

**UNIVERSIDADE E SÃO PAULO**

Faculdade de Ciências Farmacêuticas

Programa de Pós-Graduação em Ciência dos Alimentos

Área de Bromatologia

**Efeito dos compostos fenólicos da jaboticaba Sabará (*Plinia jaboticaba* (Vell.)  
Berg) na redução dos riscos à saúde causados pela obesidade**

**Effect of the phenolic compounds from Sabara jaboticaba (*Plinia jaboticaba*  
(Vell.) Berg) in reducing health risks caused by obesity**

Márcio Hércules Caldas Moura

São Paulo

2020

UNIVERSIDADE DE SÃO PAULO

Faculdade de Ciências Farmacêuticas

Programa de Pós-Graduação em Ciência dos Alimentos

Área de Bromatologia

Efeito dos compostos fenólicos da jaboticaba Sabará (*Plinia jaboticaba* (Vell.) Berg)  
na redução dos riscos à saúde causados pela obesidade

Márcio Hércules Caldas Moura

Versão Original

Tese para obtenção do título de

**Doutor**

Orientadora: Prof. Dr. Maria Inés Genovese

São Paulo

2020

Autorizo a reprodução e divulgação total ou parcial deste trabalho, por qualquer meio convencional ou eletrônico, para fins de estudo e pesquisa, desde que citada a fonte.

Ficha Catalográfica elaborada eletronicamente pelo autor, utilizando o programa desenvolvido pela Seção Técnica de Informática do ICMC/USP e adaptado para a Divisão de Biblioteca e Documentação do Conjunto das Químicas da USP

Bibliotecária responsável pela orientação de catalogação da publicação: Marlene Aparecida Vieira - CRB - 8/5562

M929e Moura, Márcio Hércules Caldas  
Efeito dos compostos fenólicos da jaboticaba Sabará (Plinia jaboticaba (Vell.) Berg) na redução dos riscos à saúde causados pela obesidade / Márcio Hércules Caldas Moura. - São Paulo, 2020.  
87 p.

Tese (doutorado) - Faculdade de Ciências Farmacêuticas da Universidade de São Paulo.  
Departamento de Alimentos e Nutrição Experimental - Programa de Pós-Graduação em Ciência dos Alimentos.  
Orientador: Genovese, Maria Inés

1. CE560.16.27.13 . 2.  
CA110.1.4.1.2.1.1.1.4.13. 3. CB330.4.13.2.2. I. T.  
II. Genovese, Maria Inés , orientador.

MÁRCIO HÉRCULES CALDAS MOURA

Efeito dos compostos fenólicos da jaboticaba Sabará (*Plinia jaboticaba* (Vell.) Berg)  
na redução dos riscos à saúde causados pela obesidade

Comissão julgadora da Tese para obtenção do grau de Doutor

---

Prof. Dr. Maria Inés Genovese  
Orientadora

---

1º examinador(a)

---

2º examinador(a)

---

3º examinador(a)

São Paulo, \_\_\_\_\_ de \_\_\_\_\_ de 2020

## Agradecimentos

Para a realização de um trabalho de pesquisa como este são necessárias inúmeras pessoas e instituições. Infelizmente não consigo agradecer a todos os envolvidos, nome a nome, por isso, antecipadamente, agradeço de coração àqueles que de alguma forma contribuíram para a conclusão desta tese e, conseqüentemente, para a realização deste grande sonho.

Agradeço a minha mãe Ozany, meus avós/pais, Maria do Socorro e Expedito (*in memoriam*), minha tia/mãe Rosilene, meus tios Eliezer, Cleide, Ozeas, Ismael, Dimas, Natanael, Georges e Jane. Cada um à sua maneira possibilitou esta conquista.

A minha amada esposa Thiara por acreditar, incentivar e apoiar irrestritamente este projeto de vida que resultou em um mestrado e um doutorado. Esta conquista é igualmente minha e sua. Minha sincera gratidão.

A minha orientadora Profa. Dra. Maria Inés Genovese pela oportunidade, orientações, conselhos e muita paciência ao longo destes anos.

Gostaria de agradecer aos meus colegas de trabalho Renata, Carlos, Rafaela, Larissa, Érika, Rosa, Elias, Gabriela Lima e Denise. A convivência foi incrível e a ajuda fundamental.

Meu muito obrigado a todos àqueles que mesmo não tendo qualquer relação direta com o trabalho se propuseram a ajudar. Agradeço especialmente a Ivanir, Luciene, Amanda e aos Prof. William e Maria O. Souza do Instituto de Ciências Biomédicas (ICB/USP).

Agradeço ao Prof. Dr. Francisco A. Thomas-Barberán e sua equipe, em especial, Carlos Garcia e Jose Alberto, pela recepção, ajuda e orientação durante o doutorado sanduíche na Espanha.

Agradeço o apoio das Instituições de fomento Conselho Nacional de Desenvolvimento Científico e Tecnológico (CNPq, #141637/2016-1) e Coordenação de Aperfeiçoamento de Pessoal de Nível Superior (CAPES, #88887.368003/2019-00) pela bolsa de estudos durante o doutorado e doutorado sanduíche, respectivamente.

## Figures

- Figure 1.** Main classes and subclasses of bioactive food compounds (BFC) and phenolic bioactive compounds (BPC)..... 14
- Figure 2.** Relation between excess energy intake, WAT inflammation and metabolic syndrome..... 17
- Figure 3.** Relation between obesity, insulin resistance and type 2 diabetes mellitus (T2M), and points where bioactive phenolic compounds may act (★)..... 19
- Figure 4.** Sabara jaboticaba (*Plinia jaboticaba* (Vell.) Berg) tree and fruits. ....22
- Figure 5.** Experimental protocol to evaluate the effect of daily gavage administration of the phenolic extract from jaboticaba (PEJ) to mice induced to obesity by a high-fat, high-sucrose diet (HFSD). ....29
- Figure 6.** Chromatogram at 280 (A) and 520 nm (B) obtained through HPLC-DAD of the phenolic extract from jaboticaba (PEJ). ....36
- Figure 7.** Chromatogram at 280 (A) and 520 nm (B) obtained through HPLC-DAD-IT MS/MS of the phenolic extract from jaboticaba (PEJ). ....38
- Figure 8.** Chromatogram at 280 and 360 nm obtained through HPLC-DAD of the phenolic extract from jaboticaba (PEJ) after acid hydrolysis in the supernatant (A) and precipitated (pellet) (B). ....40
- Figure 9.** Energy intake (A, B, C), food efficiency (D, E), body weight, absolute and relative body weight gain (BWG) (F – J) and absolute and relative weight of total white adipose tissue (WAT) (K, L) of mice fed with chow diet and water (CH), high-fat-sucrose diet (HFSD) and water (HFS), HFSD and phenolic extract from jaboticaba (PEJ) at the dose of 50 mg gallic acid equivalent (GAE)/kg of body weight (BW) (PEJ1) by daily gavage and HFSD and PEJ at the dose of 100 mg GAE/kg BW (PEJ2) by daily gavage. ....43
- Figure 10.** Absolute and relative weights of subcutaneous (sc), retroperitoneal (rt), inguinal (ig), epididymal (ep) and total white adipose tissue (WAT) (A – J), distribution of adipocyte areas frequency (AAF) (K and L) and representative H&E stained of epWAT (M) of mice fed with chow diet and water (CH), high-fat-sucrose diet (HFSD) and water (HFS), HFSD and phenolic extract from jaboticaba (PEJ) at the dose of 50 mg gallic acid equivalent (GAE)/kg of body weight (BW) (PEJ1) by daily gavage and HFSD and PEJ at the dose of 100 mg GAE/kg BW (PEJ2) by daily gavage.....45
- Figure 11.** Cytokine concentrations in the epididimal adipose tissue (WAT) (A – G) and plasma (H – O) of mice fed with high-fat-sucrose diet (HFSD) and water (HFS), HFSD and phenolic extract from jaboticaba (PEJ) at the dose of 50 mg gallic acid equivalent (GAE)/k g of body weight (BW) (PEJ1) by daily gavage and HFSD and PEJ at the dose of 100 mg GAE/kg BW (PEJ2) by daily gavage.....47

**Figure 12.** Effect of the PEJ on several parameters related to glucose metabolism (**A – J**), AKT and mTOR concentrations in liver, WAT and gastrocnemius muscle (GM) (**K – R**), and GLUT4 expression in GM (**S**) of mice fed with high-fat-sucrose diet (HFSD) and water (HFS), HFSD and phenolic extract from jaboticaba (PEJ) at the dose of 50 mg gallic acid equivalent (GAE)/kg of body weight (BW) (PEJ1) by daily gavage and HFSD and PEJ at the dose of 100 mg GAE/kg BW (PEJ2) by daily gavage.....51

**Figure 13.** Effect of the PEJ on pancreatic lipase activity (**A**), fecal lipid content (FLC) (**B**), plasma and hepatic cholesterol and TAG levels (**C – K**), plasma and hepatic TAG levels (**F, K**), plasma NEFA levels (**H**), hepatic proinflammatory cytokines (**L – P**), and representative liver images (**Q**) of mice fed with high-fat-sucrose diet (HFSD) and water (HFS), HFSD and phenolic extract from jaboticaba (PEJ) at the dose of 50 mg gallic acid equivalent (GAE)/kg of body weight (BW) (PEJ1) by daily gavage and HFSD and PEJ at the dose of 100 mg GAE/kg BW (PEJ2) by daily gavage. ....56

**Figure 14.** PEJ effect on energy metabolism of mice fed with chow diet and water (CH), high-fat-sucrose diet (HFSD) and water (HFS), HFSD and phenolic extract from jaboticaba (PEJ) at the dose of 50 mg gallic acid equivalent (GAE)/kg of body weight (BW) (PEJ1) by daily gavage and HFSD and PEJ at the dose of 100 mg GAE/kg BW (PEJ2) by daily gavage. ....60

**Figure 15.** PEJ effect on intestinal microbiome of mice fed with chow diet and water (CH), high-fat-sucrose diet (HFSD) and water (HFS), HFSD and phenolic extract from jaboticaba (PEJ) at the dose of 50 mg gallic acid equivalent (GAE)/kg of body weight (BW) (PEJ1) by daily gavage and HFSD and PEJ at the dose of 100 mg GAE/kg BW (PEJ2) by daily gavage. ....63

**Figure 16.** PEJ effect on beta diversity of the intestinal microbiome in the 14<sup>th</sup> week (**A, unweighted, and B, weighted**) and in the 28<sup>th</sup> week (**C, unweighted, and D, weighted**) of mice fed with chow diet and water (CH), high-fat-sucrose diet (HFSD) and water (HFS), HFSD and phenolic extract from jaboticaba (PEJ) at the dose of 50 mg gallic acid equivalent (GAE)/kg of body weight (BW) (PEJ1) by daily gavage and HFSD and PEJ at the dose of 100 mg GAE/kg BW (PEJ2) by daily gavage.....65

**Figure 17.** PCA and PLS-DA score plots of urinary metabolites of mice fed with chow diet and water (CH), high-fat-sucrose diet (HFSD) and water (HFS), HFSD and phenolic extract from jaboticaba (PEJ) at the dose of 100 mg gallic acid equivalent (GAE)/kg of body weight (BW) (PEJ2) by daily gavage.....67

**Figure 18.** VIP scores of urinary metabolites of mice fed with chow diet and water (CH), high-fat-sucrose diet (HFSD) and water (HFS), HFSD and phenolic extract from jaboticaba (PEJ) at the dose of 100 mg gallic acid equivalent (GAE)/kg of body weight (BW) (PEJ2) by daily gavage. ....68

**Figure 19.** Biplot and heatmap of urinary metabolites of mice fed with chow diet and water (CH), high-fat-sucrose diet (HFSD) and water (HFS), HFSD and phenolic extract from jaboticaba (PEJ) at the dose of 100 mg gallic acid equivalent (GAE)/kg of body weight (BW) (PEJ2) by daily gavage. ....69

## Tables

<b>Table 1.</b> Chemical characterization of the phenolic extract from jaboticaba (PEJ)....	37
<b>Table 2.</b> Tentative identification of polyphenols present in the phenolic extract from jaboticaba (PEJ) by HPLC-DAD-IT MS/MS.....	39
<b>Table 3.</b> Ellagitannin and gallotannin quantification of the phenolic extract from jaboticaba (PEJ) administered to the animals. ....	41
<b>Table 4.</b> Main metabolites tentatively identified in urine of mice by UPLC-ESI-QTOF. ....	70

## Summary

<b>1. Introduction</b> .....	<b>13</b>
1.1. Bioactive food compounds .....	13
1.2. Obesity, inflammation and BPC .....	15
1.3. Glucose and lipid metabolisms and BPC .....	17
1.4. Thermogenesis and BPC .....	20
1.5. BPC on intestinal microbiome .....	20
1.6. Untargeted metabolomics .....	21
1.7. BPC from jaboticaba .....	21
<b>2. Objectives</b> .....	<b>24</b>
<b>3. Material and methods</b> .....	<b>25</b>
3.1. Plant material and phenolic extract .....	25
3.1.1. <i>Plant material</i> .....	25
3.1.2. <i>Preparation of the phenolic extract from jaboticaba (PEJ)</i> .....	25
3.1.3. <i>Chemical characterization of the PEJ</i> .....	26
3.2. Effect of daily PEJ administration in diet-induced obesity .....	27
3.2.1. <i>Animal and experimental design</i> .....	27
3.2.2. <i>Energy intake, body weight and food efficiency</i> .....	28
3.2.3. <i>Histology of the epididimal white adipose tissue (epWAT)</i> .....	28
3.2.4. <i>Assessment of inflammatory status</i> .....	29
3.2.5. <i>Analysis related to glucose</i> .....	31
3.2.6. <i>Analysis related to lipids</i> .....	31
3.2.7. <i>Analysis related to thermogenesis</i> .....	32
3.2.8. <i>Statistical analysis</i> .....	33
3.2.9. <i>Metagenomic analysis</i> .....	33
3.2.10. <i>Untargeted metabolomic analysis</i> .....	35

<b>4. Results and discussion</b> .....	<b>36</b>
4.1. Chemical characterization of the PEJ.....	36
4.2. Effect of daily administration of the PEJ against obesity .....	41
4.2.1. <i>Energy intake, food efficiency, body weight gain, adiposity, and adipocyte hypertrophy</i> .....	42
4.2.2. <i>Inflammation</i> .....	46
4.2.3. <i>Glucose metabolism</i> .....	50
4.2.4. <i>Lipid metabolism</i> .....	55
4.2.5. <i>PEJ effect on energy metabolism</i> .....	59
4.2.6. <i>PEJ effect on microbiota</i> .....	62
4.2.7. <i>Untargeted metabolomics</i> .....	66
<b>5. Conclusions</b> .....	<b>72</b>
<b>6. References</b> .....	<b>73</b>

## Resumo

MOURA, Márcio Hércules Caldas. **Efeito dos compostos fenólicos da jabuticaba Sabará (*Plinia jaboticaba* (Vell.) Berg) na redução dos riscos à saúde causados pela obesidade.** Faculdade de Ciências Farmacêuticas – Universidade de São Paulo, São Paulo, 2020.

A jabuticaba Sabará (*Plinia jaboticaba* (Vell.) Berg) é um fruto nativo da Mata Atlântica brasileira, rico em polifenóis e apreciado para o consumo tanto *in natura* quanto em preparos variados. O objetivo deste trabalho foi avaliar se compostos fenólicos da jabuticaba Sabará, na forma de extrato fenólico (PEJ), são capazes de reduzir os riscos à saúde causados pela obesidade e problemas de saúde associados induzidos por uma dieta rica em lipídios e sacarose (HFSD) em camundongos C57BL/6J. Inicialmente, durante 14 semanas, 66 animais machos com oito semanas de vida foram distribuídos aleatoriamente em dois grupos: controle negativo (CH), alimentado com dieta padrão AIN96M e água *ad libitum*; controle positivo (HFS), alimentado com HFSD e água *ad libitum*. Ao final desta etapa, 10 animais de cada grupo foram eutanasiados sob anestesia e seus órgãos e tecidos coletados. Os animais restantes foram redistribuídos em quatro grupos por mais 14 semanas: grupo CH, alimentado com dieta padrão e água; grupo HFS, alimentado com HFSD e água; grupo PEJ1, alimentado com HFSD e PEJ na dose de 50 mg equivalente de ácido gálico (EAG)/kg de massa corporal (m.c.); grupo J100 alimentado com HFSD e PEJ na dose de 100 mg EAG/kg m.c. O consumo de ração, a massa corporal e a glicemia de jejum (FBG) foram medidos semanalmente e as gavagens de água (CH e HFS) ou PEJ (PEJ1 e PEJ2) foram realizadas diariamente. Na 26<sup>a</sup> semana foi realizado o teste intraperitoneal de tolerância à insulina (ipITT), na 27<sup>a</sup> o teste oral de tolerância à glicose (oGTT) e na 28<sup>a</sup> as análises relacionadas a homeostase energética. Ao final do experimento os animais foram eutanasiados sob anestesia e seus órgãos e tecidos coletados. Quando comparados ao grupo HFS, animais que receberam o PEJ apresentaram ganho de massa corporal aprox. 30% menor e aprox. 45% menos massa total de tecidos adiposos brancos (TAB). Além disso, os grupos PEJ apresentaram adipócitos menos hipertrofiados. Marcadores de inflamação foram significativamente reduzidos em ambos os grupos tratados. A FBG foi aprox. 13% inferior para os grupos PEJ em relação ao grupo HFS. Além disso, os valores médios de ipITT, oGTT, insulina e HOMA-IR demonstraram que o PEJ aumentou a sensibilidade à insulina e diminuiu a intolerância à glicose. A expressão do GLUT4 no músculo estava aumentada nos grupos tratados. O conteúdo lipídico fecal dos grupos PEJ foi superior ao do grupo HFS, sugerindo que, assim como ocorreu *in vitro*, o extrato inibiu a atividade da lipase pancreática *in vivo*. Os níveis de colesterol total (PEJ1), LDL e NEFA foram reduzidos e os de HDL aumentados. A concentração hepática de TAG também foi reduzida pelo PEJ. O gasto energético e a expressão de UCP1 foram superiores para ambos os grupos suplementados quando comparados ao grupo HFS. PEJ alterou positivamente a microbiota intestinal e a análise de metabólitos mostrou que os animais tratados com PEJ possuíam perfil metabólico diferente. Em conjunto, estes resultados demonstraram que os CFJS podem ser usados como adjuvantes no combate a obesidade e problemas de saúde associados.

**PALAVRAS-CHAVES:** polifenóis, jabuticaba, obesidade, microbiota intestinal, metabólica.

## Abstract

MOURA, Márcio Hércules Caldas. **Effect of the phenolic compounds from Sabara jaboticaba (*Plinia jaboticaba* (Vell.) Berg) in reducing health risks caused by obesity.** Faculty of Pharmaceutical Sciences - University of São Paulo, São Paulo, 2020.

Sabara jaboticaba (*Plinia jaboticaba* (Vell.) Berg) is a Brazilian native fruit from Atlantic Forest, rich in polyphenols and appreciated for consumption both *in natura* and in various preparations. This study aimed to evaluate whether phenolic compounds of Sabara jaboticaba, in the form of phenolic extract (PEJ), can reduce the health risks caused by obesity and associated health problems induced by a fat-sucrose-rich diet (HFSD) in C57BL/6J mice. Initially, for 14 weeks, 66 8-week-old male mice were randomly distributed into two groups: negative control (CH), fed with standard AIN96M diet and water *ad libitum*; positive control (HFS), fed with HFSD and water *ad libitum*. At the end of this stage, 10 animals from each group were euthanized under anesthesia and their organs and tissues collected. The remaining animals were redistributed into four groups for another 14 weeks: group CH, fed a standard diet and water; HFS group, fed with HFSD and water; PEJ1 group, fed with HFSD and PEJ at the dose of 50 mg equivalent of gallic acid (GAE)/kg of body weight (BW); group J100 fed with HFSD and PEJ at the dose of 100 mg GAE/kg BW. Food intake, BW, and fasting blood glucose (FBG) were measured weekly and water (CH and HFS) or PEJ (PEJ1 and PEJ2) were daily administered. In the 26<sup>th</sup> week the intraperitoneal insulin tolerance test (ipITT) was performed, in the 27<sup>th</sup>, the oral glucose tolerance test (oGTT), and, in the 28<sup>th</sup>, the analyzes related to energy homeostasis. At the end of the experiment, the animals were euthanized under anesthesia and their organs and tissues were collected. When compared to the HFS group, animals that received PEJ showed decrease in BW gain of approx. 30% and of approx. 45% in the gain of total white adipose tissues (WAT). In addition, the PEJ groups showed less hypertrophied adipocytes. Inflammation markers were significantly reduced in both treated groups. The FBG was approx. 13% lower for the PEJ groups compared to the HFS group. In addition, the mean values of ipITT, oGTT, insulin and HOMA-IR demonstrated that PEJ increased insulin sensitivity and decreased glucose intolerance. GLUT4 expression in the muscle was also increased in the treated groups. The fecal lipid content was lower in the PEJ groups when compared to the HFS group, suggesting that PEJ inhibited pancreatic lipase activity both *in vitro* and *in vivo*. In the PEJ groups, the levels of total cholesterol, LDL and NEFA were reduced and those of HDL increased. The hepatic concentration of TAG was also reduced by PEJ. Energy expenditure and UCP1 expression were higher for both supplemented groups when compared to the HFS group. PEJ positively altered the intestinal microbiota and the analysis of metabolites showed that animals treated with PEJ had different metabolomic profile. Together, these results demonstrated that polyphenols from jaboticaba may be used as adjuvants against obesity and associated health problems.

**KEYWORDS:** polyphenols, jaboticaba, obesity, intestinal microbiota, metabolomics.

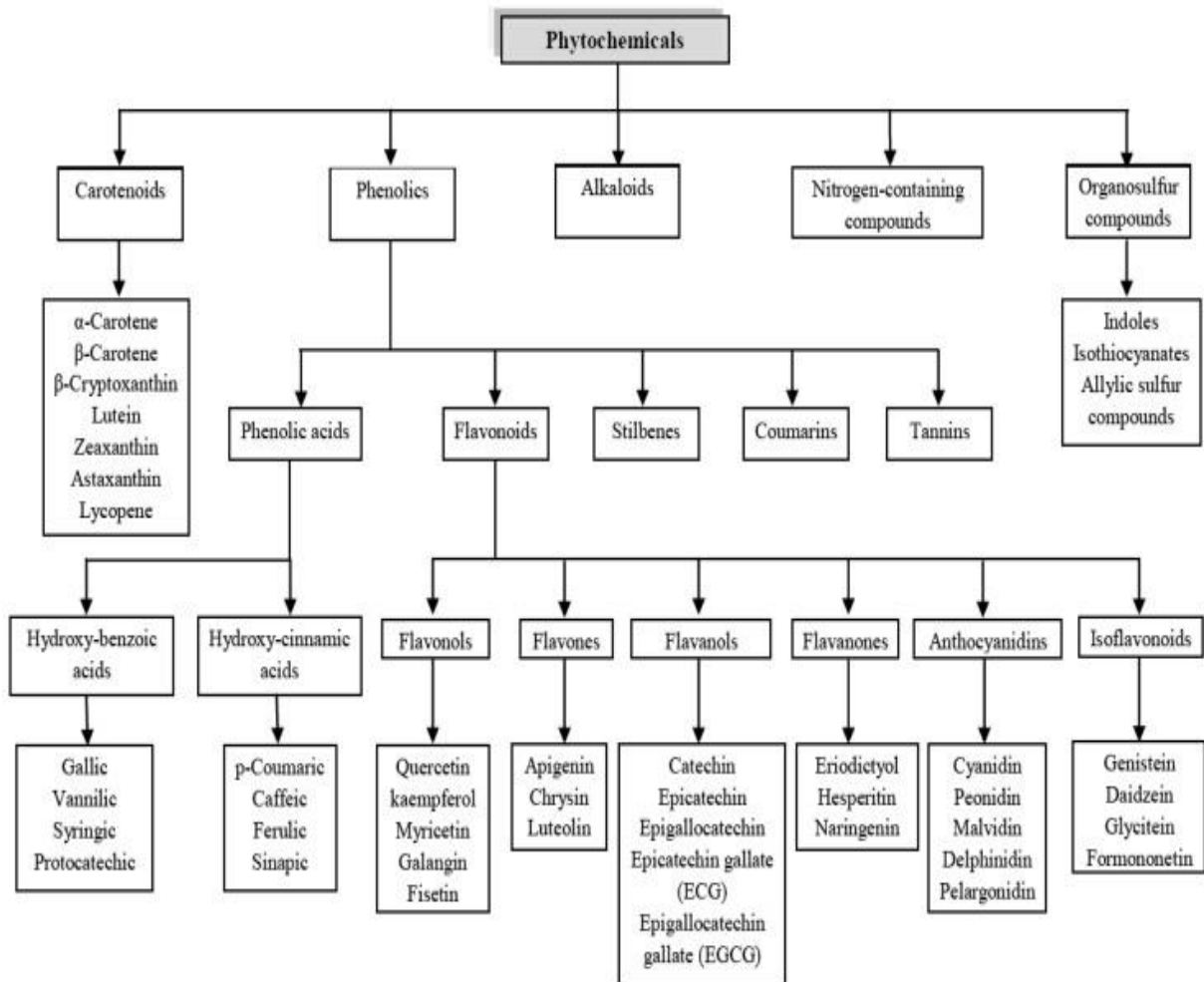
## 1. Introduction

### 1.1. Bioactive food compounds

Fruits and vegetables-rich diets have been strongly associated with several beneficial health effects. Such foods are essential sources of macro and micronutrients for the healthy growth and development of the organism. In recent decades, many studies have demonstrated that part of the health benefits attributed to these foods are due to phytochemicals also known as bioactive food compounds (BFC) (BASTOS; ROGERO; ARÉAS, 2009; DEL RIO et al., 2013). BFC are secondary metabolites in plants that play little or no role in usual biochemical processes, such as photosynthesis, respiration, growth, and development. Although extranutritional constituents, they are usually found in high concentrations. BFC are used in plant defense against various damages, biosignalizers in some metabolic syntheses, and as attractive for pollinating animals. Bioactive phenolic compounds (BPC) constitute the mostly of the BFC and are chemically characterized by having at least one aromatic ring mono- or polysubstituted by hydroxyls (CROZIER; JAGANATH; CLIFFORD, 2009).

BPC are divided into two groups: flavonoids and non-flavonoids. Flavonoids have a basic structure formed by two aromatic rings linked by three carbons (C<sub>6</sub>-C<sub>3</sub>-C<sub>6</sub>), being, therefore, diphenylpropanes. BPC are the most numerous in the plant kingdom, being commonly found in the leaves of plants and in the skin of fruits. Among flavonoids, flavan-3-ols stand out because their chemical structures vary from simple monomers to oligomers and complex polymers. The polymers of flavan-3-ols are named proanthocyanidins, also known as condensed tannins (CROZIER; JAGANATH; CLIFFORD, 2009; DEL RIO et al., 2013). Phenolic acids are the most important non-flavonoids. They are classified into hydroxybenzoic or hydroxycinnamic acids and their derivatives. Gallic and ellagic acid are the main hydroxybenzoic acids and are, respectively, precursors of the gallic tannins (gallotannins) and ellagic tannins (ellagitannins). Since they are hydrolysable under acid or basic conditions, they are also known as hydrolysable tannins. Hydroxycinnamic acids usually occur in the conjugated form with other compounds and are collectively referred to as chlorogenic acids. The stilbenes are in a much lower proportion than the other non-flavonoids, being the resveratrol their main representative (**Figure 1**) (DEL RIO et al., 2013).

**Figure 1.** Main classes and subclasses of bioactive food compounds (BFC) and phenolic bioactive compounds (BPC).



Source: Bellik et al. (2012).

Flavonols are widely distributed in plants, being the most common quercetin, myricetin and kaempferol, which are found mainly in glycosylated forms. Quercetin derivatives are found in high concentrations in onions (*Allium cepa*) and are present in the daily diet of different populations and countries. Several beneficial properties have been associated to quercetin, such as anti-carcinogenic, anti-inflammatory, and antiviral activities. Flavones and flavanones are commonly found in citrus fruits. Sour orange (*Citrus aurantium*) and grapefruit (*Citrus paradise*) are examples of rich fruits in conjugates of the flavanones hesperidin and naringenin, compounds with cardioprotective properties. Legumes are almost exclusive sources of isoflavones that, due to their structural similarity to estrogen, have estrogenic properties, and are

classified as phytoestrogens. Soy (*Glycine max*) is rich in daidzein and genistein, two isoflavones widely consumed.

Fruits like raspberry, strawberry, blackberry, pomegranate, and jaboticaba are diversified sources of anthocyanins, ellagitannins and proanthocyanidins, compounds with a wide range of positive biological actions to health. Regardless of the species, coffee beans are sources of chlorogenic acids and, due to the high consumption of this drink, these phenolics are part of the daily diet of thousands of people around the world. Red wines are also appreciated worldwide and are resveratrol and derivatives-rich drinks. Both chlorogenic acids and resveratrol have proved beneficial effects on human health (ALEZANDRO et al., 2013; CROZIER; JAGANATH; CLIFFORD, 2009; DEL RIO et al., 2013). BPC are already part of the daily diet of people, making it necessary to stimulate an adequate and diversified daily consumption, safely spreading their health benefits, and expanding access to them.

## **1.2. Obesity, inflammation, and BPC**

Overweight and obesity are defined as an abnormal or excessive accumulation of body fat which is potentially dangerous to health. The body mass index (BMI in  $\text{kg}/\text{m}^2$ ) is the most common standard for classifying overweight and obesity. Adults are considered with overweight when their BMI is equal or higher than 25, and with obesity when this value is equal to or higher than 30. In the case of children and adolescents, the index used is the BMI-for-age, which considers the standard average child growth rate established by the WHO (z-score). Children and adolescents with z-score values twice as high as the average are considered overweight and three times more are considered obese (WHO, 2014). Since 1975 obesity has practically tripled worldwide. According to the World Health Organization (WHO), in 2016, 39% of adults aged 18 and over were overweight, and of these, 11% of men and 15% of women were obese. Even more worrying is the fact that, in that same year, around 41 million children under the age of 5 and 340 million children aged between 5 and 19 were overweight or obese (WHO, 2014). In Brazil, more than half of the population (56.9%) aged 18 or over is overweight, and of this total, obesity affects almost a third of men (16.8%) and more one third of women (24.4%) (IBGE, 2015).

Obesity increases the risk for diabetes, cardiovascular diseases, certain types of cancers, osteoarthritis, and sleep apnea, in addition to impairing reproductive

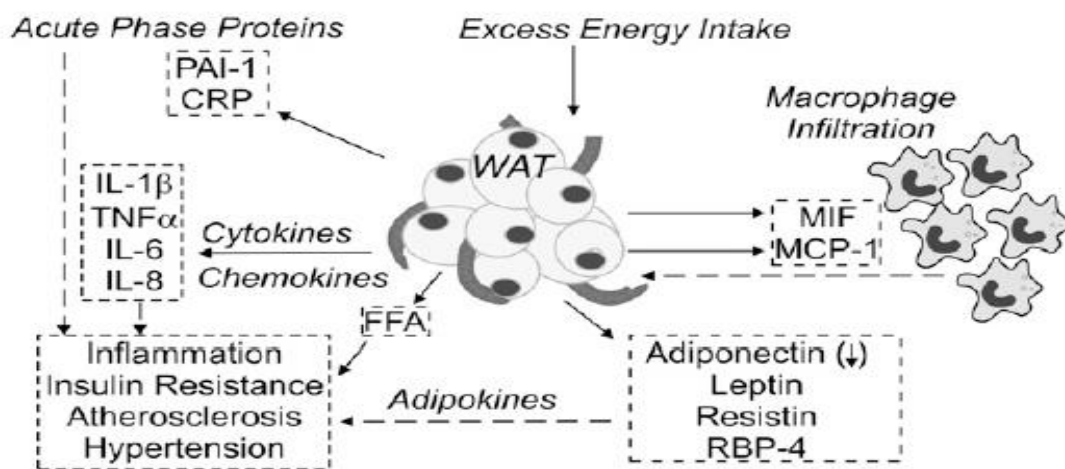
performance. According to the OMS, 4 million death each year may be directly associated with overweight or obesity, and, until this moment, more severe symptoms, and complications of coronavirus disease (COVID-19) have been reported in obese people. The white adipose tissue (WAT) plays a much more complex role in the organism than simply to store energy and, therefore, negative changes in its metabolic and endocrine functions impair glucose homeostasis, energy metabolism, food intake, body mass regulation, hemostasis and immune system functions (PHE, 2020; WHO, 2014).

Adipocyte hypertrophy/hyperplasia, caused by excessive energy intake, is one of the ways in which the WAT ends up being dysregulated. This improper WAT functioning increases secretion of several adipocyte factors with proinflammatory properties, such as tumor resistin, necrosis factor-alpha (TNF $\alpha$ ), interleukin 6 (IL6) plasminogen activator inhibitor 1 (PAI1), and monocyte chemo-attracting protein (MCP1), among others. MCP1 mediates the migration of blood monocytes to WAT, mainly in the visceral, where they differ in type 1 (M1) macrophages, which are pro-inflammatory and secrete more pro-inflammatory cytokines, restarting the cycle, resulting in local inflammation (PATEL; BURAS; BALASUBRAMANYAM, 2013). Adipocyte expansion can also compromise the local blood supply and lead to hypoxia, causing necrosis which increase the infiltration of M1 macrophages in WAT, with consequent overproduction of inflammatory factors (EMANUELA et al., 2012). WAT is also related to local or systemic inflammation and high blood concentration of lipopolysaccharides (LPS). LPS is the main glycolipid in the outer membrane of gram-negative intestinal bacteria and powerful endotoxin, capable of activating several inflammatory pathways by binding to the toll-like receptor 4 (TLR4), causing metabolic endotoxemia (BOUTAGY et al., 2016). Thus, together, adipocyte hypertrophy, the abnormal synthesis of pro-inflammatory cytokines by WAT, hypoxia and endotoxemia produce a persistent systemic inflammatory state, but of low intensity. For this reason, obesity has been defined as a chronic low-grade inflammatory state. It is important to highlight that inflammation is related to atherosclerosis, hypertension, and insulin resistance, which, in turn, is strongly associated with the genesis of diabetes (**Figure 2**) (ROBERTS; HEVENER; BARNARD, 2014).

Different BPC from many food sources have been associated to modulation of inflammatory response induced by obesity by both inhibiting metabolic pathways and reducing the expression of key proteins involved in the inflammatory process (WANG

et al., 2014). In addition to these anti-inflammatory properties, clinical trials, and *in vitro* and *in vivo* studies highlight the potential of BPC in the prevention and reduction of health risks caused by obesity through other mechanisms, such as decreased food intake, reduced absorption of lipids, regulation of glucose and lipid metabolisms, increased energy expenditure, and modulation of the gut microbiome (DEL RIO et al., 2013; XIE et al., 2018).

**Figure 2.** Relation between excess energy intake, WAT inflammation and metabolic syndrome.



WAT: white adipose tissue. IL-1 $\beta$ , IL6, IL-8: interleukins 1 $\beta$ , 6 and 8. TNF $\alpha$ : tumor necrosis factor-alpha. PAI1: plasminogen activator inhibitor 1. CRP: C-reactive Protein. MCP1: monocyte chemo-attracting protein. RBP-4: retinol binding protein 4.

Source: Kennedy et al. (2008).

### 1.3. Glucose and lipid metabolisms and BPC

A dysfunctional glucose metabolism may result, among other health problems, in type 2 diabetes mellitus (T2M). According to the WHO, individuals with fasting blood glucose values equal to or greater than 126 mg/dL are considered diabetic. When diabetes is characterized by resistance to action of insulin, it is called T2M. T2M increases the risk of cardiovascular disease (CVD), kidney problems, blindness, and limb amputation, and is therefore an important cause of premature death and incapacity. The prevalence of this disease has been increasing worldwide with an estimated global rate of 8.5% in 2014, affecting 422 million individuals, including children and adolescents. In addition, in 2012, 1.5 million deaths were directly

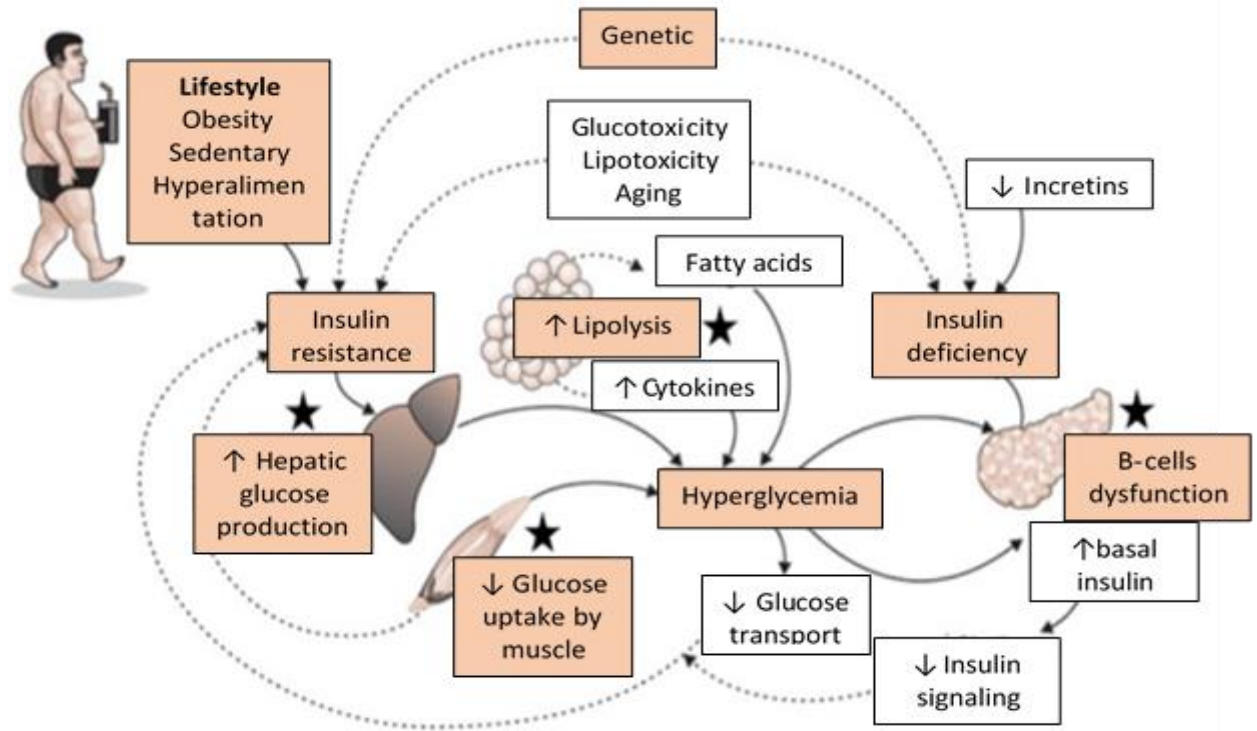
associated with DMT2, being also responsible for the drastic reduction in the quality of life of several populations (WHO, 2016).

Although the etiology of T2D is not yet fully understood, studies point to impaired insulin action followed by IR as precursors of diabetes, i.e., initially, the secretion of insulin is increased to compensate the reduction in insulin action, maintaining normoglycemia. When insulin production declines to an inefficient level to compensate the IR, T2D manifests. Obesity, IR and T2D are so strongly related that the term “diabesity” is widely used by experts. Transition from obesity to T2D occurs through progressive defects in the secretion and action of insulin in its main target tissues, namely, muscle, adipose tissue and liver, caused by the excessive accumulation of body fat (SILVA, 2015; ZIMMET; ALBERTI; SHAW, 2001).

Even without a complete elucidation of the mechanisms of action, many studies report that BPC have hypoglycemic properties, and can act as adjuvants in the regulation of glucose metabolism. These compounds can decrease postprandial glycemia, possibly by inhibiting digestive enzymes, such as  $\alpha$ -glycosidase and  $\alpha$ -amylase, and/or the active sodium-dependent glucose transporter (SGLT1) in the small intestine. They can also induce translocation of the glucose transporter 4 (GLUT4) from cytoplasmatic vesicles to plasmatic membrane in adipose tissue and skeletal muscle, reducing the plasma glucose concentration by modulating the insulin receptor/protein kinase B (IRS-Akt) pathway. Phenolics also decreased the expression of enzymes associated with glycogenolysis and gluconeogenesis, which can lead to a reduction in plasma glucose levels, in addition to protecting  $\beta$ -pancreatic cells from glucotoxicity (**Figure 3**) (HANHINEVA et al., 2010; OOI et al., 2018).

The Insulin action depends on complex mechanisms based on vary events of phosphorylations and dephosphorylations. The abnormal hepatic lipid accumulation not caused by alcohol consumption is known as non-alcoholic fatty liver disease (NAFLD) and has been associated with defects in these mechanisms, leading to both IR in the liver and in the skeletal muscle. NAFLD is present in approx. 20-30% general people and more than 90% of obese with T2M have NAFLD, and IR is present in both latter conditions (PERRY et al., 2014). There is also the lipotoxicity, result of the lipid accumulation in other organs when the storage capacity of the WAT is exceeded. Several studies already proved that there is a close relationship between lipotoxicity, IR and T2M. Therefore, a disorder in lipid metabolism has negative consequences on glucose metabolism causing many other health problems (BIDEN et al., 2014).

**Figure 3.** Relation between obesity, insulin resistance and type 2 diabetes mellitus (T2M), and points where bioactive phenolic compounds may act (★).



Source: Silva (2015).

BPC can regulate the lipid metabolism of several ways. *In vitro* and *in vivo* experiments with phenolic extracts from different sources, such as fruits, fruit seeds and plants, showed that these compounds inhibited the action of pancreatic lipase, a key enzyme of lipid digestion, thus reducing the absorption of lipids by the intestine (YU et al., 2017). Other studies have shown that BPC through multiple mechanisms reduced plasma concentrations of the total-, LDL-, VLDL-cholesterols and triacylglycerols (TAG) accompanied of increase in the plasma HDL concentration, therefore, having hypocholesterolemic properties (DI DONNA et al., 2014; MOURA et al., 2018; ZHANG et al., 2020). In addition, studies have also reported that BPC may positively modulate the mammalian target of rapamycin (mTORC) protein, a serine/threonine kinase with several cell functions, including lipogenesis and lipolysis (Ooi et al., 2018). Through other mechanism, the chronic supplementation with phenolic extracts of grape seeds was able to regulate the hepatic gene expression of

micro-RNAs associated with obesity and the metabolic syndrome (BASELGA-ESCUDERO et al., 2015).

#### **1.4. Thermogenesis and BPC**

In thermodynamic terms, obesity is result of the relation between high energy intake and low energy expenditure (EE). Thus, finding ways to increase the EE may help fight obesity. Mammals have two types of adipose tissue, the WAT, and the brown adipose tissue (BAT), a mitochondrial-rich tissue, whose main function is to dissipate energy as heat, increasing the EE. The BAT plays this function through protein uncoupling protein 1 (UCP1) in a process namely thermogenesis (XIE et al., 2018).

In contrast to HFSD, fruit and vegetable-rich diets have been strongly associated with several beneficial health effects. Part of the health benefits are related to phytochemicals also known as bioactive phenolic compounds (BPC), secondary plant metabolites used in plant defense (CROZIER; JAGANATH; CLIFFORD, 2009; DEL RIO et al., 2013). BPC from many food sources were shown to fight adiposopathy, hyperglycemia and dyslipidemia, and increase EE (HANHINEVA et al., 2010; WANG et al., 2014; XIE et al., 2018).

#### **1.5. BPC on intestinal microbiome**

The relation between intestinal microbiome and obesity has been widely studied. It has been proposed that gut microbiota can triggers obesity and metabolic disorders through different ways, such as increasing or decreasing energy intake/expenditure and inflammation (increasing or decreasing endotoxemia). The gut microbial community is strongly dependent of the host but may be changed by many endogenous and exogenous factors. In humans, the microbiota is composed by 5 main phyla, Bacteroidetes, Firmicutes, Actinobacteria, Proteobacteria, and Verrucomicrobia, the first two representing approx. 90% of the total (CASTANER et al., 2018). Microbiota of obese and lean humans or animals are distinct, and the Firmicutes/Bacteroidetes (F/B) ratio has been considered, although in a non-consensual way, as a possible marker of obesity-related health problem. Studies, mainly in animals, have reported an increase in the F/B ratio in obese and/or diabetic

individuals, and, more recently, the increase in the Firmicute rate was associated with a severe deterioration of the NAFLD in mice (KAN et al., 2020).

BPC can positively alter the intestinal microbial community by creating a favorable environment to beneficial bacteria strains. For example, polyphenols increased the gut mucin production, benefiting expansion of *Akkermansia muciniphila*, a specie that has been linked to healthy status (ANHÊ et al., 2017). BPC were also associated to decrease of LPS-producing bacteria, lowering, therefore, endotoxemia (KANG et al., 2017).

### **1.6. Untargeted metabolomics**

The field of study about molecules in the organism under different conditions is named omics. Genomics/epigenomics (DNA), transcriptomics (mRNA), proteomics (proteins) and metabolomics/lipidomics (small molecules and lipids) are the main omics disciplines and subdisciplines. Untargeted metabolomics is an approach increasingly used to discovery new biomarkers or to broaden the understanding about changes in biological pathways caused by drugs, toxins and diseases (GORROCHATEGUI et al., 2016). The main techniques used to identify and quantify metabolites are nuclear magnetic resonance (NMR), spectroscopy and mass spectroscopy (MS). A growing number of techniques, mathematical models, library and softwares have been developed aiming to get insight about relations between phytochemicals and genotype-phenotype (SHEIKHOLESLAMI et al., 2020)

### **1.7. BPC from jaboticaba**

Brazil has approximately one third of the world's flora distributed in 10 biomes and, consequently, presents a magnificent biodiversity. The Atlantic Forest is one of these biomes and extends in heterogeneous way along the Brazilian coast. The amount of endemism in this tropical forest makes it more important, as there are 8,000 plant species and 700 endemic animal species (MYERS et al., 2000; TABARELLI, 2005).

The jaboticaba tree (*Plinia* spp.), belonging to Myrtaceae family, is predominant in the Atlantic Forest biome and native to the South, Southeast and Midwest regions

of Brazil. It is a tree with an average size between 10 and 15 m, soft trunk with 30 to 40 cm in diameter, pyramidal shape, and elongated crown. Its leaves are simple, opposite, and lanceolate. Since it is a cauliflory type plant, its white and pedicel flowers extend over the trunk and branches. The fruits are small, soft, and rounded berries, with dark purple skin when ripe and with whitish and sweet pulp (SUGUINO et al., 2012). There are nine species, one of which is now extinct, five found in research centers and three spread in nature or cultivated. Of these, the Paulista jaboticaba (*Plinia cauliflora* (DC.) Berg) and the Sabara jaboticaba (*Plinia jaboticaba* (Vell.) Berg) are the most known, cultivated and widely commercialized, with Sabara being the most common (**Figure 4**) (CITADIN; DANNER; SASSO, 2010).

**Figure 4.** Sabara jaboticaba (*Plinia jaboticaba* (Vell.) Berg) tree and fruits.



Source: the author (2018).

Jaboticaba stands out among Brazilian native fruits for its high commercial potential, since it is appreciated both for fresh consumption and in various preparations, such as sweets and drinks. Both cultivar, Paulista and Sabara, are rich in anthocyanins, proanthocyanidins and ellagitannins, phenolics associated with reduced risk of several chronic non-communicable diseases (NCD) (DEL RIO et al., 2013). According to Alezandro et al. (2013), Sabara surpasses Paulista in terms of phenolic content, *in vitro* antioxidant capacity, proanthocyanidin content and concentration of free and total ellagic acid. These authors also demonstrated that in the fully ripe fruit the concentrations of these compounds are more elevated in

proportions equitable with some type of berries, fruits that have been associated with several health benefits, but that are scarce in Brazil. For these reasons, Sabara jaboticabas entire (peel, seed, pulp) and fully ripe were chosen for this work.

In last years, the number of studies reporting benefits to health of jaboticaba (*Plinia* spp.) has considerably increased. Aqueous dispersion of the fruit powder attenuated oxidative stress, and improved the lipid profile of rats induced to diabetes by streptozotocin (ALEZANDRO; GRANATO; GENOVESE, 2013). The peel intake attenuated oxidative stress and improved the endogenous antioxidant system of obese rats (BATISTA et al., 2014). Similarly, meals containing the peel increased serum antioxidant concentrations and decreased glucose and insulin levels in healthy adults (PLAZA et al., 2016). Fruit extract attenuated diabetic nephropathy by decreasing oxidative stress and inflammation (HSU et al., 2016). Phenolic-rich extracts administered for 8 weeks to C57BL/6 mice fed with high-sucrose/high-fat diet (HSHF) prevented the excessive weight gain by minimizing the white adipose tissues accumulation. In addition, the glucose and lipid metabolisms were improved. Therefore, using a HFSD-induced obesity animal model, we here investigated, for the first time, whether long-term supplementation with BPC from Sabara jaboticaba, as phenolic extract (PEJ), had a positive impact on health of obese mice.

## 2. Objectives

The general objective of this work was to evaluate the effect of the phenolic-rich extract from Sabara jaboticaba (PEJ) on the health of obese C57BL/6J mice.

The specific objectives were:

- Chemically characterize the PEJ in relation to total phenolic content, proanthocyanidins, flavonoids, phenolic acids, and tannins.
- Evaluate the effects of oral daily administration for 14 weeks of the PEJ at two doses, 50 and 100 mg gallic acid equivalent (GAE)/kg of body weight (BW), in the BW gain, inflammation, glucose and lipid metabolisms and energy homeostasis in obese C57BL/6J mice.
- Evaluate, after 14 weeks, the effect of oral daily administration of the PEJ at two doses (50 and 100 GAE/kg BW), in intestinal microbiome of obese C57BL/6J mice.
- Evaluate the metabolites produced by obese C57BL/6J mice after 14 weeks of oral daily administration of the PEJ at two doses (50 and 100 GAE/kg BW).

### 3. Material and methods

#### 3.1. Plant material and phenolic extract

##### 3.1.1. Plant material

Ripe Sabara jaboticabas (*Plinia jaboticaba* (Vell.) Berg) were acquired from a local producer (Jaboticabal-SP, at 21° 16' S latitude and 48° 19' W longitude) through the São Paulo Central Market (CEAGESP – Companhia de Entrepósitos e Armazéns Gerais de São Paulo, São Paulo, Brazil). After cleaning, the whole fruits were frozen in liquid nitrogen, lyophilized, powdered in analytic mill, and stored at – 20 °C for further analysis.

##### 3.1.2. Preparation of the phenolic extract from jaboticaba (PEJ)

Phenolic compounds were extracted using a hydromethanolic solution (methanol/water/acetic acid; 70:30:0.5 v/v/v) at a 1:25 (w/v) powder-to-solvent ratio for 2 h at 4 °C followed by more two times of 30 min each one. The mixture was filtered under pressure with filter paper (Whatman N° 1), concentrated in rotatory evaporator (Rotavapor R-120; Büchi, Switzerland) at 37 °C until methanol elimination and resuspended with distilled water for the solid-phase extraction (SPE). The SPE was performed in manually crafted octadecylsilane (C18, Sigma-Aldrich Co. LLC, Supelclean™ LC-18 SPE) columns using 60 mL polypropylene tubes. The columns were preconditioned with methanol followed by distilled water at a 1:20:60 (w/v/v) polymer-to-solvent ratio (p/s). The extract was passed through the columns at a 3% of total phenolic-to-polymer ratio. After distilled water washing (at a 1:60 p/s), the phenolic compounds were eluted with methanol (at a 1:50 p/s). The eluates were totally dried on a rotatory evaporator (Rotavapor R-120; Büchi, Switzerland) and resuspend in water for *in vivo* assays and chemical analysis. This extract was named phenolic extract from jaboticaba (PEJ).

### **3.1.3. Chemical characterization of the PEJ**

The PEJ was chemically characterized in relation to total phenolic concentration according to Magalhães et al. (2010). The results were expressed as gallic acid equivalent (GAE)/mL extract. Proanthocyanidin content was quantified by DMAC (4-dimetilaminocinamaldeído) methodology according to Prior et al. (2010) using a standard curve of proanthocyanidin B2 (PB2). The results were expressed as PB2 equivalent/mL extract. The total ellagic acid content was quantified by acid hydrolysis according to Genovese et al. (2008). Flavonoids and phenolic acids were determined and quantified through high performance liquid chromatography with diode array detection (HPLC-DAD), as follows: after drying in rotatory evaporator at 37 °C of 1 mL of the PEJ, it was resuspended in methanol and filtered through 0,22 µm PTFE membrane (Millipore, MA, E.U.A.). The chromatograph used was the Hewlett-Packard 1100 model, with automatic sample injector, quaternary pump and DAD detector, column Prodigy 5 µm ODS 3 250 × 4.60 nm (Phenomenex Ltda., United Kingdom), controlled by ChemStation software. The solvent gradient consisted of A (water/tetrahydrofuran/trifluoroacetic acid, 98:2:0.1) and B (acetonitrile), in the proportion of 17% B for 2 min, increasing to 25% B after 5 min, to 35% B after another 8 min and 50% B after 5 min. The quantification was performed by comparing the retention times and UV spectral characteristics of these compounds with external standards purchased from Sigma (Chemicals Co., St. Louis, USA) and Extrasynthèse (Genay, France).

The chemical structures was confirmed through high performance liquid chromatography with diode array detection coupled to mass spectrometer with ion trap analyzer (HPLC-DAD-IT MS/MS) at Research Group on Quality, Safety and Bioactivity of Plant Foods (CEBAS-CSIC), Murcia, Spain, as follows: 1 mL of the PEJ was dried under vacuum, resuspended in methanol, filtered through a 0.22 µm PDVF filter (Millipore Ltd., Bedford, MA) before analysis on an Agilent 1100 HPLC system (Agilent Technologies, Waldbronn, Germany) using a reverse phase Pursuit XR<sub>s</sub> C18 column (250 mm x 4 mm, 5 µm particle size) (Agilent Technologies, Waldbronn, Germany). The mobile phases were (A) 1% formic acid in water and (B) acetonitrile following an elution gradient with 3% B at 0 min; 9%, 5 min; 16%, 15 min; 50%, 45 min; 90%, 47 min; 3%, 52 min; 3%, 57 min. The flow rate was of 800 µL/min, the scan wavelength was performed between 200 and 600 nm with UV chromatograms recorded at 280 and

360 nm. The ion trap (IT) was equipped with electrospray interface (ESI) under the following conditions: N<sub>2</sub> as nebulizer and drying gas at 350 °C, flow of 11 L/min and pressure of 65 psi; capillary voltage at 4 kV; mass scan (MS) in negative mode in the range of *m/z* 50 – 1000 with target mass of 301; compound stability set at 75%; maximum accumulation time set at 100 ms with 3 MS repetitions for MS average spectra acquisition. The found peaks were compared to authentic reference standards.

Ellagitannins were quantified according to García-Villalba et al. (2015) with modifications. Into Kjeldahl tubes, 1.66 µL of 37% HCl was added to 3.34 µL of PEJ (final concentration 4 mol/L), mixed in vortex, and placed on digester block for 24 h at 90 °C. After returning to room temperature, the mix was transferred to a plastic tube where the pH was adjusted to 2.5 (±0.2) with 4 M HCl and 2.5 M NaOH and then centrifuged at 3000 *g* for 40 min at 4 °C. The supernatant was adjusted to 10 mL with ultra-pure water and filtered through 0.22 µm PDVF filter (Millipore Ltd., Bedford, USA). The pellet was re-extracted with 10 mL of DMSO/MeOH (50/50, v/v), mixed and filtered through 0.22 µm PDVF filter. The hydrolyzed samples were analyzed on an Agilent 1200 HPLC system (Agilent Technologies, Waldbronn, Germany) under the chromatographic conditions described above. The hydrolyzed products were identified by comparison of their retention time and UV spectra with commercial standards or with information disponible in the literature and quantified using a standard ellagic acid curve at 360 nm and a gallic acid curve at 280 nm.

### **3.2. Effect of daily PEJ administration in diet-induced obesity**

#### **3.2.1. Animal and experimental design**

All procedures were approved by Ethical Committee for Animal Research of Faculty of Pharmaceutical Science of University of São Paulo (CEUA/FCF/USP/522). Sixty to seventy 8-weeks-old C57BL/6J male mice were kept at 22 ± 1 °C, under 12 h light-dark cycle and fed with standard diet (NUVILAB CR-1, Nuvital Nutrientes S/A, PR, Brazil) and water *ad libitum* until the beginning of the experiment.

To start the experimental protocol, the animals were randomly distributed in two groups for 14 weeks, as follows: the negative control group, chow group (**CH**), fed with AIN-93M diet (3.8 kcal/g, in which, 13.6% from protein, 10.7% from lipids and 75.7% from carbohydrates) (REEVES; NIELSEN; FAHEY, 1993) and water *ad libitum*, and

the positive control group, HFS group (**HFS**), fed with high-sucrose-fat diet (HFSD) manually prepared according to Lemieux et al. (2003) (4.6 kcal/g, in which 20% from protein, 39% from lipids and 41% from carbohydrates) and water *ad libitum*. After this period, 10 animals per group were euthanized by cardiac puncture under anesthesia (isoflurane). The plasma was separated from blood by centrifugation at 3000 *g* at 4 °C for 20 min, organs and tissues were removed, weighted under constant refrigeration, and stored at – 80 °C for further analysis.

For 14 more weeks, the remaining CH animals were fed with AIN-93M diet and water by daily gavage. The remaining HFS animals were randomly distributed in three groups: the HFS group, fed with the HFSD and water by daily gavage; the lower-dose PEJ group (**PEJ1**), fed with the HFSD and the PEJ at the dose of 50 mg GAE/kg of body weight (BW) by daily gavage; the higher-dose PEJ group (**PEJ2**), fed with the HFSD and the PEJ at the dose of 100 mg GAE/kg BW by daily gavage. At the end of 28<sup>th</sup> week, the animals were euthanized, and the plasma, organs and tissues collected as described above. The **Figure 5** summarizes the experimental protocol.

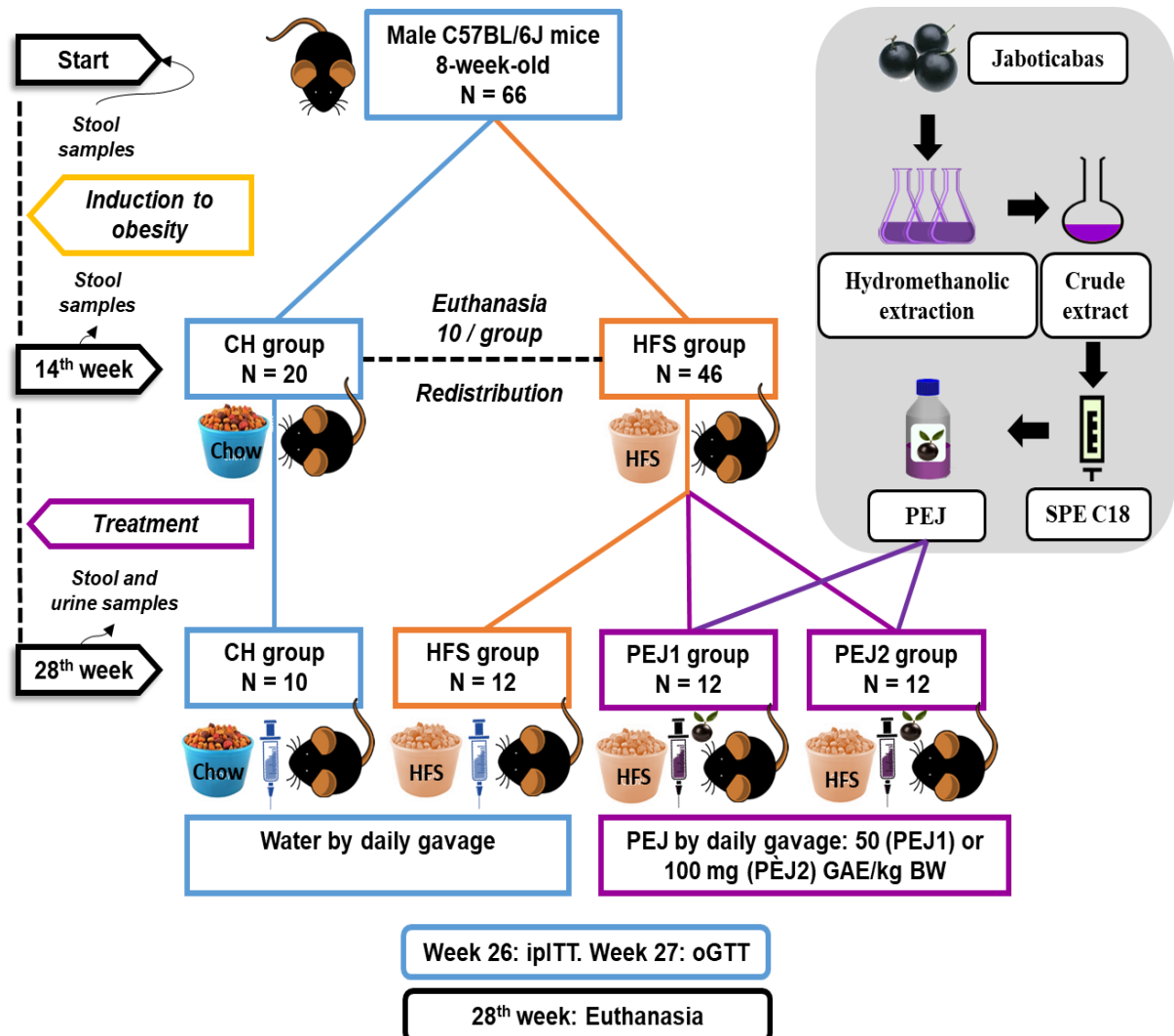
### **3.2.2. Energy intake, body weight and food efficiency**

The body weight and the energy intake were recorded weekly. The food efficiency was calculated as the gain of body weight (g) divided by energy intake (kcal) multiplied by 100, for each animal.

### **3.2.3. Histology of the epididimal white adipose tissue (epWAT)**

Fragments (approx. 100 mg) of the same section of epWAT were placed in 10% formalin at 4 °C for 72 h, transferred to 70% aqueous ethanol for 48 h, embedded in paraffin and cut in sections of approx. 5 µm. After that, these sections were stained with hematoxylin-eosin (H&E) for histological analysis. The area of adipocytes was measured using the software ImageJ2 (National Institute of Health, USA) on images acquired using a microscope Axio Imager 2 with the software AxioVision LE 4.8.2.0 (Carl Zeiss, Jena, Germany) in three different sections and approx. 120 cells per section for each animal. The adipocyte distribution frequency was calculated according to Parlee et al. (2014) with some modifications in objects with area  $\geq 350 \mu\text{m}^2$ , since small objects may be a mixture of adipocytes and stromal vascular cells.

**Figure 5.** Experimental protocol to evaluate the effect of daily gavage administration of the phenolic extract from jaboricaba (PEJ) to mice induced to obesity by a high-fat, high-sucrose diet (HFSD).



SPE: Solid phase extraction. C18: octadecylsilane. GAE: Gallic acid equivalent. BW: body weight. ipITT: Intraperitoneal insulin tolerance test. oGTT: Oral glucose tolerance test.

### 3.2.4. Assessment of inflammatory status

#### 3.2.4.1. Adipokines and cytokine quantification

Concentrations of leptin, resistin, adiponectin, TNF $\alpha$ , IL6, MCP1 and PAI1 were determined in plasma, epWAT and liver by immunofluorescence assay using Milliplex® map kits (MADKMAG-71K and MADPNMAG-70K-01) purchased from Merck-Millipore (Millipore Corporation, Billerica, MA, USA) following the manufacturer's guidelines.

Briefly, plasma samples were analyzed neat and epWAT and liver homogenates were prepared as follows: the tissue (50-100 mg) was homogenized (T10, Ultra-Turrax, IKA, Staufen, Germany) in 500  $\mu$ L of lysis buffer (RIPA lysis buffer, Merck KGaA, Darmstadt, Germany) with protease inhibitor cocktail (Calbiochem – 539191, EMD Millipore corporation, CA, USA) under constant refrigeration. The mixture was centrifuged at 10000 rpm for 60 min at 4 °C for twice (Eppendorf, 5427 R model). The supernatant was carefully collected and stored at – 80 °C for further analysis. For epWAT and liver, the final concentrations were normalized using the total protein content of each sample determined by commercial kit (Pierce BCA, ThermoFisher Scientific, USA).

#### 3.2.4.2. *Western blotting*

In the liver, the phosphorylated and total nuclear factor  $\kappa$ B (pNF- $\kappa$ B and NF- $\kappa$ B) and  $\beta$ -actin were detected in the same portion as follows: the tissue (50-80 mg) was homogenized (T10, Ultra-Turrax, IKA, Staufen, Germany) in lysis buffer (1% Triton-X 100, 100 mM Tris (pH 7.4), pyrophosphate 100 mM sodium fluoride, 10 mM EDTA, 100 mM sodium orthovanadate, 2 mM PMSF and 0.01 mg/mL aprotinin). The mixture was centrifuged at 14000  $g$  (Eppendorf, 5427 R model) at 4 °C for 60 min. The supernatant was carefully collected, and total protein content was determined by a commercial kit (Pierce BCA, ThermoFisher Scientific, Rockford, USA). After denaturation by heating in Laemmli buffer, the proteins were loaded in polyacrylamide gel (Bolt™, 4-12% Bis-Tris Plus gel, ThermoFisher Scientific, Rockford, USA) and automatized dry-transferred to PVDF membranes (iBlot™ 2, gel transfer device, ThermoFisher Scientific, Rockford, USA). The membranes were incubated for 12 h under agitation with primary antibodies against NF- $\kappa$ B and pNF- $\kappa$ B (p65 (Ser536), #3033 and p65 #3987) and  $\beta$ -actin (#3700) (Cell Signaling Technology, Beverly, USA), washed in water, incubated with peroxidase-conjugated secondary antibody for 2-3 h and revealed by chemiluminescence (ECL, GE Healthcare, USA). The software ImageJ2 (National Institute of Health, USA) was used to determine the densitometry of the bands.

### **3.2.5. Analysis related to glucose**

The fasting blood glucose (FBG) was weekly determined, after 4-h fasting, using a glucometer Accu-check Performa (Roche, Mannheim, Germany) from blood of caudal vein. The intraperitoneal insulin tolerance test (ipITT) was performed in the 26<sup>th</sup> week, after 2-h fasting. The insulin (Humulin R, 100 U/mL) was diluted 1000 X in PBS buffer (pH 7.2) previously diluted 10 X in distilled water. The injected volume ( $\mu\text{L}$ ) of the final solution was calculated multiplying the body weight of animal by 10. The glucose concentration was determined as described above in the times 0, 5, 10, 15, 30 and 45 min after the insulin injection and the values were expressed as percentual decay rate per minute ( $k_{\text{ITT}} = 0.693/t_{1/2}$ , where  $t_{1/2}$  was calculated between 5 and 15 min after injection). The oral glucose tolerance test (oGTT) was performed in the 27<sup>th</sup> week, after 4h-fasting. The dose was of 1.0 g of glucose in distilled water/kg BW, administered by gavage. The glucose concentration was determined as described above in times 0, 15, 30, 45 and 90 min after gavage. The plasma insulin concentration was determined in collected blood at 0, 30 and 90 min by ELISA kit (Rat/Mouse Insulin ELISA Kit, Millipore, MA, U.S.A). The insulin resistance homeostatic index (HOMA-IR) was determined by the formula:  $\text{HOMA-IR} = \{[\text{Fasting glucose (mmol/L)}] \times [\text{Fasting insulin } (\mu\text{U/mL})]\} / 22.5$ . The concentrations of total and phosphorylated AKT (AKT1, ser473) and mTOR (mTOR complex 1, ser2448) were determined by Milliplex® map kits (48-611MAG and 48-612MAG) purchased from Merck-Millipore (Millipore Corporation, Billerica, MA, USA) according manufacturer's guidelines as previously described in section 2.2.4.1. The GLUT4 and tubulin expressions were determined in the gastrocnemius muscle as previously described in the section 3.2.4.2 using primary and second antibody purchased from purchased from ThermoFisher Scientific (Rockford, USA) (#MA5-17176) and Cell Signaling Technology (Beverly, USA) (#2146).

### **3.2.6. Analysis related to lipids**

The *in vitro* inhibitory activity of the PEJ on pancreatic lipase (Sigma chemical Co., St. Louis, E.U.A.; 1 mg/mL) was evaluated according to Buchholz & Melzig (2016), using orlistat (PHR1445, Sigma chemical Co., St. Louis, USA 1 mg/mL) as standard. The results were expressed as  $\text{IC}_{50}$  calculated from the equation obtained by

concentration ( $\mu\text{g GAE/mL}$ ) versus percentage of inhibition  $\{\% \text{inhibition} = [(AB - AS)/AB] \times 100$ ; where AB = absorbance of blank, and AS = absorbance of sample}.

The fecal lipid content was determined by Soxhlet in samples collected before starting the experiment and in the 14<sup>th</sup> and 28<sup>th</sup> week, after drying in the oven at 75 °C for 7 h (AOAC 920.39) (AOAC, 2005). The plasma lipid profile (Total-, HDL-, LDL-cholesterols) and triacylglycerol (TAG) was determined using commercial kits according to manufacturer guidelines (LABTEST, Lagoa Santa, MG, Brazil). VLDL cholesterol was calculated by formula TAG/5. The hepatic contents of TC and TAG were quantified according to Hara & Radin (1978), with modifications as follows: in a 2 mL plastic microtube, 50-80 mg of tissue were homogenized (T10, Ultra-Turrax, IKA, Staufen, Germany) for 2 min with 1 mL of hexane/isopropanol (3:2) and shaken for 24 h at 4 °C and 300 rpm (Eppendorf, 5427 R model). The mixture was centrifuged at 1000 g (Eppendorf, 5427 R model) for 15 min and the supernatant quantitatively transferred to an assay tube in which 1.5 mL of sodium sulphate (6.6%) were added. After 15 min decantation, a supernatant aliquot of 200  $\mu\text{L}$  was totally dried under  $\text{N}_2$  e resuspended with 0.5 mL of isopropanol. The hepatic contents of TC and TAG were determined using a commercial kit according to manufacturer's guidelines (LABTEST, Lagoa Santa, MG, Brazil). The non-esterified fatty acid (NEFA) plasma concentration was determined by commercial kit according manufacturer's guidelines (FUJIFILM Wako Chemicals, Neuss, Germany).

### **3.2.7. Analysis related to thermogenesis**

The indirect calorimetry was performed in the last experimental week. Animals were housed in the Comprehensive Animal Laboratory Monitoring System (Oxymax®-CLAMS; Columbus Instruments, Columbus, OH, USA) of the Department of Physiology and Biophysics of the Institute of Biomedical Science, University of São Paulo (SP, Brazil) for 24 h, with an equal period of adaptation, to measure the oxygen consumption ( $\text{VO}_2$ , mL/kg/min), the carbon dioxide production ( $\text{VCO}_2$ , mL/kg/min), respiratory exchange ratio (RER,  $\text{VCO}_2/\text{VO}_2$ ), heat production  $\{\text{kcal/kg/min}; \text{VO}_2 \times [3.815 + (1.232 \times \text{RER})]\}$  and activity (in the x and y planes). The animals had *ad libitum* access to food and water while in cages. The expressions of UCP1 and tubulin were determined in BAT as previously described in the section 3.2.4.2 using primary

and secondary antibody purchased from ThermoFisher Scientific (Rockford, USA) (#PA1-24894) and Cell Signaling Technology (Beverly, USA) (#2146).

### **3.2.8. Statistical analysis**

The statistical analysis was performed using the GraphPad Prism (V8.4.2, GraphPad Prism Software, LLC, San Diego, CA, USA). Initially the data were analyzed regarding the nature of their distribution by the Shapiro-Wilk test. Unpaired *t*-test followed by Welch's test were used for normal distributions or Unpaired *t*-test followed by Mann-Whitney test for non-parametric distributions, and One-way ANOVA followed by Tukey's test to normal distributions or Kruskal-Wallis followed by Dunn's test for non-parametric distributions.

### **3.2.9. Metagenomic analysis**

Feces were collected before the experiment and at the 14<sup>th</sup> and 28<sup>th</sup> week in sterile tubes and stored at – 80 °C. DNA extraction from samples was carried out using the QIAmp DNA Stool Mini Kit (Qiagen, HiLDen, Germany) in total accordance with the instructions and stored at – 20 °C until utilization. The DNA concentration was measured by fluorometry (Qubit 4 fluorometer, Thermo Fisher Scientific Inc., Carlsbad, CA, USA). The fecal microbiome characterization was done from amplification of the 16S rRNA ribosomal bacterial segment in the V4 domain with V4 forward (5' – TCG TCG GCA GCC AGT GAT GTG TAT AAG AGA CAG GTG CCA GCM GCC GCG GT – 3') and reverse (5' – GTC TCG TGG GCT CGG AGA TGT GTA TAA GAG ACA GGG ACT ACH VGG GTW TCT AAT – 3') primers. The 16S metagenomic sequencing library preparation was carried out according to the manufacturer protocol (ILLUMINA, 2013). The PCR reaction mix contains 2.5 µL Buffer II, 5 µL forward and reverse primer, 0.2 µL Taq DNA polymerase, 2.5 µL sample (at 5 ng/mL DNA concentration), and sterile water to 25 µL (AccuPrime™ Taq DNA Polymerase System, Thermo Fisher Scientific Inc., Carlsbad, CA, USA). The PCR amplification was performed under the following conditions: 95 °C for 3 min, followed by 25 cycles of 95 °C for 30 s, 55 °C for 30 s and 72 °C for 5 min using the Veriti™ 96-well Thermal Cycler (Thermo Fisher Scientific Inc., Carlsbad, CA, USA). The PCR products were purified by magnetic

beads following the instructions of the PCR Purification AMPure XP kit (Agencourt, Beckmann-Coulter, USA). Then the purified PCR products were indexed and connected to sequencing adapters using the Nextera XT Index Kit V2 (Illumina, San Diego, CA, USA). After that, the PCR fragment containing 250 bp came to have 412 bp. A new PCR reaction was performed using a solution containing 5  $\mu$ L Buffer II, 5  $\mu$ L forward and reverse primer, 1.3  $\mu$ L Taq DNA polymerase, 5  $\mu$ L samples, and sterile water to 50  $\mu$ L (AccuPrime™ Taq DNA Polymerase System, Thermo Fisher Scientific Inc., Carlsbad, CA, USA). The PCR conditions were the following: 95 °C for 3 min, 8 cycles at 95 °C for 30 s, 55 °C for 30 s, 72 °C for 30 s, 72 °C for 5 min, using the same equipment described above. A new purification step was performed using the kit described above. After each PCR reaction and purification, 1% agarose gel electrophoresis was utilized to verify the length of DNA fragment. The final DNA concentration was remeasured by fluorometry as previously described, and the samples concentrations were adjusted to 4 nmol/L. The final pooled library was sequenced using the Miseq Reagent Kit V2 500 cycles (Illumina, San Diego, CA, USA) in a Illumina® Miseq equipment by Core Facility for Scientific Research – University of Sao Paulo (CEFAP/USP) using a 20% PhiX as internal control.

The sequencing results were assessed using the software QIIME2 (Quantitative Insights into Microbial Ecology, V2020.2, <https://qiime2.org/>). QIIME2 was used to align and filter sequences, identify and filter chimeric sequences, construct the operational taxonomic units (OTU) and the phylogenetic tree, and obtain the diversity metrics and statistics to the microbial community. The used pipeline is described in QIIME2 docs (Moving Pictures tutorial) changing the import step to CASAVA 1.8.2 files and adding one step more related to the chimeric analysis with q2-vsearch (QIIME2, 2020). The final sequences were grouped in OTU with 97% similarity against GreenGenes data bank 13.8 according to the QIIME2 instructions (QIIME2, 2020). Graphics and related statistics were performed using the softwares OriginLab (V2020, Originlab corp., Northampton, MA, USA), GraphPad Prism (V8.4.2, GraphPad Prism Software, LLC, San Diego, CA, USA).

### **3.2.10. Untargeted metabolomic analysis**

The untargeted metabolomic was performed at Research Group on Quality, Safety and Bioactivity of Plant Foods (CEBAS-CSIC, Murcia, Spain) in urine samples collected through metabolic cages. The animals were placed in the cages with water and food *ad libitum* and the samples were collected 12 h after the gavage of the PEJ at the dose of 100 mg GAE/kg BW, dried under vacuum and stored at – 80 °C. The metabolites were extracted from urine according to García et al. (2018) with slight modifications. Dried samples were mixed with 1 mL of MeOH and filtered through 0.22 µm PTFE membranes then analyzed by ultraperformance liquid chromatography coupled with electrospray ionization tandem quadrupole time-of-flight mass spectrometry (UPLC-ESI-QTOF). The chromatographic system was an UPLC Agilent 1290 Infinity (Agilent Technologies, WaLDbrohn, Germany) coupled to a mass QTOF detector (6550 Accurate, Agilent) with ESI technology and a C18 column (Poroshell 120, 3 x 100 mm, 2.7 µm pore size). The chromatography and spectrometry conditions were the following: mobile phases of water with 0.1% formic (A) and acetonitrile with 0.1% formic acid (B) at a flow rate of 0.4 mL/min. N<sub>2</sub> was used as nebulizer and drying gas (35 psi, 9 L/min and 280 °C, 9 L/min, respectively). The range *m/z* to acquisition of spectra was of 100-1100 in negative mode using 100 V to produce the fragments with an acquisition rate of 1.5 spectra/s and target mass between 50 and 800 *m/z*.

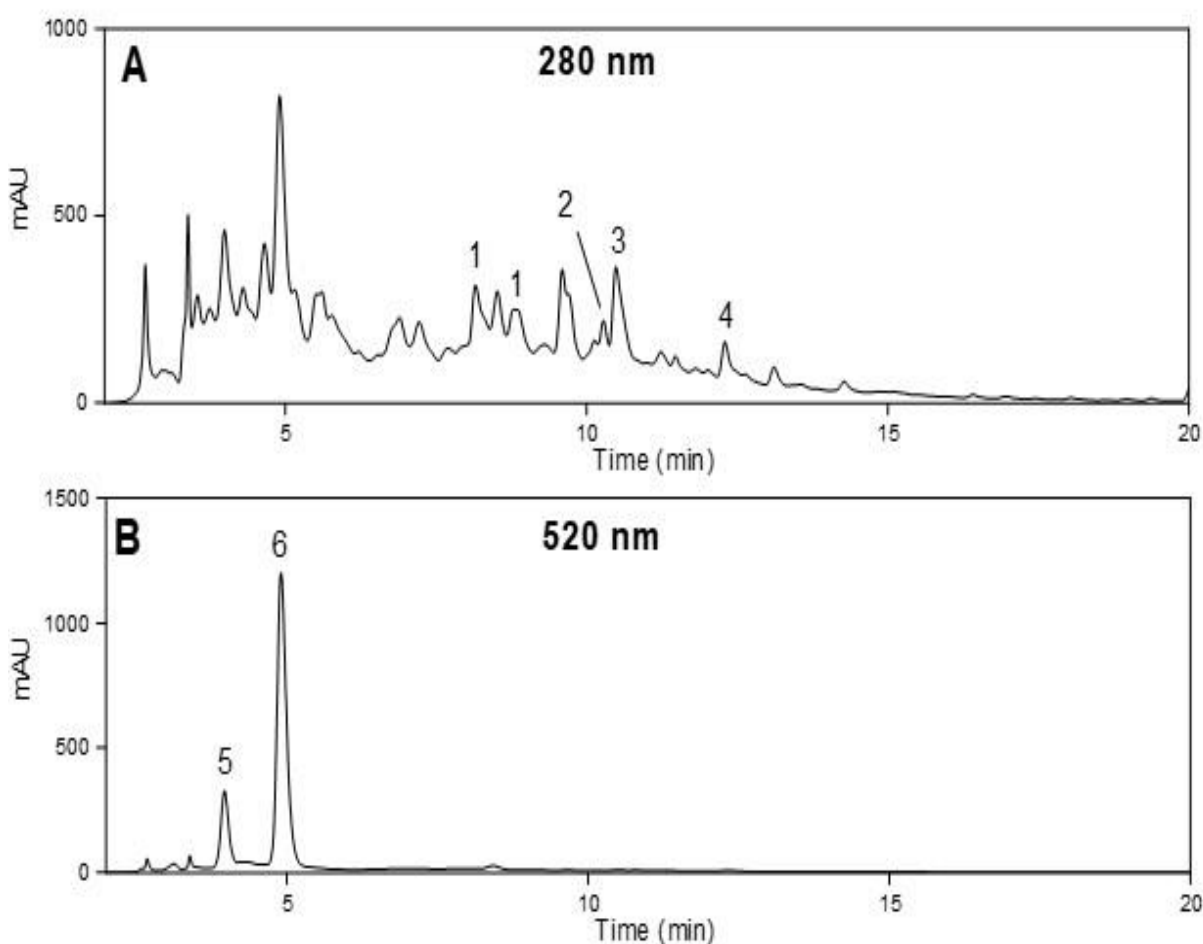
Raw data were initially processed with the Agilent Mass Hunter Qualitative software according to the Molecular Feature Extraction (MFE) algorithm previously configured with the appropriated information about retention time, *m/z* range, and filters to peaks, masses, and ions. After that, the data were treated by the Mass Profiler Professional software, producing a global entities matrix. The softwares SIMCA (Umea, Sweden) and MetaboAnalyst (Xia Lab, v4.0, Canada) were also used.

## 4. Results and discussion

### 4.1. Chemical characterization of the PEJ

The PEJ was obtained by SPE using C18 as adsorbent, being rich in both types of phenolic compounds, flavonoids, and non-flavonoids, i.e., phenolic acids and tannins. The chemical characterization through HPLC-DAD tentatively identified five compounds, two anthocyanidin glucosides (delphinidin and cyanidin), two flavonol glucosides (myricetin and quercetin) and one phenolic acid, ellagic acid (**Figure 6**).

**Figure 6.** Chromatogram at 280 (A) and 520 nm (B) obtained through HPLC-DAD of the phenolic extract from jaboticaba (PEJ).



1 – Ellagic acid derivatives. 2 – Myricetin 3-O-rhamnoside (Myricitrin). 3 – Ellagic acid. 4 – Quercetin 3-O-rhamnoside (Quercitrin). 5 – Delphinidin 3-O-glucoside (Myrtillin). 6 – Cyanidin 3-O-glucoside (Kuromanin).

The PEJ was also characterized in relation to the total content of phenolics and proanthocyanidins, and total and free ellagic acid (ellagitannins by difference). The main compounds found in the PEJ were ellagitannins (approx. 40%) followed by anthocyanins (approx. 10%), proanthocyanidins (less than 5%), free ellagic acid (less than 3%) and much smaller quantities of myricetin and quercetin (approx. 0.5% each) (**Table 1**). With few exceptions, all these compounds have already been reported in 'jaboticaba (INADA et al., 2020; MOURA et al., 2018; PEREIRA et al., 2017; PLAZA et al., 2016; QUATRIN et al., 2019; SILVA et al., 2016).

**Table 1.** Chemical characterization of the phenolic extract from jaboticaba (PEJ).

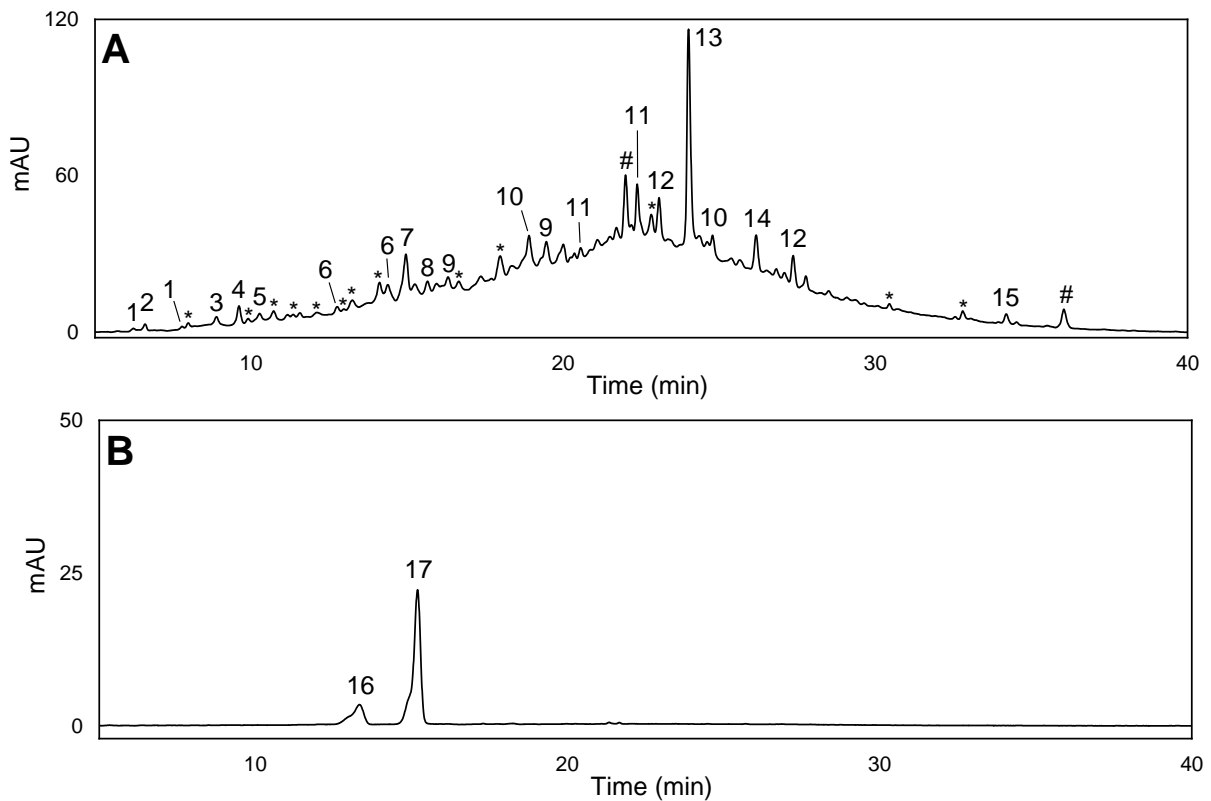
Total phenolics ( $\mu\text{g}$ GAE/mL)	11450 $\pm$ 370
Proanthocyanidins ( $\mu\text{g}$ PB2/mL)	663 $\pm$ 11
Flavonoids, phenolic acids, and derivatives ( $\mu\text{g}$ /mL)	
<i>Delphinidin 3-O-glucoside</i> *	294 $\pm$ 14
<i>Cyanidin 3-O-glucoside</i> *	800 $\pm$ 5
<i>Myricetin 3-O-rhamnoside</i> *	26 $\pm$ 1
<i>Quercetin 3-O-rhamnoside</i> *	32 $\pm$ 4
<i>Total ellagic acid (TEA)</i>	4508 $\pm$ 15
<i>Free ellagic acid (FEA)</i>	133 $\pm$ 12
<i>Ellagitannins</i> #	4374 $\pm$ 24

Results are expressed as mean  $\pm$  SD. ( $n = 3$ ). GAE: gallic acid equivalent. PB2: proanthocyanidin B2. #Calculated by difference: TEA – FEA. \*commercial standard myrtillin, kuromanin, myricitrin, quercitrin, respectively.

Except for myricetin 3-O-rhamnoside, all other compounds previously quantified and tentatively identified by HPLC-DAD had their chemical structure confirmed by mass spectrometry (HPLC-DAD-IT MS/MS). In addition, 12 more phenolic compounds were tentatively identified, totaling 17: 4 flavonoids, 3 phenolic acid, 3 ellagic acid glucosides and 7 tannins, totalizing 17, and highlighted the large amount of ellagitannins present in the extract (**Figure 7**).

The fragmentation pattern is shown in **Table 2** below. The identification was performed by comparison between the fragments of the molecular ions on the data bases (MassBank, ReSpect, Metlin) and in the literature. Some compounds were identified through of the comparison of their retention times (RT) and UV spectra with commercial standards.

**Figure 7.** Chromatogram at 280 (A) and 520 nm (B) obtained through HPLC-DAD-IT MS/MS of the phenolic extract from jaboticaba (PEJ).



1 – Punicalcortein. 2 – Gallic acid. 3 – Pedunculagin. 4 – Galloyl-punicalin. 5 – Protocatechuic acid. 6 – Galloyl-Bis-HHDP-glucose. 7 – Casuarictin. 8 – Galloyl-methyl-gallate. 9 – Tellimagrandin I. 10 – Ellagic acid hexoside. 11 – Ellagic acid pentoside. 12 – Ellagic acid rhamnoside. 13 – Ellagic acid. 14 – Quercetin 3-O-rhamnoside. 15 – Quercetin. 16 – Delphinidin 3-O-glucoside. 17 – Cyanidin 3-O-glucoside. \*Not identified ellagitannins. #Not identified compounds.

In relation to tannins, two punicalcortein isomers ( $m/z$  633,  $C_{27}H_{21}O_{18}$ ), RT 6.3 and 7.8 min, were tentatively identified. In addition to pomegranate (*Punica granatum* L.), in which four punicalcortein isomers, A, B, C and D, were identified, these ellagitannins are also present in blackberry (*Rubus fruticosus* L.), chestnut shells (*Castanea sativa* Mill. (Fagaceae)), and in the black myrobalan (*Terminalia chebula* Retz), an important fruit in the Indian traditional medicine (CERULLI et al., 2020; CLIFFORD; SCALBERT, 2000; KITRYTĚ et al., 2020; LEE et al., 2017). Pedunculagin ( $m/z$  783, Bis-hexahydroxydiphenoyl (HHDP)-glucose,  $C_{34}H_{24}O_{22}$ ), galloyl-punicalin ( $m/z$  933, 2-O-galloylpunicalin,  $C_{41}H_{26}O_{26}$ ), trisgalloyl HHDP glucose isomer ( $m/z$  951,  $C_{41}H_{28}O_{27}$ ), casuarictin ( $m/z$  935, Bis-HHDP-galloylglucose,  $C_{41}H_{27}O_{26}$ ), galloyl methyl gallate ( $m/z$  335,  $C_{15}H_{11}O_9$ ) and tellimagrandin I ( $m/z$  785, HHDP-digalloylglucose,  $C_{34}H_{25}O_{22}$ ), RT 9.0, 9.6, 12.9/14.1, 15.6, 16.3/19.6, respectively, were also tentatively identified.

**Table 2.** Tentative identification of polyphenols found in the phenolic extract from jaboticaba (PEJ) by HPLC-DAD-IT MS/MS.

#	Compound	RT	UV (nm)	[M-H] <sup>-</sup>
1	Punicacortein	6.3; 7.9	236	<b>633</b> : 301, 275, 249
2	Gallic acid	6.6	236	<b>169</b> :125
3	Pedunculagin	9.0	236, 278	<b>783</b> : 301, 484, 275
4	Galloyl-punicalin	9.6	236, 282	<b>933</b> : 631, 915, 897
5	Protocatechuic acid	10.4	nd	<b>153</b> : 109
6	Trisgalloyl HHDP glucose	12.9; 14.5	238, 278	<b>951</b> : 907, 783
7	Casuarictin	15.1	238, 280	<b>935</b> : 633, 571, 329
8	Galloyl-methyl-gallate	15.6	238, 276	<b>335</b> : 183, 169, 165
9	Tellimagrandin I	16.3; 19.6	240, 270	<b>785</b> : 301, 483, 765
10	Ellagic acid hexoside	19.0; 24.8	242, 294,	<b>463</b> : 301
11	Ellagic acid pentoside	20.4; 22.5	250, 294,	<b>433</b> : 300, 301, 302
12	Ellagic acid rhamnoside	23.2; 27.2	246, 360	<b>447</b> : 300
13	Free ellagic acid	24.1	252, 366	<b>301</b> : 228, 257, 185
14	Quercetin 3-O-rhamnoside	27.2	252, 350	<b>447</b> : 301, 179
15	Free quercetin	34.4	252, 370	<b>301</b> : 151, 179, 255
16	Delphinidin 3-O-glucoside	13.4	238, 274,	<b>463</b> : 301, 300, 337
17	Cyanidin 3-O-glucoside	15.3	238, 278,	<b>447</b> : 285

Values in bold are the molecular ions. nd: not determined.

Galloyl-punicalin is a ellagitannin commonly reported in the fruit and in the heartwood from pomegranate, and galloyl-methyl-gallate is a gallotannin found in acorns of Kermes oak (*Quercus coccifera*), a small evergreen shrub found in Mediterranean countries, (MOLINA-GARCÍA et al., 2018). It is worth noting that although the fragmentation patterns of punicacortein, galloyl-punicalin and galloyl-methyl-gallate correspond to those found in the literature.

Three phenolic acids were tentatively identified in the RT 6.7, 10.3 and 24.1 min, respectively: gallic acid ( $m/z$  169, C<sub>7</sub>H<sub>6</sub>O<sub>5</sub>), protocatechuic acid ( $m/z$  153, C<sub>7</sub>H<sub>6</sub>O<sub>4</sub>) and ellagic acid ( $m/z$  301, C<sub>14</sub>H<sub>6</sub>O<sub>8</sub>). This was preceded by three of its glycosidic derivatives, i.e., pentoside, hexoside and rhamnoside in the RT 19.0, 22.5, 23.2 min, respectively. In contrast to preliminary chemical characterization shown in **Table 1**,

ramnoside of myricetin was not identified and free quercetin was identified in RT 34.4 min. In the wavelength 520 nm, the anthocyanins delphinidin 3-O-glucoside ( $m/z$  463,  $C_{21}H_{21}O_{12}$ ) and cyanidin 3-O-glucoside ( $m/z$  301,  $C_{21}H_{21}O_{11}$ ) were identified in RT 13.4 and 15.3 min, respectively. With few exceptions, all these compounds have already been reported in jaboticaba (INADA et al., 2020; MOURA et al., 2018; PEREIRA et al., 2017; PLAZA et al., 2016; QUATRIN et al., 2019; SILVA et al., 2016).

Depending on their chemical structure, the tannins are classified in non-hydrolysable and hydrolysable tannins. Hydrolysables, in turn, are classified in two groups: gallotannins or gallic tannins and ellagitannins or ellagic tannins. In gallic tannins, the hydrolysis of the galloyl groups releases gallic acid, and in ellagic tannins, the HHDP groups when hydrolyzed rearrange into ellagic acid (BRESCIANI et al., 2017; CLIFFORD; SCALBERT, 2000). **Figure 8** shows the chromatographic profile of the supernatant and precipitated (pellet) of the PEJ after acid hydrolysis at 280 and 360 nm, and **Table 3** their quantification.

**Figure 8.** Chromatogram at 280 and 360 nm obtained through HPLC-DAD of the phenolic extract from jaboticaba (PEJ) after acid hydrolysis in the supernatant (**A**) and precipitated (pellet) (**B**).

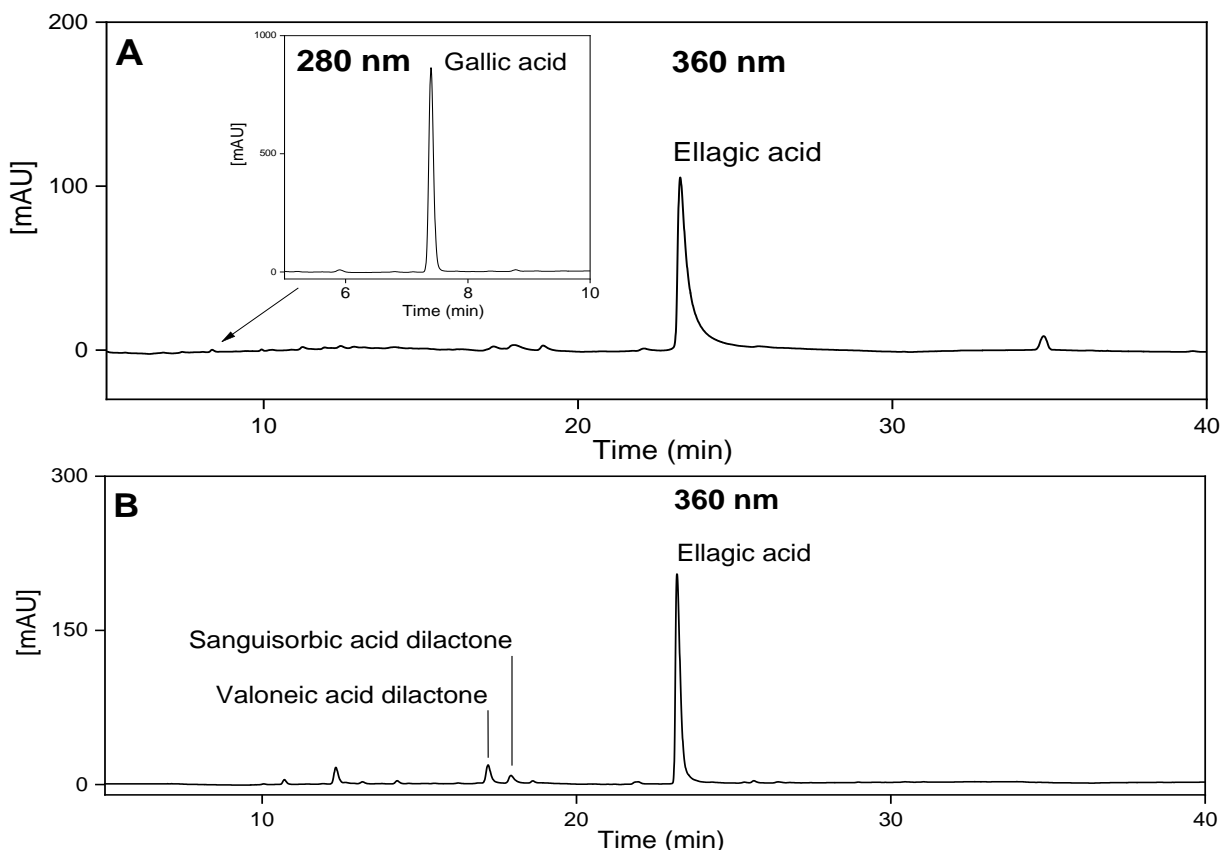


**Table 3.** Ellagitannin and gallotannin quantification of the phenolic extract from jaboticaba (PEJ) administered to the animals.

	$\mu\text{g/mL}$	PEJ1 ( $\mu\text{g/kg/day}$ )	PEJ2 ( $\mu\text{g/kg/day}$ )
Gallic acid	$357 \pm 50$	$51 \pm 4$	$97.5 \pm 7.5$
Ellagic acid	$660 \pm 60$	$93 \pm 7$	$180 \pm 15$
Valoneic acid dilactone	$46.5 \pm 3.5$	$6.5 \pm 0.5$	$12.5 \pm 1$
Sanguisorbic acid dilactone	$23 \pm 2$	$3.3 \pm 0.5$	$6.3 \pm 0.5$

The main identified and quantified compounds were gallic acid, ellagic acid and dilactones of the valoneic and sanguisorbic acids. A similar chromatographic profile was previously reported for pomegranate with the presence of these isomeric dilactones indicate galloyl groups linked to esters of HHDP belonging to structurally complex ellagitannins (GARCÍA-VILLALBA et al., 2015).

#### 4.2. Effect of daily administration of the PEJ against obesity

The potential health benefits of the PEJ were assessed through daily administration of two doses, namely 50 (PEJ1) and 100 (PEJ2) mg GAE/kg BW, for 14 weeks to obese C57BL/6J mice. These doses were based in previous studies performed by ALEZANDRO et al. (2013) and MOURA et al. (2018) showing that phenolic compounds from Sabara jaboticaba efficiently decreased oxidative stress and hyperlipidemia, prevented the excessive gain of body weight and WAT, and decreased hyperglycemia and IR in a diet-induced obesity model.

According to **Table 3**, the PEJ1 animals received approx. 103  $\mu\text{g/kg}$  of ellagitannins (PEJ2 animals the double). In terms of human consumption, these concentrations represent between 223 and 446 mg/kg/day, close to the estimated consumption for the adult Brazilian population, of  $378 \pm 15$  mg/day (MIRANDA et al., 2016). In this way, PEJ was administered to obese mice in doses equivalent to daily human consumption.

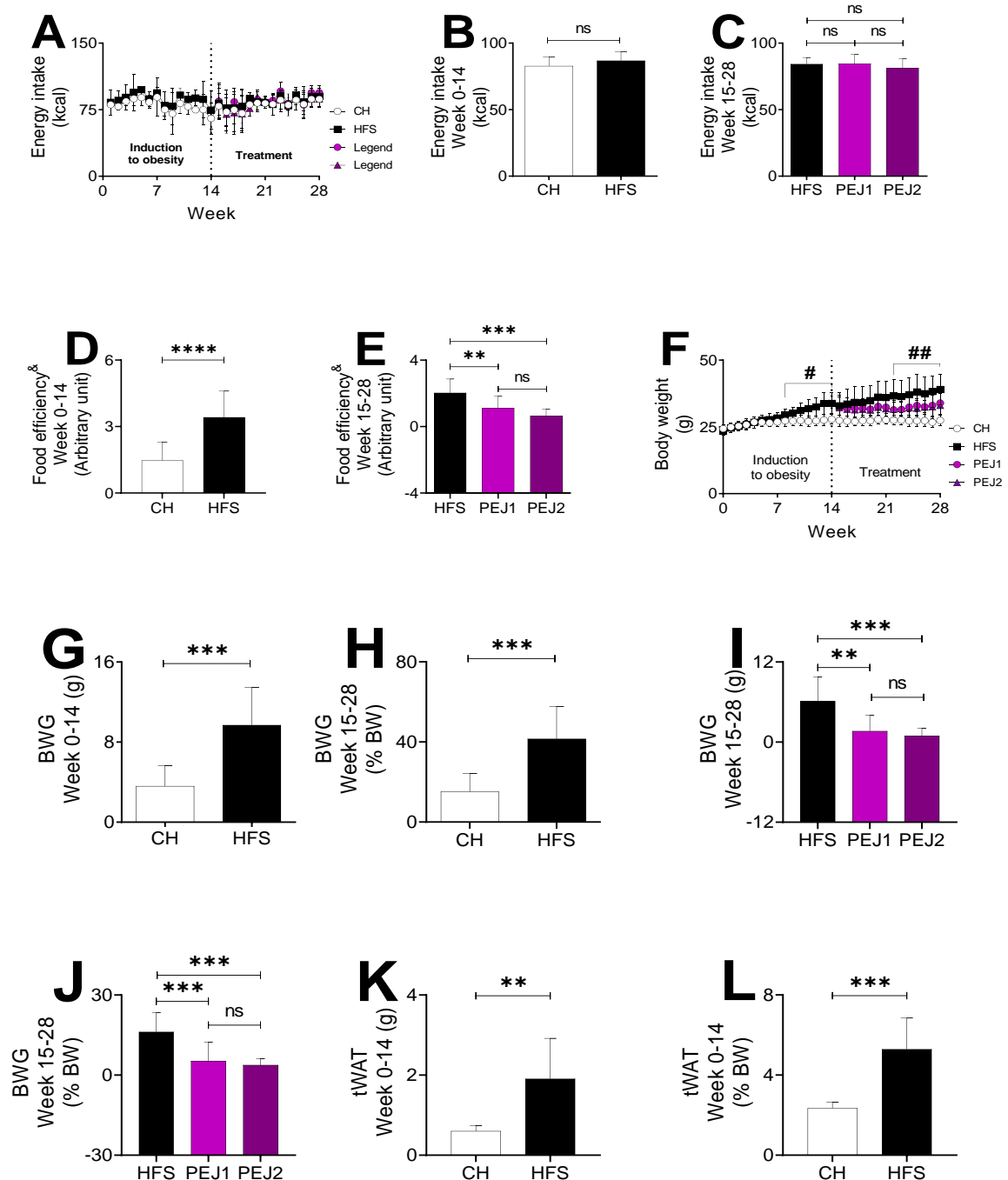
#### **4.2.1. Energy intake, food efficiency, body weight gain, adiposity, and adipocyte hypertrophy**

Twice a week the feed was weighed and converted to energy, according to values previously explained in section 2.2.1 (AIN93M = 3.8 kcal/g or HFSD = 4.6 kcal/g). There was no statistical difference in energy intake among the groups in any experimental stages, that is, neither during the first stage (week 0-14), called induction to obesity, nor during the last stage (week 15-28), called treatment (**Figures 9A, B and C**). Studies have reported that phenolic compounds can act as appetite suppressants, by modulation of hormone pathways related to center of appetite in hypothalamus (XIE et al., 2018). Although the PEJ is a phenolic-rich extract, there was no decrease in energy intake of treated groups, suggesting, therefore, that phenolic compounds from jaboticaba did not suppress appetite of the animals.

Despite these similar values for energy intake, the HFS group showed food efficiency statistically higher than the CH group in the first stage (approx. 57%), and higher than the supplemented groups in the last stage (approx. 45% and 69% vs. PEJ1 and PEJ2 respectively) (**Figures 9D and E**). These values showed that the HFS animals were more efficient in converting energy in body weight. The absolute and relative body weight gain (BWG) are shown in **Figures 9F – 9J**. In the first 14 weeks, from the 7<sup>th</sup> week the HFS animals showed BW statistically higher than the CH animals. To both average values, absolute and relative, the BWG of the HFS group was more than double that of the CH group (9.7 vs. 3.6 g and 41.5 vs. 15.2%, respectively) (**Figures 9G and H**).

In the treatment stage, the groups that received the PEJ showed absolute and relative BWG statistically lower than HFS group after seven weeks of treatment, in the 22<sup>nd</sup> experimental week. At the end of this period, both PEJ groups presented absolute BWG equal to 1.6 and 0.9 g, respectively, and relative BWG equal to 5.3 and 3.8%, respectively, while these values for the HFS group were 6.2 g and 16.2%, therefore exceeding the supplemented groups in almost four times (**Figures 9I and J**). However, after 14 weeks of PEJ administration, no statistically significant difference was observed between the initial and final means of body weights neither in the PEJ1 group nor in the PEJ2 group ( $p = 0.3310$  and  $p = 0.6398$ , respectively). These results showed that phenolic compounds from jaboticaba, regardless the administered dose, did not revert but prevented the excessive BWG even in animals with already established

**Figure 9.** Energy intake (**A, B, C**), food efficiency (**D, E**), body weight, absolute and relative body weight gain (BWG) (**F – J**) and absolute and relative weight of total white adipose tissue (WAT) (**K, L**) of mice fed with chow diet and water (CH), high-fat-sucrose diet (HFSD) and water (HFS), HFSD and phenolic extract from jaboticaba (PEJ) at the dose of 50 mg gallic acid equivalent (GAE)/kg of body weight (BW) (PEJ1) by daily gavage and HFSD and PEJ at the dose of 100 mg GAE/kg BW (PEJ2) by daily gavage.



Values are mean  $\pm$  standard deviation.  $n = 12-46/\text{group}$ . n.s.: not significant. \* $p < 0.05$ , \*\* $p < 0.01$ , \*\*\* $p < 0.001$  or  $< 0.0001$ . 8B, D, G, H and L: unpaired  $t$  test with Welch's correction. 8C, E, I and J: One-way ANOVA with Tukey's test. &Calculated as: [Gain of body weight (g)/Energy intake (kcal)]. #CH vs HFS ( $p < 0.005$ ). ##HFS vs PEJ1 and PEJ2 ( $p < 0.005$ ). Kruskal-Wallis with Dunn's test. 9F and 9G:  $n = 10/\text{group}$ ; Unpaired  $t$  test with Welch's correction.

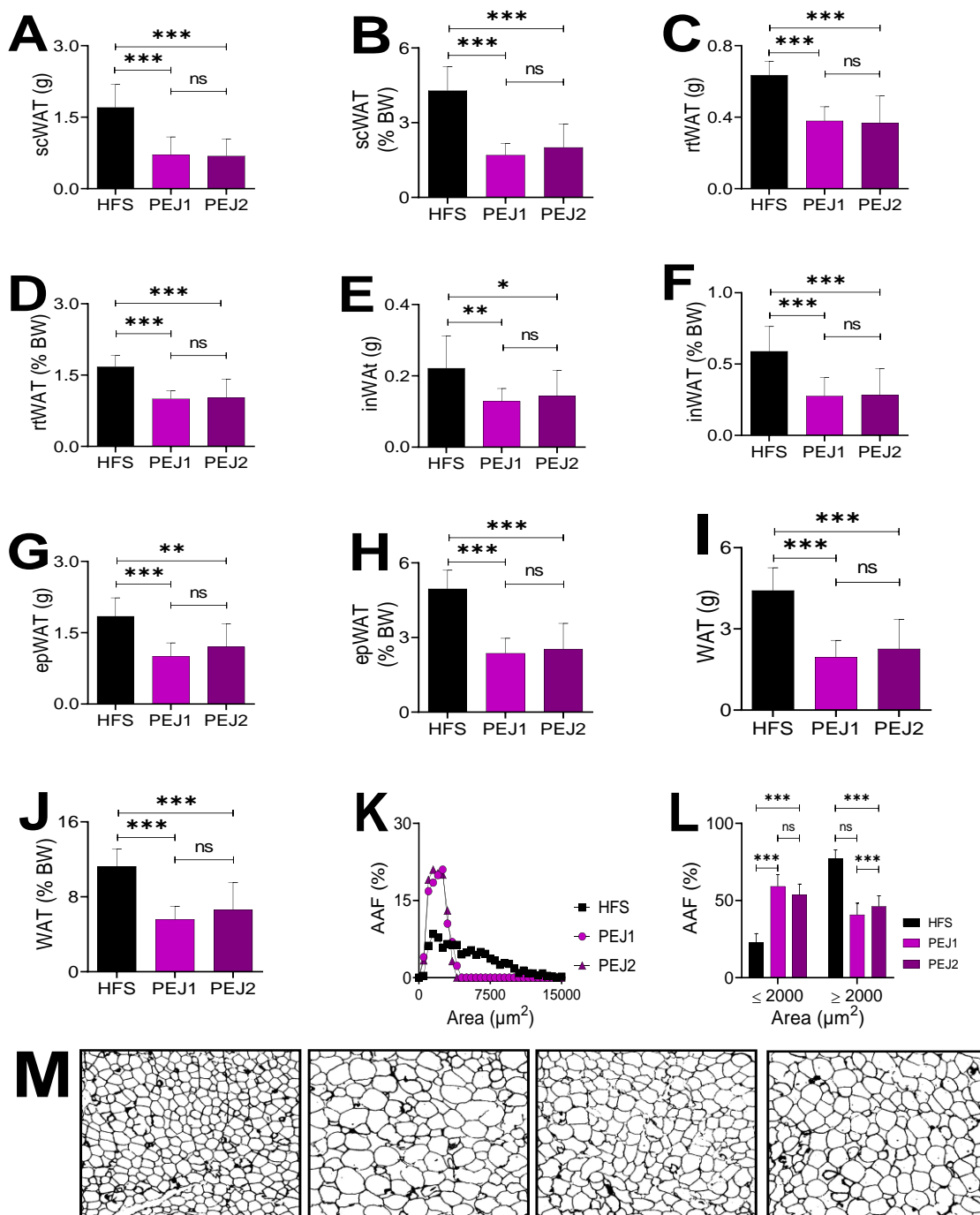
obesity, thus having preventive anti-obesogenic properties, as previously reported (MOURA et al., 2018).

At the end of the 14<sup>th</sup> week, ten animals of each group were euthanized according to conditions previously described in section 3.2.1. From this procedure, the absolute and relative weights of the total white adipose tissue (WAT), which is the sum of the subcutaneous, retroperitoneal, inguinal and epididymal WAT, were determined (**Figures 9K end L**). The values of both WAT, absolute and relative, of the HFS group exceed in more than twice the values of the CH group (1.9 g and 5.3% vs. 0.6 g and 2.3% respectively). BWG and WAT gain confirm that the HFSD efficiently induced obesity with a marked WAT gain during the initial 14 weeks, validating this animal model (HARIRI; THIBAUT, 2010).

At the end of the experiment, the animals were properly euthanized as described in the section 3.2.1 and their organs and tissues were collected. The absolute and relative average weights of subcutaneous (sc), retroperitoneal (rt), inguinal (ig), epididymal (ep) and total (t) WAT are presented in **Figure 10**. The HFS group showed all WAT weights statistically higher than the supplemented groups. Proportionately, the averages of the HFS group surpassed those of the PEJ1 and PEJ2 groups at approx. 61 and 53% for the scWAT, 40 and 37% for the rtWAT, 53 and 52% for the igWAT, 52 and 49% for the epWAT, and 50 and 41% for the WAT, respectively. In general, the PEJ1 group had lower average WAT gain than the PEJ2 group, however without statistical difference among them (**Figures 10A – 10J**).

The WAT growth occurs through hyperplasia (number) and/or hypertrophy (size). Thus, in addition to the absolute and relative WAT weights, a histomorphometry analysis was performed to deepen the understanding of the diet-induced WAT remodeling. The distribution of adipocyte areas (**Figures 10K and 10L**) shows that the PEJ1 and PEJ2 groups had WAT mostly composed by small adipocytes, with mean area below 2000  $\mu\text{m}^2$  (60% and 53% respectively), while the HFS group had higher number of adipocytes with mean area above 2000  $\mu\text{m}^2$  (77%). In both measures, there was marked statistical difference between the supplemented groups and the HFS group ( $p = 0.0001$  for both). The representative **Figure 10M** make evident the difference in adipocyte size among groups and show that the adipose composition of the PEJ1 and PEJ2 groups was more similar to the CH group, with smaller adipocytes than the HFS group. The PEJ1 cells were a little less hypertrophied than the PEJ2 cells.

**Figure 10.** Absolute and relative weights of subcutaneous (sc), retroperitoneal (rt), inguinal (ig), epididymal (ep) and total white adipose tissue (WAT) (**A – J**), distribution of adipocyte areas frequency (AAF) (**K and L**) and representative H&E stained of epWAT (**M**) of mice fed with chow diet and water (CH), high-fat-sucrose diet (HFSD) and water (HFS), HFSD and phenolic extract from jaboticaba (PEJ) at the dose of 50 mg gallic acid equivalent (GAE)/kg of body weight (BW) (PEJ1) by daily gavage and HFSD and PEJ at the dose of 100 mg GAE/kg BW (PEJ2) by daily gavage.



Values are mean  $\pm$  standard deviation. N = 6 - 10/group. n.s.: not significant. \* $p < 0.05$ , \*\* $p < 0.01$ , \*\*\* $p < 0.001$  or  $< 0.0001$ . All: One-way ANOVA with Tukey's test.

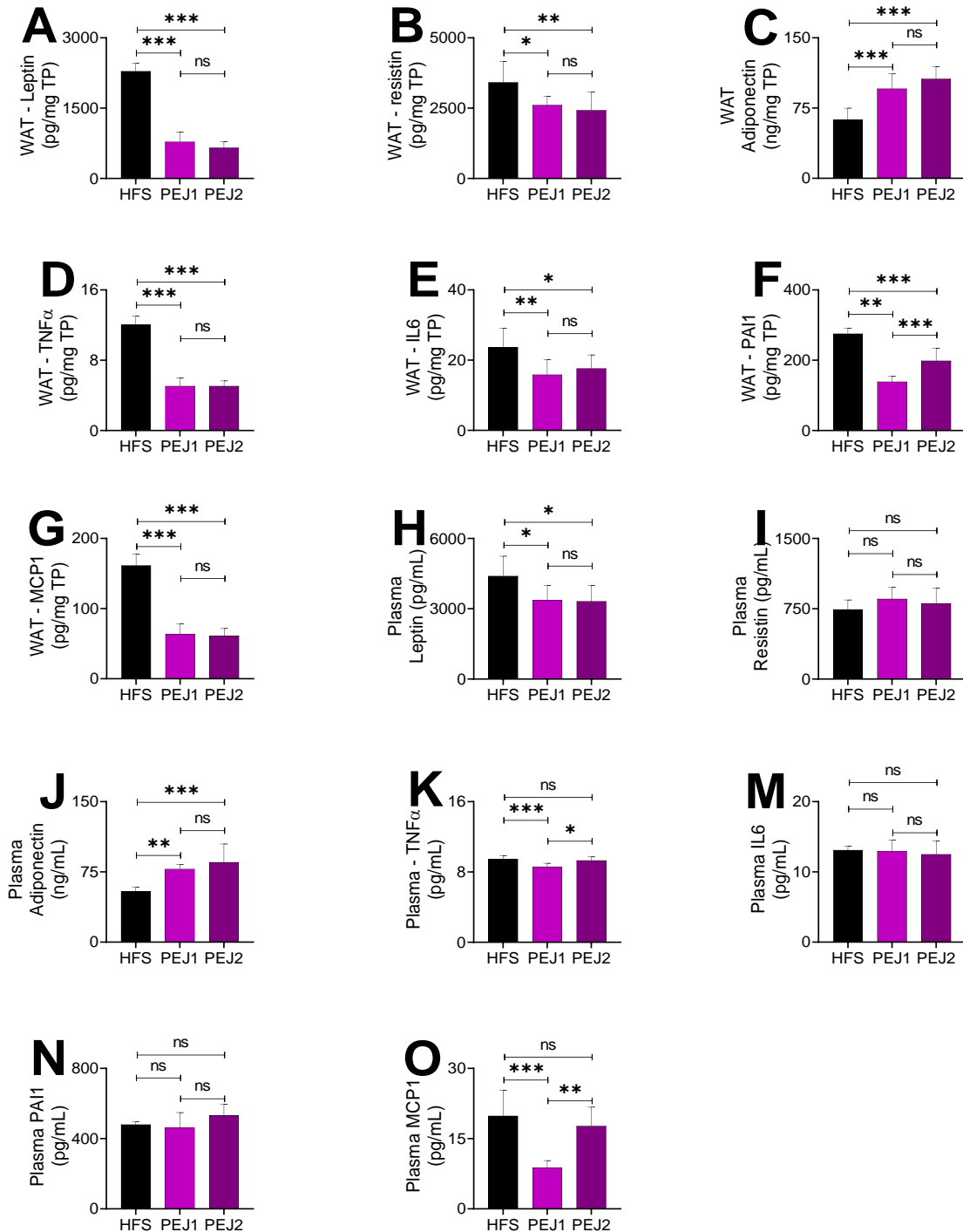
Under obesity, adipose tissue is mostly composed by hypertrophic adipocytes overburdened with lipids. This condition leads to a pathologically change in adipose tissue, resulting in a dysfunctional condition called adiposopathy. Adiposopathy is linked to several metabolic comorbidities, since adipocytes have become large producer of proinflammatory cytokines resulting in local inflammation. Additionally, the lipids non-stored into adipocytes reach other organs, such as liver, muscle and pancreas where become ectopic deposits. Together, overproduction of proinflammatory cytokines and ectopic lipid storage trigger systemic IR and hyperinsulinemia, the T2D pathologic basis. When the storage capacity of adipocytes is exceeded, precursor stem cells differentiate in mature adipocytes. This process is called adipogenesis and results in adipocyte hyperplasia. The hyperplasia inhibition is suggested for many authors as a strategy to prevent adipose tissue growth and consequently obesity. However, on the other hand, an enhanced adipogenesis may contribute with non-hypertrophic adipocytes, fighting the adiposopathy, ectopic fat deposition and IR (PARLEE et al., 2014; PERDICARO et al., 2020).

Studies report that phenolic compounds prevent diet-induced adipocyte hypertrophy. Decreased inflammation-related genes, with lower production of pro-inflammatory adipokines, was reported in C57BL/6J mice fed for 9 weeks with gallic acid-supplemented HFSD. In addition, their WAT adipocyte areas were reduced (TANAKA et al., 2020). In another similar study, Sprague Dawley rats fed for 6 weeks with quercetin-supplemented HF diet had their WAT adipocyte areas reduced without, however, reducing WAT gain. The authors positively associated these results to increased expression of proteins involved in adipogenesis/angiogenesis and adipocyte maturation (PERDICARO et al., 2020).

#### **4.2.2. Inflammation**

The adipose tissue has a key role in systemic inflammatory processes. The way in which it expands, that is, as occur its remodeling, is linked to lower or higher plasma release of adipocyte factors as peptide hormones, such as leptin, resistin, adiponectin, and pro-inflammatory cytokines, such as TNF $\alpha$ , IL6, PAI1, MCP1, among others (NELSON; COX, 2014). Concentrations of these proteins in the WAT are shown in the **Figure 11**. Excepting the adiponectin values, the HFS group presented values statistically higher than the PEJ1 and PEJ2 groups for leptin, resistin, TNF $\alpha$ , IL6, MCP1

**Figure 11.** Cytokine concentrations in the epididimal adipose tissue (WAT) (**A – G**) and plasma (**H – O**) of mice fed with high-fat-sucrose diet (HFSD) and water (HFS), HFSD and phenolic extract from jaboticaba (PEJ) at the dose of 50 mg gallic acid equivalent (GAE)/k g of body weight (BW) (PEJ1) by daily gavage and HFSD and PEJ at the dose of 100 mg GAE/kg BW (PEJ2) by daily gavage.



Values are mean  $\pm$  standard deviation.  $n = 8$ /group. n.s: not significant. \* $p < 0.05$ , \*\* $p < 0.01$ , \*\*\* $p < 0.001$  or  $< 0.0001$ . All: One-way ANOVA with Tukey's test. TNF $\alpha$ : tumoral necrose factor alpha. IL6: interleukin 6. PAI1: plasminogen activator inhibitor 1. TP: total protein. MCP1: monocyte chemoattractant protein 1.

and PAI1, proportionally more than double for all (**Figures 11A, B, D – G**, respectively). The PEJ supplemented groups showed statistically higher adiponectin concentrations than the HFS group, 35 and 41% respectively (**Figure 11C**).

Since the WAT has an important contribution to anti- and pro-inflammatory cytokine circulating concentrations, these adipocyte factors were also determined in the plasma. When compared to the PEJ1 and PEJ2 groups, the HFS group showed statistically higher leptin concentration and statistically lower adiponectin concentration (**Figures 11H and J**, respectively). There was no statistical difference in the resistin value among groups (**Figures 11B**). The TNF $\alpha$  and MCP1 plasma concentrations were statistically reduced in the PEJ1 animals compared to other groups (**Figures 11K and O**, respectively), with no statistical difference in the IL6 and PAI1 averages (**Figures 11M and N**, respectively).

Leptin, resistin and adiponectin are important peptide hormones related to adipocyte endocrine function. The leptin production is directly associated to adipocyte hypertrophy, i.e., large fat cells release more leptin than small ones. The leptin role is to decrease the appetite by acting on anorexigenic neurons (appetite-suppressants) present in the hypothalamic arcuate nucleus, which, in summary, inhibit food intake and fat synthesis and stimulate fat acid oxidation. Similar to insulin, the leptin excess may result in leptin resistance (NELSON; COX, 2014).

Resistin is a small cysteine-rich protein mainly produced by adipocytes in mouse, cattle, and sheep, and by monocytes and macrophages in humans. Several studies have positively associated resistin with insulin resistance and obesity, maybe acting as a key hormone. Circulating concentration of these hormones are usually elevated in animals with diet-induced obesity, and recent studies have suggested that they do not only interact with each other, in a similar and opposite way, but also a chronic elevated resistin concentration leads to leptin resistance, a clinical condition like IR (ZIEBA; BIERNAT; BARĆ, 2020).

The adiponectin is almost exclusively produced by the adipose tissue and commonly has a low production rate under chronic HFSD consumption and WAT hypertrophy. Although not fully understood, it has a key role sensitizing other organs to insulin action, inhibiting inflammatory responses, acting on muscle metabolism of fatty acids, increasing the uptake and  $\beta$ -oxidation, and on glucose hepatic metabolism, enhancing the uptake and catabolism (NELSON; COX, 2014; PERDICARO et al., 2020). In face of this, the above results suggest that PEJ-supplemented animals could

be more protected against adiposopathy when compared to the non-supplemented ones, since they presented high leptin and resistin concentrations accompanied by low adiponectin concentration.

A dysfunctional adipose tissue significantly contributes to systemic inflammation through large secretion of pro-inflammatory adipocytokines, notably TNF $\alpha$ , a key cytokine in the adipocyte dysfunction. This cytokine promotes macrophage infiltration into adipose tissue, through release of IL6, PAI1 and MCP1, decreasing the levels of anti-inflammatory factors, such as adiponectin. Macrophages, but also adipocytes, when overexpress TNF $\alpha$ , restart the cycle (KOWALSKA et al., 2019; NELSON; COX, 2014; SHIMIZU et al., 2014). Regarding these cytokines, our results suggest that PEJ animals had adipose tissues less inflamed than the HFS animals, since they had lower concentrations of inflammatory cytokines in the adipose tissue. Although not all plasma results allow us to conclude that the PEJ efficiently prevented a systemic inflammation status, the PEJ1 animals presented decreased levels of two important inflammatory cytokines, TNF $\alpha$  and MCP1, indicating potential positive effect against inflammation.

Several studies associate polyphenols from various food sources to improvement in adipose function and regulation of proinflammatory cytokines production. For example, raspberry (*Rubus idaeus* L.) extract, also an anthocyanin-rich extract, when added to hypertrophied 3T3-L1 cell culture (mouse adipocyte), substantially increased the expression of the antioxidant enzymes superoxide dismutase (SOD2), glutathione peroxidase (GPx) and catalase, down-regulated the expression and secretion of the pro-inflammatory proteins IL6, MCP1, interleukin 1 $\beta$  (IL-1 $\beta$ ), and up-regulated the expression and secretion of the anti-inflammatory protein interleukin 10 (IL10). In addition, similar to the results observed for PEJ, the leptin and resistin expressions were decreased and that of the adiponectin increased (KOWALSKA et al., 2019). Anthocyanin-rich extracts from purple and red maize (*Zea mays* L.) modulated the inflammation in both mono- and co-cultures of adipocytes (3T3-L1) and macrophages (RAW264.7) by reducing the TNF $\alpha$  and MCP1 production, pointing to the important paracrine interaction between these cell types. According to Zhang et al (2019), an underlying mechanism is that anthocyanins present in the extracts regulated the NF- $\kappa$ B and c-Jun N-terminal kinase (JNK) dependent of mitogen-activated protein kinases (MAPK) pathways. In other words, anthocyanins inactivated or decreased the expression of these proteins with subsequent decrease

in the transcription of genes with an inflammatory role, such as (inducible nitric oxide synthase) iNOS, cyclooxygenase 2 (COX2), TNF $\alpha$  and IL6. An impaired production of these proinflammatory cytokines resulted, through paracrine interaction, in a lower inflammatory condition in the adipocyte. Less inflamed adipocytes resulted, among other things, in lowered release of free fatty acid and proinflammatory cytokines. As well as the lipopolysaccharides (LPS), cytokines may activate the previously described pathways, restarting the macrophage-adipocyte inflammatory paracrine loop. In addition, as positive side effects, oxidative damage, lipolysis, and insulin resistance were mitigated (ZHANG; LUNA-VITAL; MEJIA, 2019).

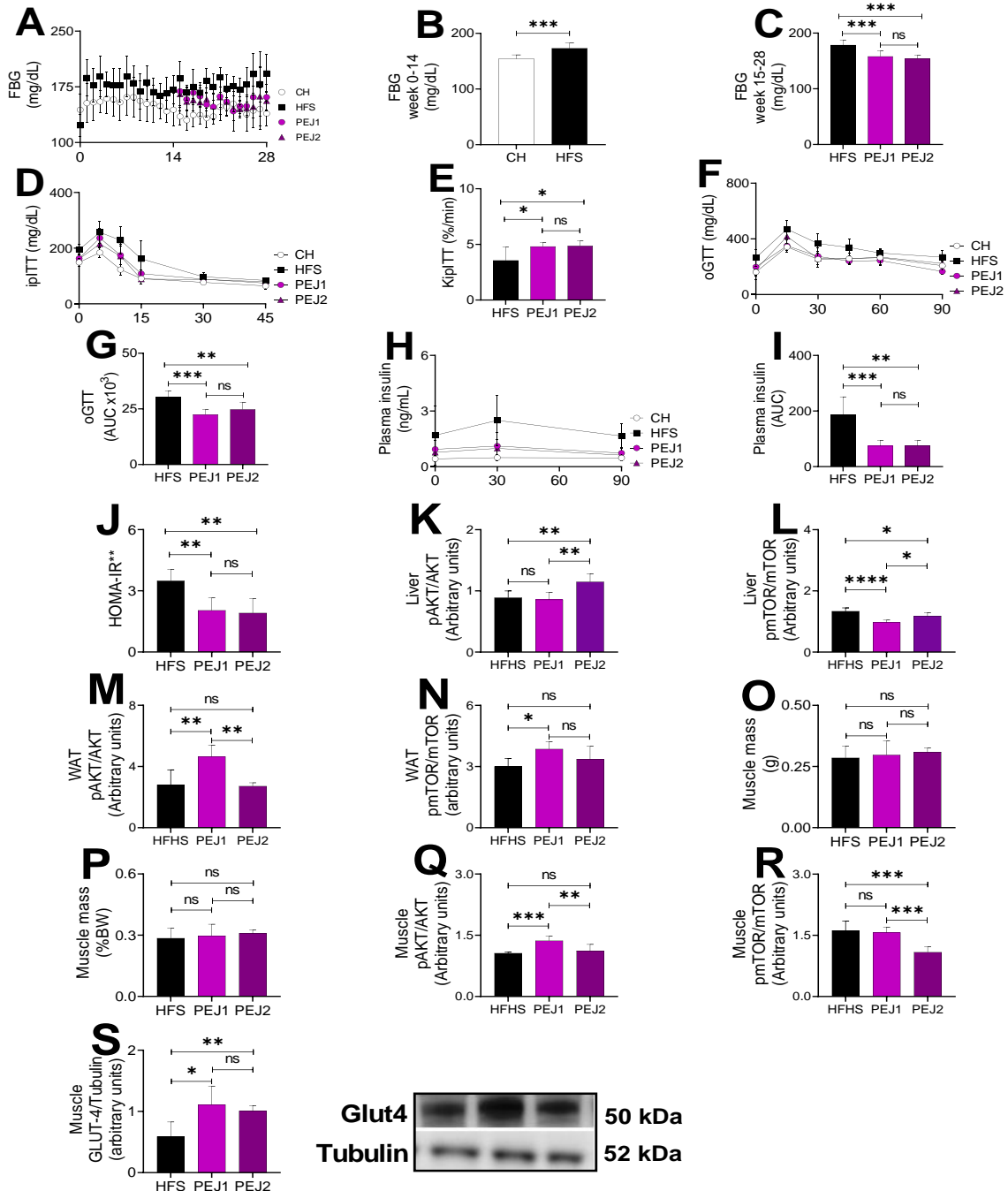
These results suggest that the PEJ has antiobesogenic and anti-inflammatory properties, probably acting by the mechanisms explained above. The PEJ prevented the excessive body weight gain, as well as the excessive WAT gain and its hypertrophy. It also increased the adiponectin concentration in the WAT and plasma, decreased the leptin, TNF $\alpha$ , MCP1, IL6 and MCP1 concentration in WAT, and decreased the leptin, TNF $\alpha$  and MCP1 concentration in the plasma. Specifically, the lower dose of the PEJ (PEJ1) showed better results than the higher dose (PEJ2). The PEJ1 group gained approx. 10% less WAT mass, presented slighted lower hypertrophy and lower cytokine proinflammatory production in the WAT and plasma.

#### 4.2.3. Glucose metabolism

The effects of PEJ-supplementation on glucose metabolism were assessed through weekly fasting blood glucose (FBG), intraperitoneal insulin tolerance test (ipITT), oral glucose tolerance test (oGTT), plasma insulin concentration, HOMA-IR index, AKT and mTOR concentrations in the liver, WAT and gastrocnemius muscle, and protein expression of GLUT4 in the GM, as well as the absolute and relative muscle mass. The results are shown in **Figure 12**.

The HFS group showed the highest FBG throughout the experiment surpassing the CH group in approx. 20% in the initial 14 weeks and in approx. 15% the PEJ groups in the final 14 weeks (**Figures 12A, B and C**, respectively), indicating positive action on glucose metabolism. The HFS animals showed high glucose concentrations for a much longer period when compared to the PEJ animals, meaning that insulin took longer to act (**Figure 12D**). This observation was confirmed by additional calculation of decay rate of glucose (KipITT), which showed that the plasma glucose concentration

**Figure 12.** Effect of the PEJ on several parameters related to glucose metabolism (**A – J**), AKT and mTOR concentrations in liver, WAT and gastrocnemius muscle (GM) (**K – R**), and GLUT4 expression in GM (**S**) of mice fed with high-fat-sucrose diet (HFSD) and water (HFS), HFSD and phenolic extract from jaboticaba (PEJ) at the dose of 50 mg gallic acid equivalent (GAE)/kg of body weight (BW) (PEJ1) by daily gavage and HFSD and PEJ at the dose of 100 mg GAE/kg BW (PEJ2) by daily gavage.



Values are mean  $\pm$  standard deviation.  $n = 6-14$ /group. n.s.: not significant. \* $p < 0.05$ , \*\* $p < 0.01$ , \*\*\* $p < 0.001$  or  $0.0001$ . All: One-way ANOVA with Tukey's test. FBG: fast blood glucose. ipITT: intraperitoneal insulin tolerance test. KipITT: constant glucose decay. oGTT: oral glucose tolerance test. HOMA-IR = {[Fasting glucose (mmol/L)] X [Fasting insulin ( $\mu$ U/mL)]}/22.5. AKT: protein kinase B. mTOR: mammalian target of rapamycin. Muscle: gastrocnemius muscle. S: representative immunoblots of glucose transporter 4 (GLUT4) and tubulin.

were reduced faster in the PEJ animals than in the HFS animals (**Figure 12E**). In relation to oGTT values, both supplemented groups showed lower average values than HFS group, suggesting faster glucose uptake by the PEJ animals (**Figures 12F and G**, respectively). The HFS group presented the highest plasma insulin concentration, indicating elevated insulin release during oGTT trial (**Figures 12H and I**, respectively). In addition, the HOMA-IR index was statistically higher for the HFS group, suggesting insulin resistance (**Figure 12J**). AKT and mTOR concentrations in the liver, WAT and muscle were not totally cohesive. When compared to the HFS group, the hepatic AKT concentration was statistically elevated only in the PEJ2 group, while in the WAT and muscle, only in the PEJ1 group (**Figures 12K, M and Q**, respectively). Regarding the mTOR, both supplemented groups showed lower concentrations than the HFS group in the liver, however, in the muscle, these values were statistically lower only for the PEJ2 group (**Figures 12L and R**). In the WAT, mTOR concentration was higher for both supplemented groups compared to the HFS group (**Figure 12N**). No statistical difference was observed in the absolute and relative muscle weight among groups (**Figures 12O and P**). GLUT4 protein expressions in the muscle were higher in the PEJ groups than in the HFS group, which is in conformity with the AKT concentration previously shown, i.e., the PEJ1 group showed statistically higher values for both AKT concentration and GLUT4 protein expression (**Figures 12Q and S**).

Studies have reported that phenolic compounds contribute to glycemic homeostasis in different ways. Phenolic compounds can decrease carbohydrate digestion and gut glucose uptake inhibiting digestive enzymes, such as  $\alpha$ -amylase and  $\alpha$ -glucosidase, and glucose transporter, for example, sodium-dependent glucose co-transporter 1 (SGLT-1). In skeletal muscle and WAT, they increase glucose uptake by stimulation of GLUT4 translocation from cytoplasm to plasmatic membrane. Polyphenols also stimulate insulin release by  $\beta$ -pancreatic cells and, in addition, the hepatic glucose production can also be modulated by them (HANHINEVA et al., 2010; XIE et al., 2018).

More specifically, polyphenols from Myrtaceae family fruits have demonstrated beneficial effects on glucose metabolism. Clarified juices from cambuci (*Campomanesia phaea* (O. Berg.) Landrum), cagaita (*Eugenia dysenterica* DC.), camu-camu (*Myrciaria dubia* Mc. Vaugh) and jaboticaba reduced the postprandial plasma glucose and insulinemia in healthy individuals (BALISTEIRO et al., 2017; PLAZA et al., 2016). In agreement with this, phenolic extracts from cambuci, cagaita

and Sabara jaboticaba reduced FBG, increased insulin sensitivity and reduced glucose intolerance in diet-induced obese animals (DONADO-PESTANA et al., 2018; MOURA et al., 2018). In another study, mice fed for 8 weeks with phenolic-rich HF diet showed enhanced glucose homeostasis and increased insulin sensitivity (LI et al., 2020a). According to authors, these positive results were due to improvement on pancreatic  $\beta$ -cell function and the hepatic TAG synthesis inhibition with enhanced lipid utilization. Among studied mechanisms are those related to AKT/mTOR phosphorylation pathway, which is responsible by increased glucose uptake from bloodstream. More recently, phenolic from cambuci were associated to AKT activation in muscle and liver of mice with consequent reduction of hyperglycemia, glucose intolerance and IR (DONADO-PESTANA et al., 2020).

Protein kinase B (PKB), also known as AKT, is a serine and threonine kinase with important physiological roles, whose dysfunction has several pathological consequences, such as IR, T2D and inflammatory diseases. Among three isoforms divided according to differences in Ser/Thr residues, the AKT1/PKB $\alpha$  is the one that is ubiquitous distributed in mammalian tissues (MANNING; TOKER, 2017). mTOR is a highly conserved serine threonine kinase with a major role in metabolism, survival, and cell growth. In mammalian, there are two complexes with different functions: mTOR complex 1 (mTORC1) and mTOR complex 2 (mTORC2). mTORC1 senses oxygen levels, energy status, mitogens and amino acids and promotes the cell growth by regulating anabolic and catabolic processes. Insulin is the main controller of glucose homeostasis by regulating glucose uptake into muscle and adipose tissues and hepatic gluconeogenesis. The food intake increases insulin, which by means of IRS pathway activates AKT. Activated AKT starts the translocation movement of GLUT4 from cytoplasmatic vesicles to cell membrane in adipocytes and myocytes. AKT also increases the glycogen synthesis in the liver and muscle. Indirectly, AKT also activates the complex mTORC1. Activated mTORC1 enhances lipid storage by inhibiting lipolysis,  $\beta$ -oxidation and ketogenesis. In addition, mTORC1 phosphorylates IRS1 in a negative-feedback regulation (YOON, 2017b).

In obesity, the reduced response of the WAT to insulin lead to diminished FFA uptake, resulting in ectopic accumulation in other tissues, such as liver. High hepatic lipid accumulation is strongly associated to NAFLD and IR. The IR decreases insulin-AKT signaling pathway leading to reduction of glucogenesis in this organ. As in the liver, in the muscle excessive lipid production and impaired elimination promote IR,

which likewise impairs the insulin-AKT pathway (HUANG et al., 2018). In contrast to the PEJ animals, the HFS animals showed higher FBG, insulin and glucose intolerance, exacerbated insulin production accompanied by reduced HOMA-IR index, and also reduced AKT concentration in the liver, WAT and muscle (vs PEJ2, PEJ1 and PEJ1 , respectively). These results suggest that the PEJ extract may have positively modulated this pathway, resulting in improved glucose homeostasis.

Overactive mTORC1 has been reported in obesity and excessive nutrient intake, probably due to hyperglycemia and hyperinsulinemia. The chronic activation of mTORC1 by nutrient overload results in excessive TAG deposition in liver and muscle. As discussed, this abnormal lipid accumulation outside WAT contributes to IR and NAFLD. Studies report that mTORC1 hyperactivation phosphorylates IRS1 via negative feedback regulation on serine residues (S636/S639), which is considered a molecular marker of IR in tissues. Therefore, the mTORC1 inhibition might be a target to treat metabolic obesity and IR. Although insulin-IRS1-AKT pathway is a canonical via to activate mTORC1, there are two other AKT-independent mTORC1-specific regulations, amino acid- or adenosine monophosphate-activated protein kinase (AMPK)-dependent. While amino acid-dependent regulation activates mTORC1 by a series of sensors and mediators, the AMPK one act in contrast, i.e., inhibit mTORC1 by phosphorylating the complexes tuberous sclerosis complex (TSC-TBC) and regulatory protein associated with mTOR (RAPTOR) (YOON, 2017a). It is worth emphasizing that mTORC1 can also be activated by TNF $\alpha$  (KHAMZINA et al., 2005). mTOR concentration was significantly elevated in the liver of the HFS group when compared to both PEJ groups, probably by another pathway other than Insulin-IRS-AKT. Unlike, in the muscle, only the PEJ2 group showed reduced mTORC1 concentration. On the other hand, in the WAT, the PEJ animals showed elevated mTORC1 concentration, but with statistical difference only to the PEJ1 group when compared to others. Taken together, AKT/mTORC1 concentrations suggest increased lipid deposition in liver and muscle of the HFS animals and decreased uptake of glucose and lipid in the WAT of these animals.

Collectively, the results of the AKT/mTOR pathway, together with those related to glucose metabolism, allow to conclude that the PEJ supplementation improved glucose metabolism, since the PEJ animals showed lower hyperglycemia (both doses), higher insulin and glucose tolerance (both doses), lower hyperinsulinemia (both doses), increased AKT concentration in the liver (PEJ2), WAT and muscle (PEJ1), and

decreased mTORC1 concentration in the liver (PEJ1) and muscle (PEJ2) accompanied of higher concentration in the WAT (both doses).

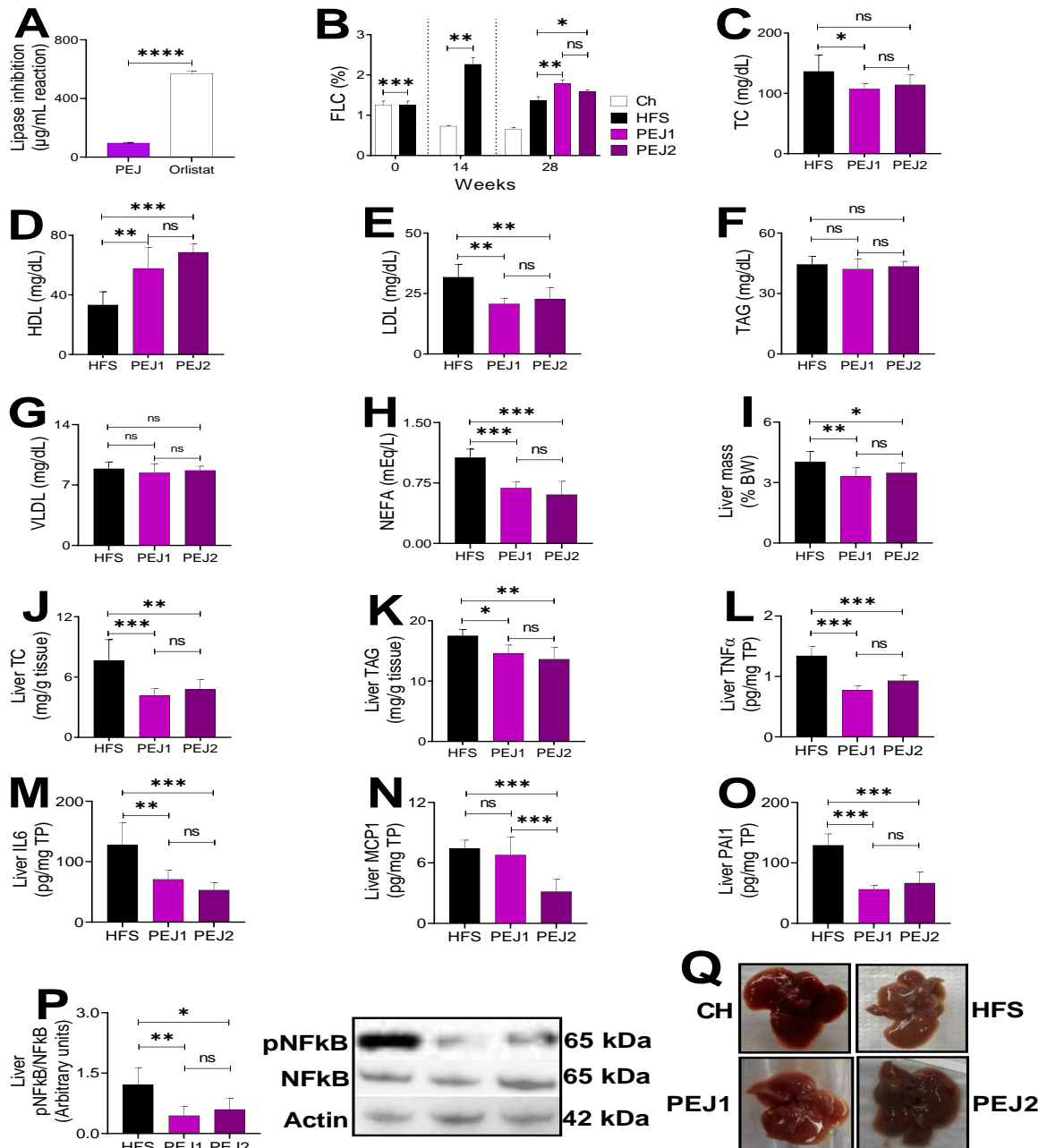
#### 4.2.4. Lipid metabolism

The PEJ effects on lipid metabolism were assessed through its *in vitro* inhibitory activity upon pancreatic lipase, fecal lipid content (FLC), plasma (total, HDL, LDL) and liver (total) cholesterol concentrations, plasma and liver TAG concentrations, plasma non-esterified fatty acids (NEFA) concentration, hepatic TNF $\alpha$ , IL6, PAI1 and MCP1 concentrations, and NF- $\kappa$ B hepatic expression (**Figure 13**).

Since pancreatic lipase plays an especially important role in lipid absorption, inhibitory drugs are an option to treat obesity. The PEJ showed to be an efficient *in vitro* pancreatic lipase inhibitor with an average IC<sub>50</sub> six-fold lower than the orlistat, a potent pancreatic lipase inhibitory drug (**Figure 13A**). Similar results were reported for jaboticaba and other fruit extracts, such as pomegranate (*Punica granatum* L.), acerola (*Malpighia emarginata*), graviola (*Annona muricata*), and cagaita (DONADO-PESTANA; BELCHIOR; GENOVESE, 2015; MARQUES et al., 2016; MOURA et al., 2018; YU et al., 2017). In fact, several studies have associated phenolic compounds to hypolipidemic and hypoglycemic effects, partly due to inhibition of lipid and carbohydrate digestive enzymes, such as pancreatic lipase,  $\alpha$ -glucosidase, and amylase (BUCHHOLZ; MELZIG, 2016; LACROIX; LI-CHAN, 2014; MARRELLI et al., 2013; XIE et al., 2018).

To evaluate whether the *in vitro* inhibition of pancreatic lipase occurred *in vivo*, FLC was quantified at the beginning of experiment, after 14 weeks under feed with obesogenic diet, and after 14 weeks under administration of the PEJ, in the 28<sup>th</sup> experimental week (**Figure 13B**). As expected, after 14 weeks, the HFS group presented a FLC approx. three times higher than the CH group. In the 28<sup>th</sup> week, the FLC of the groups PEJ1 and PEJ2 was, respectively, 23% and 13.5% superior to that of the HFS group, indicating that the PEJ, in the two dosages, increased the lipid excretion in feces. Similarly, YU and collaborators (2017) reported that phenolic extract from pomegranate leaves inhibited the pancreatic lipase *in vitro*, and, through *in vivo* inhibition, decreased the lipid absorption in small gut. Thus, the increased values of

**Figure 13.** Effect of the PEJ on pancreatic lipase activity (**A**), fecal lipid content (FLC) (**B**), plasma and hepatic cholesterol and TAG levels (**C – K**), plasma and hepatic TAG levels (**F, K**), plasma NEFA levels (**H**), hepatic proinflammatory cytokines (**L – P**), and representative liver images (**Q**) of mice fed with high-fat-sucrose diet (HFSD) and water (HFS), HFSD and phenolic extract from jaboticaba (PEJ) at the dose of 50 mg gallic acid equivalent (GAE)/kg of body weight (BW) (PEJ1) by daily gavage and HFSD and PEJ at the dose of 100 mg GAE/kg BW (PEJ2) by daily gavage.



Values are mean  $\pm$  standard deviation.  $n = 6-14/\text{group}$ . n.s.: not significant. \* $p < 0.05$ , \*\* $p < 0.01$ , \*\*\* $p < 0.001$  or  $0.0001$ . All: One-way ANOVA with Tukey's test. 15A – 15C:  $n = 6-10/\text{group}$ . One-way ANOVA with Tukey's test. FLC: fecal lipid content. TC: total cholesterol. TAG: triacylglycerol. NEFA: non-esterified fatty acid. TNF $\alpha$ : tumoral necrose factor alpha. IL6: interleukin 6. MCP1: monocyte chemoattractant protein 1. PAI1: plasminogen activator inhibitor 1. P: representative immunoblots of nuclear factor kappa B (NF- $\kappa$ B) and  $\beta$ -actin. TP: total protein.

the FLC of the PEJ groups may be related to inhibition of pancreatic lipase activity in small gut by phenolic compounds.

In relation to cholesterol, the HFS group showed concentrations higher than the PEJ1 group for both total (TC) and LDL cholesterol, and for LDL cholesterol compared to the PEJ2 group (**Figures 13C and E**, respectively). The HDL cholesterol concentration in PEJ groups was statistically higher than in the HFS group (**Figure 13D**). The PEJ had no effect on reduction of the plasma TAG and VLDL concentrations, however, in relation to plasma NEFA concentration, the supplemented groups showed a significant decrease compared to the HFS group (**Figures 13F, G and H**, respectively). The relative liver mass was smaller for animals belonging to both supplemented groups compared to the HFS group, and, both TC and TAG hepatic concentration were statistically lower in the PEJ groups than in the non-supplemented group (**Figures 13, J and K**, respectively).

Several positive effects in lipid metabolism of polyphenol-supplemented animals have been reported by numerous studies. Flavanone-rich extract from bergamot fruit (*C. bergamia* Risso) decreased, after three weeks, serum concentrations of TC, TAG, VLDL and LDL and increased HDL concentration of supplemented Wistar rats to levels equal or higher than those of animals treated with simvastatin, a hypocholesterolemic drug used to treat cardiovascular diseases that blocks the 3-hydroxy-3-methylglutaryl-CoA reductase (HMGR) in hepatocytes, a key enzyme of the cholesterol metabolism (DI DONNA et al., 2014). In another study, C57BL/6J mice fed with HFSD enriched with pomegranate extract for 4 weeks showed reduced hepatic levels of TC and TAG, according to authors, through fecal excretion of cholesterol and bile acid (YANG et al., 2018). A phenolic glycoside isolated from *Moringa oleifera* Lam., administered daily to db/db mice, for 4 weeks, reduced BWG, ameliorated glucose metabolism, decreased levels of TC, LDL, TAG and NEFA, and increased HDL levels. The main mechanism of action of this phenolic compound seemed to be its capacity to enhance the AMPK phosphorylation in the liver (BAO et al., 2020). AMPK phosphorylated (active form) regulates other critical enzymes of hepatic lipid metabolism, such as PPAR $\alpha$  and sterol regulatory element-binding protein (SREBP-1) (NELSON; COX, 2014).

NEFA plasma concentration was also reduced in animals treated with PEJ. FA are transported in blood linked to albumin in the free form (non-esterified). NEFA are both the product of fatty acid hydrolysis and the substrate for their synthesis. They are increased in obesity and are an important plasma marker for metabolic syndrome since

they are the direct product of high levels of inflammatory cytokines and intensified insulin resistance. Excess circulating NEFA impairs the insulin secretion, hepatic glycogenesis, and muscle glucose uptake. Consequently, the cells are not stimulated by insulin to uptake NEFA, aggravating the harmful state of lipotoxicity and hyperglycemia (NELSON; COX, 2014; WILLIAMSON et al., 2011). Finally, the relative masses of liver shown in **Figure 13I** are in accordance with what is expected for animals that gained less BW.

NAFLD is characterized by abnormal accumulation of fat in the liver without excessive consumption of alcohol. According to “two hit hypotheses”, NAFLD is triggered by a combination of sedentary lifestyle, high-fat diet, obesity, and IR, the first hit. The second one leads to activation of inflammatory cascades, overproduction of proinflammatory cytokines, such as TNF $\alpha$  and IL6, followed by fibrogenesis (BUZZETTI; PINZANI; TSOCHATZIS, 2016). Therefore, since the PEJ animals had less BW gain, decreased plasma and hepatic cholesterol levels and reduced fat accumulation in the liver, concentrations of inflammatory markers were determined in this organ. The TNF $\alpha$ , IL6 and MCP1 concentrations and NF- $\kappa$ B expression were considerably higher in the HFS animals, more than double compared to the PEJ groups (**Figures 13L – N and P**). Other the other hand, both HFS and PEJ1 groups showed increased concentration of MCP1 in relation to the PEJ2 group (**Figure 13O**). Despite this, the PEJ positively modulated the hepatic inflammation, a result widely supported by other studies in which phenolic compounds decreased both hepatic inflammation and hepatic lipid accumulation. For example, through AKT and AMPK pathway activation, phenolic from cambuci administered to mice for 8 weeks reduced body weight gain, inflammation, and hepatic steatosis (DONADO-PESTANA et al., 2020). Jaboticaba peel extract administered for 8 weeks to aged FVB mice positively modulated the lipid metabolism preventing NAFLD (LAMAS et al., 2018). Phenolic-rich cranberry extract reversed hepatic steatosis by downregulating several proinflammatory cytokine genes in HFSD-fed C57BL/6J mice (ANHÊ et al., 2017). In another study, phenolic extract from peach peel administered to ICR mice for 12 weeks decreased the cholesterol and TAG hepatic levels and enhanced the activity of antioxidant proteins in serum and liver, such as SOD, CAT and GPx (KAN et al., 2020). Recently, a cross-sectional cohort with 789 individuals inversely associated the high consumption of phenolic acids with liver steatosis and IR, suggesting hepatic protective effect also in humans. Specifically, the consumption of hydroxybenzoic acids, of which

gallic and ellagic acid are the main representatives, was associated with lower NAFLD and fibrosis (SALOMONE et al., 2020).

Possibly acting through the biological pathways discussed above, the PEJ showed several antidyslipidemic and anti-inflammatory properties that contribute to lipid homeostasis. It decreased TC- and LDL-cholesterol plasma levels (PEJ1 and both doses, respectively), increased HDL-cholesterol plasma level (both doses), decreased hepatic lipidic accumulation and inflammation (both doses). In addition, higher lipid excretion was observed in feces of supplemented groups, indicating *in vivo* inhibition of pancreatic lipase. Thus, these results suggest that the PEJ might be used as a food adjuvant to modulate the lipid metabolism and fight NAFLD.

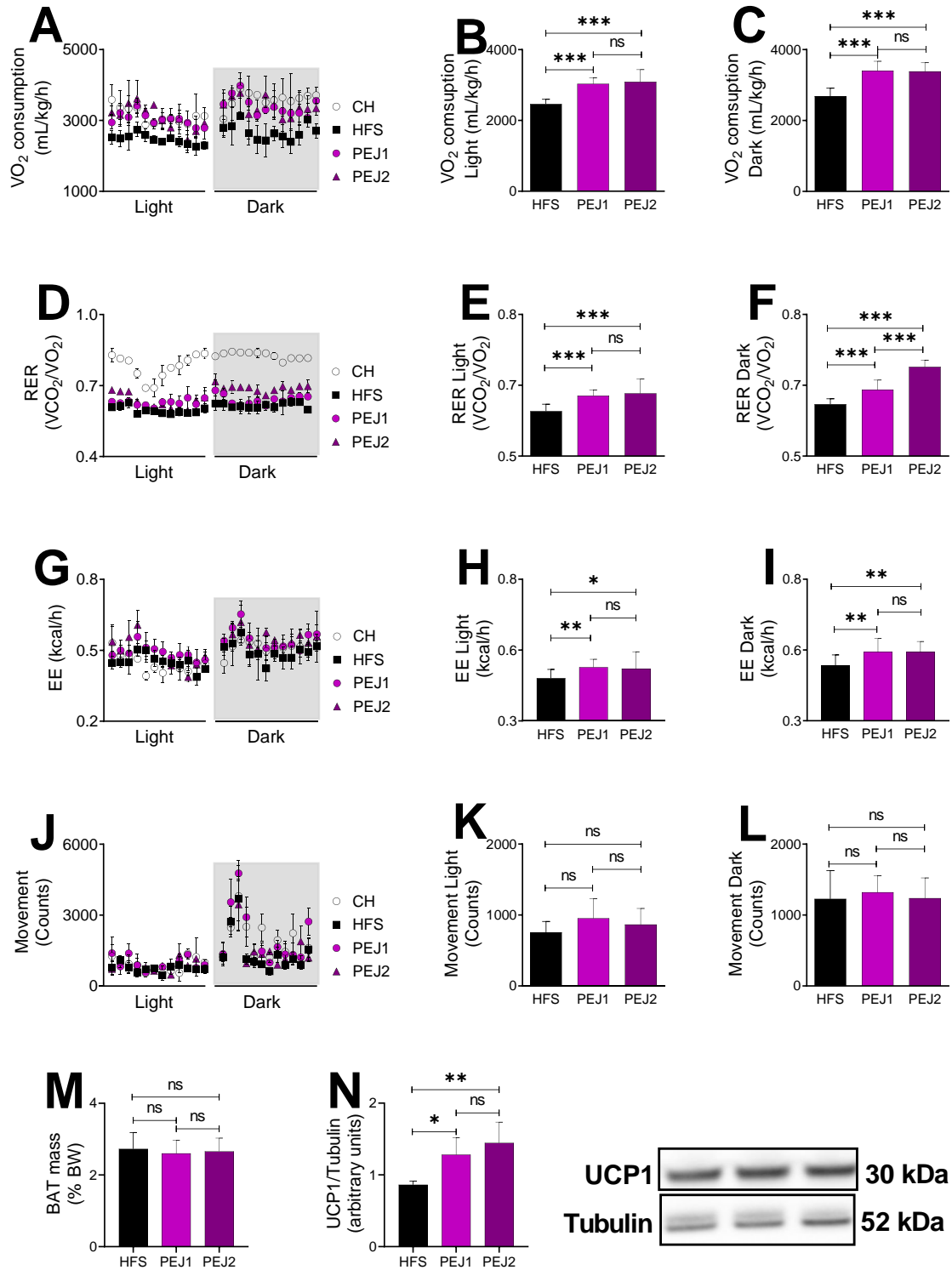
#### **4.2.5. PEJ effect on energy metabolism**

The effect of PEJ intake effect on energy metabolism was assessed through indirect calorimetry using an automatic system (CLAMS) that provided several data related to light (day) and dark (night) period of the animals for 24 h, such as O<sub>2</sub> consumption (VO<sub>2</sub>), respiratory exchange rate (RER), energy expenditure (EE) and locomotor activity. In addition, due to its importance in energy metabolism, the brown adipose tissue (BAT) mass and the UCP1 expression in it were also determined (**Figure 14**).

Regardless the dose, the supplemented groups showed VO<sub>2</sub> statistically higher than the HFS group in both periods, indicating that PEJ-supplemented animals had an increased oxidative capacity (**Figures 14A, B and C**). Similarly, average RER values were statistically superior for PEJ-treated animals when compared to non-treated ones in both periods (**Figures 14D, E and F**). RER indicates the type of energetic substrate being used. When energetic demand is less intense, fatty acid are preferentially used (RER near to 0.7). In turn, under more intense energetic demand, carbohydrates become the main energetic source (RER near to 1.0) (EVEN; NADKARNI, 2012).

As mice are night animals, they demanded less energy during the day and more energy during the night, thus we may infer that PEJ-supplemented animals, mainly the PEJ2-animals, demanded more energy in dark period, as expected for the species, while HF-animals continued to demand less energy in dark periods, which may favor the body weight gain. In accordance with this, the supplemented groups presented the highest average EE in both periods (**Figures 14G, H and I**). No statistical differences

**Figure 14.** PEJ effect on energy metabolism of mice fed with chow diet and water (CH), high-fat-sucrose diet (HFSD) and water (HFS), HFSD and phenolic extract from jaticaba (PEJ) at the dose of 50 mg gallic acid equivalent (GAE)/kg of body weight (BW) (PEJ1) by daily gavage and HFSD and PEJ at the dose of 100 mg GAE/kg BW (PEJ2) by daily gavage.



Values are mean  $\pm$  standard deviation. 13A – 13N: n = 6-10/group; One-way ANOVA with Tukey's test.

was observed in locomotor activity, suggesting that factors other than movement contributed to these positive changes in the energy homeostasis of the PEJ-treated animals (**Figures 14J, K and L**). No statistical difference was observed in the BAT mass (**Figure 14M**). When compared to the HFS group, the UCP1 expression in the BAT was increased in both supplemented groups, mainly the PEJ2 group, indicating thermogenic activity in the tissue (**Figure 14N**).

The EE is associated to mitochondrial functions, and AMPK is the main regulator of both energetic metabolism and mitochondrial biogenesis, which exert multiple functions on glucose and lipid metabolism, e.g., acting on AKT/mTOR pathway. AMPK activation increases several encoder genes of proteins considered thermogenic markers, such as UCP1. The BAT exerts its critical role in thermogenesis and energy homeostasis precisely by means of this protein that permit energy dissipation as heat, providing an alternative way for protons return to mitochondrial matrix ignoring the adenosine triphosphate synthesis (ARHA et al., 2018; NELSON; COX, 2014). Several studies have shown this positive relation among AMPK, UCP1, BAT and thermogenesis. For example, AMPK $\alpha$ 1 KO mice showed impaired thermogenesis with reduced UCP expression in BAT. On the other hand, obese mice that had lower AMPK phosphorylation also presented lower both body temperature and UCP expression in BAT, however, they had these alterations reversed by treatment with an AMPK agonist, indicating that phosphorylated AMPK is required for a normal thermogenic function (PALACIOS-GONZÁLEZ et al., 2019; YANG et al., 2016).

Like physical activities and drugs, studies report that phytochemical agents, including phenolic compounds, can induce AMPK activation and up-regulate other molecules related to energy metabolism. Flavonols from cocoa administered to mice increased the EE in association with increased levels of UCP1 mRNA expression in BAT and increased levels of UCP3, like UCP1 in BAT, mRNA expression and phosphorylated AMPK $\alpha$  in gastrocnemius muscle 2 h after supplementation (KAMIO et al., 2016). Diet containing procyanidin-anthocyanin-rich extract from black soybean seed coat (*Glycine max*) decreased, after 14 weeks, mesenteric fat depot and up-regulated gene and expression levels of UCP1 in BAT and UCP2 in WAT of high-fat diet-fed mice (KANAMOTO et al., 2011). Mice fed with genistein-supplemented diet for 60 days showed increased UCP1 expression in WAT, indicating conversion of WAT cells into brown-like adipose cells in a process named browning or beige through a

non-fully elucidated mechanism, however partially mediated by AMPK activation (PALACIOS-GONZÁLEZ et al., 2019). Phenolic extracts from cagaita (*Eugenia dysenterica* DC.), another Brazilian native fruit, even in much smaller doses, 7 and 14 mg GAE/kg BW, also increased the RER values and O<sub>2</sub> consumption of C57BL/6 mice (DONADO-PESTANA et al., 2018) supplemented for 8 weeks. Recently, C57BL/6 mice treated with coumestrol, a dietary phytoestrogen present in soybean, for two weeks, had BAT expansion caused by adipogenesis of progenitor cells in BAT resulting, among other things, in weight loss (KIM et al., 2020).

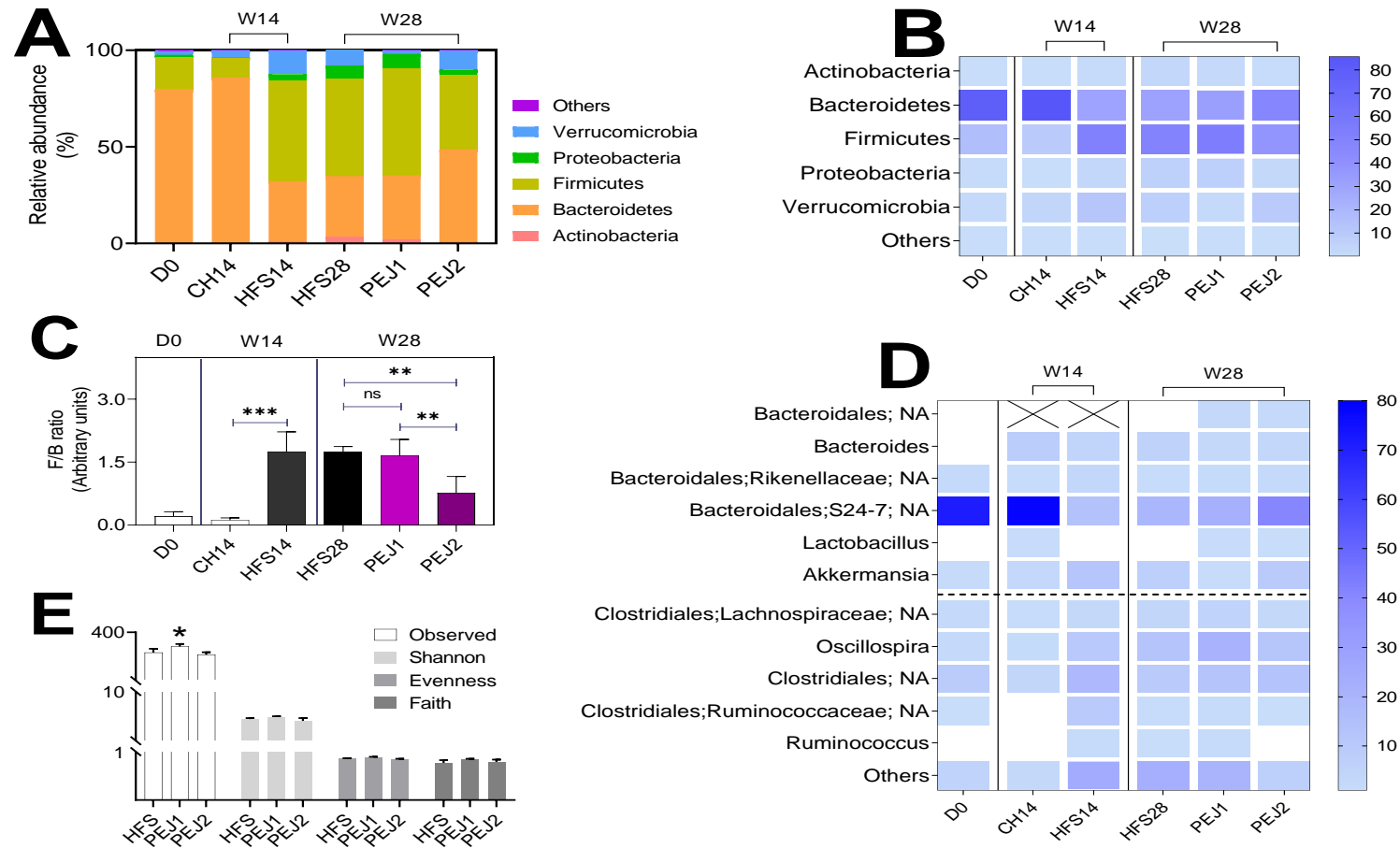
Except for BAT mass increase, our results are in accordance with these and other researches that report several positive effects of phenolic compounds on energy homeostasis, observed by increased values of VO<sub>2</sub> consumption, RER, EE and UCP1 expression in BAT, for example. These data lead us to conclude that the antiobesogenic properties of the PEJ may also be partly due to positive regulations in these parameters, probably through AMPK activation that up-regulated other molecules involved with energy homeostasis in BAT, such as UCP1.

#### **4.2.6. PEJ effect on microbiota**

The PEJ effect on intestinal microbiome was evaluated by operational taxonomic units (OTU), Firmicutes/Bacteroidetes ratio (F/B ratio), and alpha and beta diversity analysis, at three different moments: before starting the experiment (D0), in the 14<sup>th</sup> week (W14), and in the 28<sup>th</sup> week (W28), after 14 weeks of supplementation. The microbiome of the animals at the start of the experiment was compatible with microbial community of healthy C57BL/6J mice, i.e., a higher abundance of Bacteroidetes with lower Firmicutes abundance and smaller quantities of others phyla, such as Verrucomicrobia and Proteobacteria (LI et al., 2020b) (**Figure 15A and B**).

As expected, the animals fed a chow diet had no considerable alterations in microbial composition after 14 weeks. On the other hand, the animals fed a HFSD showed a considerable change, mainly in the Bacteroidetes and Firmicutes phyla (**Figure 15A and B**). Notably, supplementation of PEJ at the highest dose (PEJ2) statistically decreased the average F/B ratio to less than half, in comparison to the HFS group (1.75 vs 0.76, respectively) (**Figure 15C**). This fact indicates an important contribution to intestinal health since an increased F/B ratio has been associated to pathogenesis in obesity (CASTANER et al., 2018).

**Figure 15.** PEJ effect on intestinal microbiome of mice fed with chow diet and water (CH), high-fat-sucrose diet (HFSD) and water (HFS), HFSD and phenolic extract from jaborcaba (PEJ) at the dose of 50 mg gallic acid equivalent (GAE)/kg of body weight (BW) (PEJ1) by daily gavage and HFSD and PEJ at the dose of 100 mg GAE/kg BW (PEJ2) by daily gavage.



W14: week 14. W28: week 28. F/B ratio: Firmicutes/Bacteroidetes ratio. n = 6/group. \*p < 0.05, \*\*p < 0.01, \*\*\*p < 0.001 or 0.0001. C: W14: unpaired *t* test with Welch's correction. W28: one-way ANOVA with Tukey test.

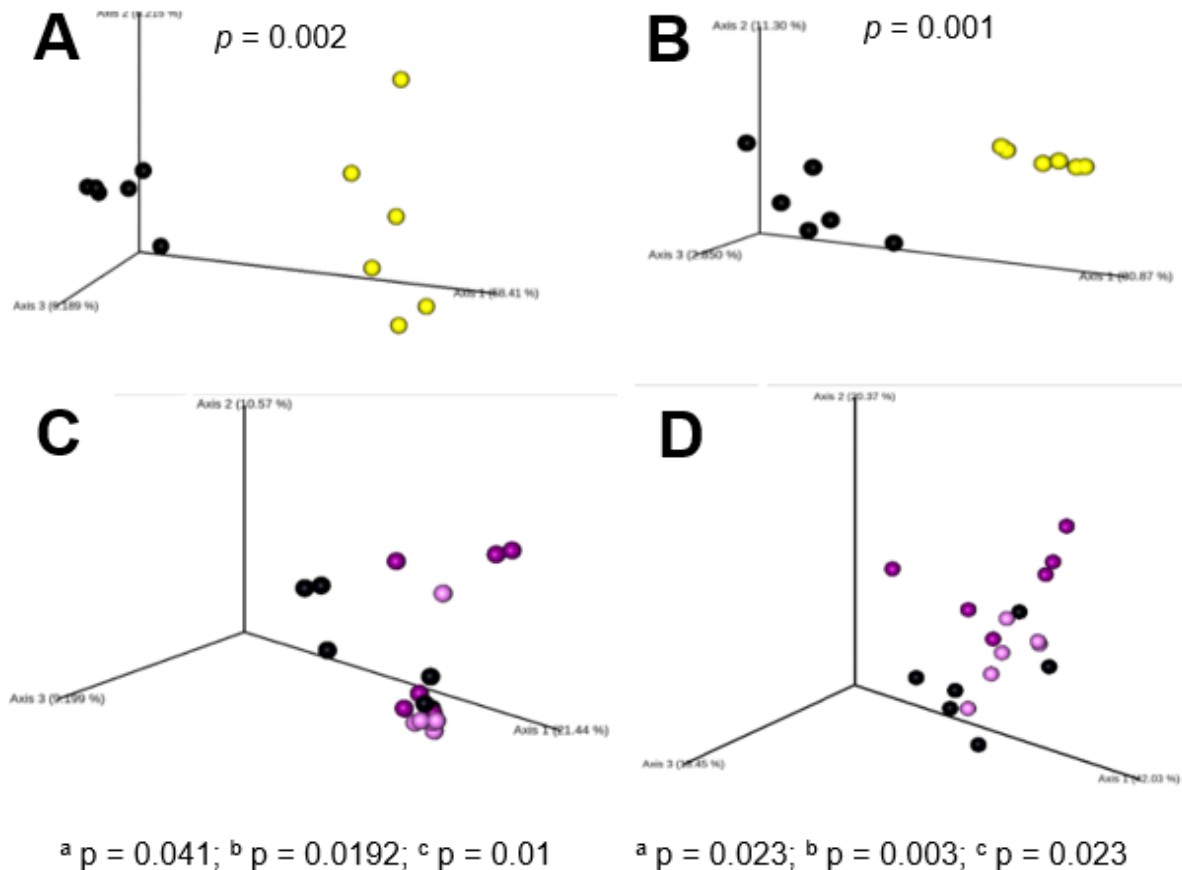
The 11 most abundant genera are presented in **Figure 15D**. The family S24-7, recently renamed *Muribaculaceae*, was the dominant family of gut *Bacteroidales*, being increased in the CH and supplemented groups when compared to the HFS group, corresponding to approx. 80% (CH), 22-29 (PEJ1 and PEJ2), and 13-19% (HFS). Above of dot line are genera inversely correlated with obesity, and below, the opposite. The gut bacterial community of the PEJ2 group was mostly composed for beneficial bacteria, numerically, 61% vs 46% when compared to the HFS.

Alpha diversity is an indicator of abundance and diversity of species in microbial community and was evaluated by *Observed features* (qualitative measure), *Shannon's diversity index* (quantitative measure), *Evenness* or *Pielou* (evenness measure) and *Faith's phylogenetic diversity* (phylogenetic qualitative measure) (**Figure 15E**). PEJ supplementation increased *Observed features* values of the PEJ1 group when compared to the HFS group, suggesting higher abundance of gut microorganisms. There was no statistical difference for the other alpha indexes.

The *beta diversity* assesses the difference among groups (clusters) according to genus through principal coordinate analyses (PCoA) using phylogenetic distance matrixes *Unifrac* unweighted (qualitative measure) and weighted (quantitative measure) in relation to community dissimilarity. Through beta diversity the distance between groups CH and HFS was evidenced in the 14<sup>th</sup> week both qualitatively and quantitatively (**Figure 16A and B**). In the same way, in the 28<sup>th</sup> week, *beta diversity* revealed that, when clustered, the supplemented groups were statistically distant of the HFS group of both forms, unweighted and weighted (**Figure 16C and D**).

The relation between intestinal microbiome and health status is increasingly clear. Numerous studies have associated gut microbiome profiles with obesity and metabolic disorders, such as T2D and NAFLD (CASTANER et al., 2018). In contrast, polyphenols from vary food sources have showed several benefit effects on health, including gut microbiome modulation. For example, supplementation with cranberry extract for 8 weeks considerably decreased the F/B ratio and increased genera inversely related to obesity, such as *Akkermansia*, in C57BL/6J mice (ANHÊ et al., 2017). Similarly, peach peel extract administered to ICR mice for 12 weeks significantly increased alpha diversity indexes and decreased harmful bacterial genera, such as *Oscillospira* and *Rominococcus* (KAN et al., 2020). Polyphenolic extract from walnut reversed the diet-induced negative disbalance in microbiota of rats, increasing, for example, family *Bacteroidales* s24-7 (LI et al., 2020b).

**Figure 16.** PEJ effect on beta diversity of the intestinal microbiome in the 14<sup>th</sup> week (**A, unweighted, and B, weighted**) and in the 28<sup>th</sup> week (**C, unweighted, and D, weighted**) of mice fed with chow diet and water (CH), high-fat-sucrose diet (HFSD) and water (HFS), HFSD and phenolic extract from jaboticaba (PEJ) at the dose of 50 mg gallic acid equivalent (GAE)/kg of body weight (BW) (PEJ1) by daily gavage and HFSD and PEJ at the dose of 100 mg GAE/kg BW (PEJ2) by daily gavage.



All results: PERMANOVA.  $n = 6$ /group. a: HFS vs PEJ1. b: HFS vs PEJ2. c: PEJ1 vs PEJ2.

Endotoxemia has been pointed as the main developer of the chronic low-grade inflammation, which has crucial role in the pathogenesis of obesity (HOTAMISLIGIL, 2006). To fight endotoxemia through positive alteration in gut microbioma has been suggested as a possible mechanism of action of polyphenols to reduce risks to health caused by obesity. After studying the effect of dietary capsaicin, the major polyphenol in red chili (*Capsicum* genus), on metabolic endotoxemia, Kang et al. (2017) proposed that positive alteration in the gut microbiota decreased LPS-producer bacteria, resulting in lower intestinal permeability and, therefore, reduced inflammatory cytokines production with consequent suppression of low-grade chronic inflammation.

Mainly in the higher dose, PEJ altered the gut microbiome of animals fed with HFSD, which can be verified by differences in *beta diversity* analyses. In addition, the F/B ratio was reduced, suggesting protective effect against harmful intestinal bacteria. As far we know, it was demonstrated for the first time that phenolic compounds from jaboticaba can positively alter the gut microbiome of mice, suggesting protective effect against diet-induced obesity. Further studies are needed to understand in detail the underlying mechanisms and which species may be associated with the observed results.

#### **4.2.7. Untargeted metabolomics**

The untargeted metabolomics analysis was performed to verify alterations in the urinary metabolomic profile of mice supplemented with PEJ. After alignment and baseline processing, a matrix of global entities (GEM) composed of 8800 molecules was obtained. The variable importance in projection (VIP) score was applied on GEM to determine the contribution of each entity by group within dataset. This procedure reduced the entities initially obtained to 800 in three groups, CH, HFS and PEJ2. All entities extracted by VIP were tested against external and internal data banks or literature, resulting in 102 tentatively identified entities.

Principal component analysis (PCA) and partial squares discriminant analysis (PLS-DA) were utilized to verify class differences among groups (**Figure 17**). The calculated PCA model gave 2 significant components, describing 72.6% of the variation ( $X = 49.9\%$ ;  $Y = 22.7\%$ ). According to cross-validation, the PLS-DA model gave 2 significant components, describing 54,9% of the variation ( $X = 22.6\%$ ;  $Y = 32.3\%$ ,  $R^2 = 0.96$ ,  $Q^2 = 0.84$ ). After a new ranking by VIP score ( $VIP > 1$ ), the entities were reduced to 34 with high contribution to the model (**Figure 18 and 19**). Finally, after analysis by one-way ANOVA followed by Fisher's LSD test, 30 compounds presented statistical difference ( $p < 0.05$ ) when compared among groups and were then sorted by concentration (**Table 4**).

As expected, most of metabolites were derived from consumption of protein, fatty acid, and polyphenols submitted to biotransformation processes, such as glucuronidation and sulfation. However, two metabolites associated to disorders in mitochondrial fatty acid and  $\beta$ -oxidation or other inborn errors of metabolism were

**Figure 17.** PCA and PLS-DA score plots of urinary metabolites of mice fed with chow diet and water (CH), high-fat-sucrose diet (HFSD) and water (HFS), HFSD and phenolic extract from jaboticaba (PEJ) at the dose of 100 mg gallic acid equivalent (GAE)/kg of body weight (BW) (PEJ2) by daily gavage.

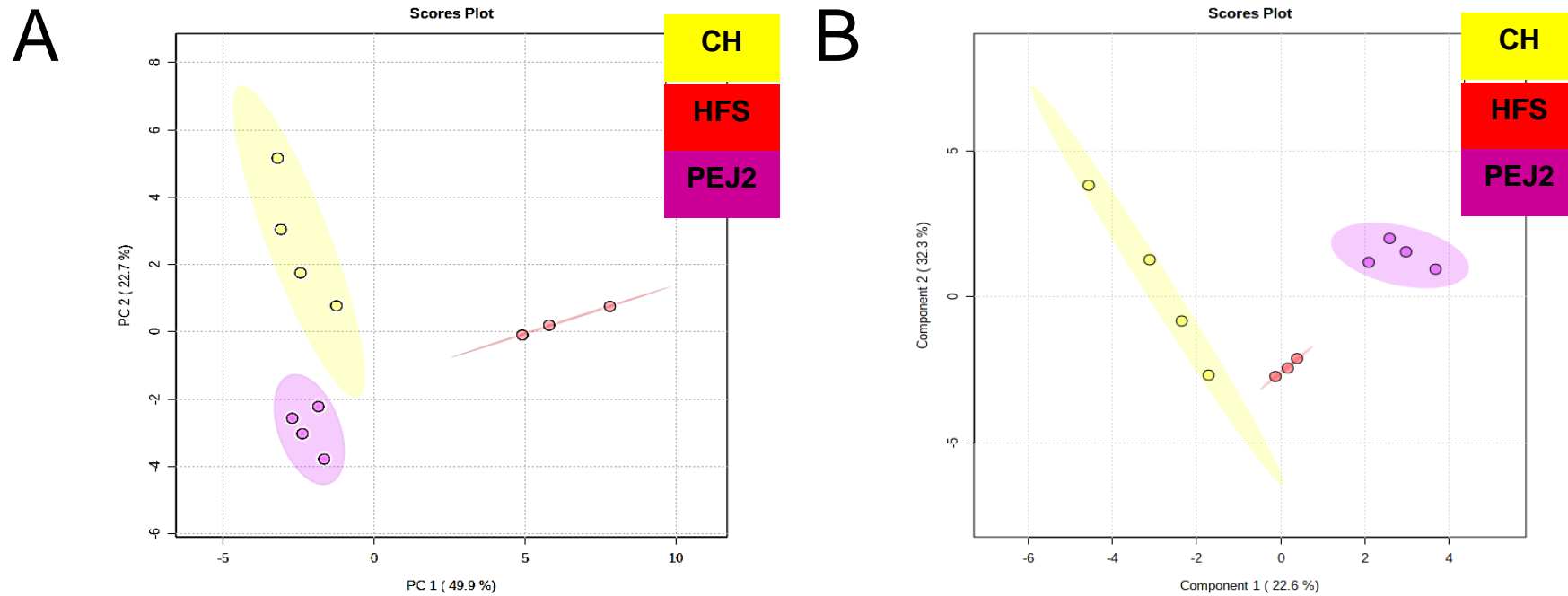


**Figure 18.** VIP scores of urinary metabolites of mice fed with chow diet and water (CH), high-fat-sucrose diet (HFSD) and water (HFS), HFSD and phenolic extract from jaboticaba (PEJ) at the dose of 100 mg gallic acid equivalent (GAE)/kg of body weight (BW) (PEJ2) by daily gavage.

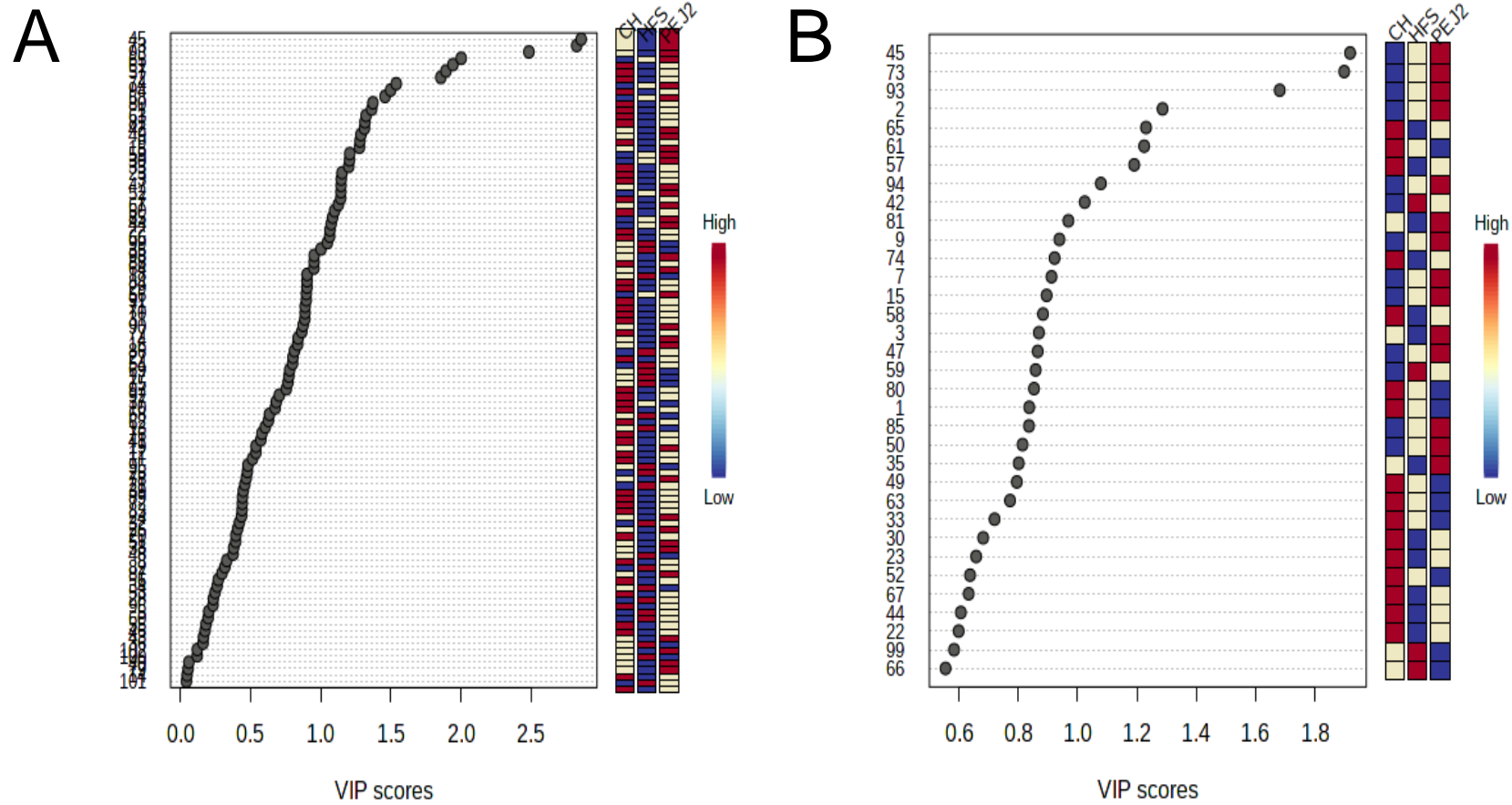
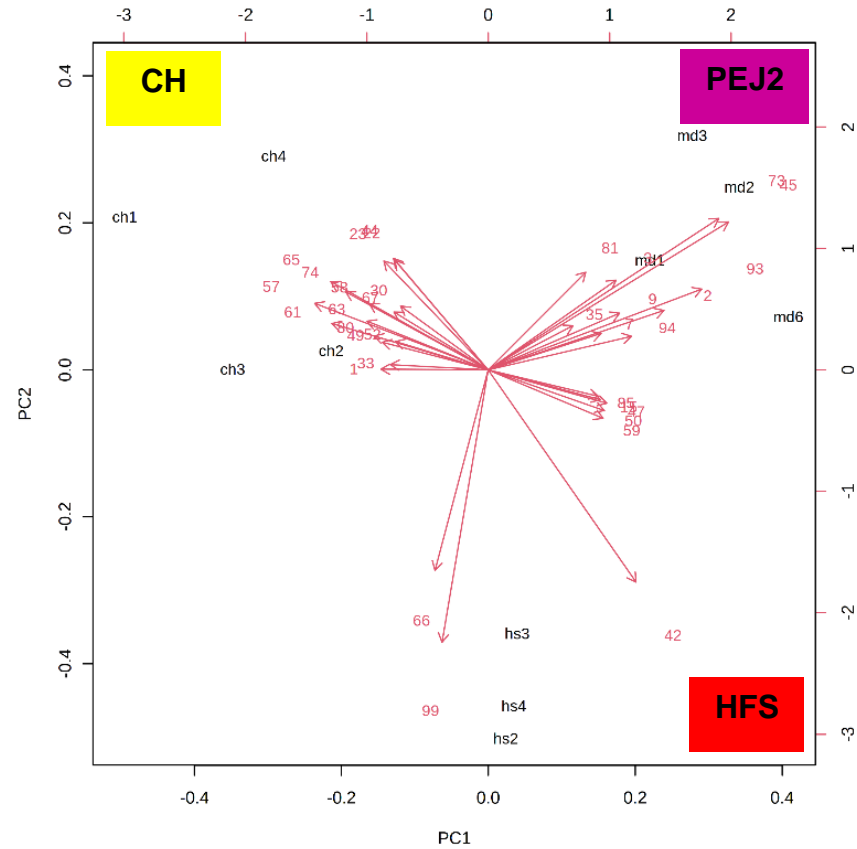


**Figure 19.** Biplot and heatmap of urinary metabolites of mice fed with chow diet and water (CH), high-fat-sucrose diet (HFSD) and water (HFS), HFSD and phenolic extract from jaboricaba (PEJ) at the dose of 100 mg gallic acid equivalent (GAE)/kg of body weight (BW) (PEJ2) by daily gavage.

**A**



**B**

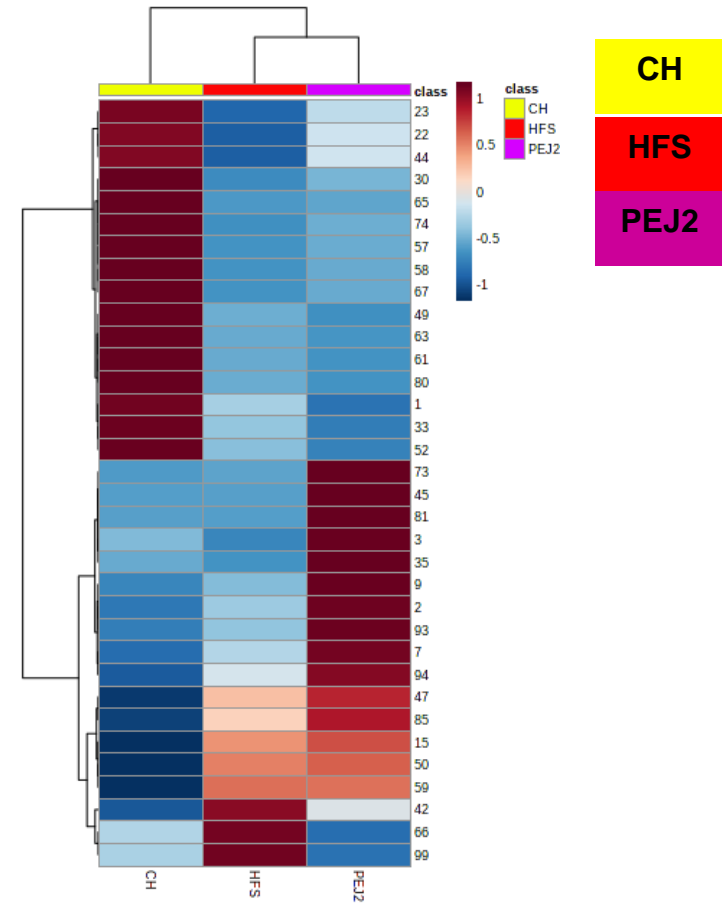


**Table 4.** Main metabolites tentatively identified in the urine of mice by UPLC-ESI-QTOF.

Group	ID	[M-H] <sup>-</sup>	RT (min)	Formula	Name
CH	1	100.0766	7.2	C <sub>5</sub> H <sub>11</sub> NO	Betaine aldehyde
	22	136.0404	2.6	C <sub>7</sub> H <sub>7</sub> NO <sub>2</sub>	p-Aminobenzoic acid
	23	138.0552	2.4	C <sub>7</sub> H <sub>9</sub> NO <sub>2</sub>	3,4-Dihydroxybenzylamine
	30	151.0389	10.8	C <sub>8</sub> H <sub>8</sub> O <sub>3</sub>	p-Hydroxyphenylacetic acid
	33	156.0663	20.0	C <sub>7</sub> H <sub>11</sub> NO <sub>3</sub>	2-Ethyl-2-methyl-3-hydroxysuccinimide
	49	193.0348	10.3	C <sub>6</sub> H <sub>10</sub> O <sub>7</sub>	D-Glucuronic acid
	52	194.0454	16.5	C <sub>9</sub> H <sub>9</sub> NO <sub>4</sub>	α-Hydroxyhippuric acid
	58	217.0169	3.0	C <sub>8</sub> H <sub>10</sub> O <sub>5</sub> S	Tyrosol 4-sulfate
	61	224.0559	12.0	C <sub>10</sub> H <sub>11</sub> NO <sub>5</sub>	4-Amino-4-deoxychorismic acid
	65	245.0914	2.7	C <sub>13</sub> H <sub>14</sub> N <sub>2</sub> O <sub>3</sub>	N-Acetyl-D-tryptophan
	67	246.9912	1.1	C <sub>8</sub> H <sub>8</sub> O <sub>7</sub> S	Vanillic acid 4-sulfate
	80	336.0707	11.8	C <sub>15</sub> H <sub>15</sub> NO <sub>8</sub>	2,8-Dihydroxyquinoline-beta-D-glucuronide
HFS	15	121.0287	14.9	C <sub>7</sub> H <sub>6</sub> O <sub>2</sub>	Benzoic acid
	42	179.0461	1.2	C <sub>8</sub> H <sub>8</sub> N <sub>2</sub> O <sub>3</sub>	Nicotinuric acid*
	50	193.0485	13.4	C <sub>10</sub> H <sub>10</sub> O <sub>4</sub>	ferulic acid
	59	219.0770	17.8	C <sub>11</sub> H <sub>12</sub> N <sub>2</sub> O <sub>3</sub>	5-Hydroxytryptophan
	66	246.0971	17.4	C <sub>10</sub> H <sub>17</sub> NO <sub>6</sub>	Malonylcarnitine*
PEJ2	2	102.0555	1.4	C <sub>4</sub> H <sub>9</sub> NO <sub>2</sub>	D-2-Aminobutyric acid
	7	113.0607	2.2	C <sub>6</sub> H <sub>10</sub> O <sub>2</sub>	4-methyl-4-pentenoic acid
	45	187.0068	18.8	C <sub>7</sub> H <sub>8</sub> O <sub>4</sub> S	Methylphenol sulfate
	47	189.0403	6.5	C <sub>7</sub> H <sub>10</sub> O <sub>6</sub>	3-Dehydroquinic acid
	73	283.0815	12.0	C <sub>13</sub> H <sub>16</sub> O <sub>7</sub>	Methylphenol glucuronide
	81	337.1490	2.2	C <sub>21</sub> H <sub>22</sub> O <sub>4</sub>	Chalcone
	93	413.1265	12.7	C <sub>22</sub> H <sub>22</sub> O <sub>8</sub>	Quercetin 3,3'-dimethyl ether 4'-(2-methylbutyrate)
94	423.1432	1.3	C <sub>24</sub> H <sub>24</sub> O <sub>7</sub>	Flavone	

Mice fed with chow diet and water (CH), high-fat-sucrose diet (HFSD) and water (HFS), HFSD and phenolic extract from jaboticaba (PEJ) at the dose of 100 mg gallic acid equivalent (GAE)/kg of body weight (BW) (PEJ2) by daily gavage. Compounds #57, 44, 99, 63 and 74 were not shown because had only the molecular formula. \**p* < 0.05 vs other groups.

statistically highlighted in the HFS group when compared other groups: nicotinuric acid and malonylcarnitine. Nicotinuric acid was also pointed as a CVD biomarker (WANG et al., 2018).

Untargeted metabolomics performed in the urine of mice after acute administration of the PEJ revealed a clear tendency of separation among groups CH, HFS and PEJ2. Among 30 statistically different metabolites, two compounds associated with impaired fatty acid metabolism were found mostly in the HFS group. Although the PEJ2 group do not show strong similarity with the CH group, the clustering of its metabolites was different when compared to the HFS group, suggesting distinct metabolic profile.

## 5. Conclusions

PEJ showed several therapeutic properties against diet-induced obesity. PEJ prevented excessive BWG and excessive WAT gain in mice with already established obesity. Animals treated with PEJ showed decreased adipocyte hyperplasia and inflammation caused by adiposopathy.

PEJ improved the glucose metabolism by reducing FBG, glucose intolerance, insulinemia and insulin resistance and modulating the AKT/mTORC pathway in liver, skeletal muscle, and WAT, as well as increase GLUT4 expression in skeletal muscle.

Similarly, PEJ also improved lipid metabolism, decreasing TC and LDL-cholesterol plasma levels, TC and TAG hepatic levels, NEFA plasma concentration and hepatic inflammation, fighting NFLD. Along this, PEJ increased EE and UCP1 expression in WAT, contributing with energy homeostasis.

PEJ also positively altered the gut microbiome, supplemented animals showed reduced F/B ratio and changed beta diversity pattern. Finally, untargeted metabolomic revealed that supplemented animals had changed metabolic production in relation to obese group.

Thus, our findings indicate that the long-term PEJ supplementation might be used as adjuvant against obesity, dysglycemia, dyslipidemia, in addition, have potential to positively alter the gut microbial community.

Additional analyses are needed to understand other important mechanisms of action of these compounds in inflammation and intestinal barrier, for example. Similarly, it is needed to expand the knowledge about gut microbiome under PEJ supplementation. Another information that should be better comprehend is related to the metabolic production after PEJ ingesting to try identifying possible health/disease marker. To conclude, we suggest submitting the PEJ or similar extract from jaboticaba to clinical trials.

## 6. References

ALEZANDRO, Marcela Roquim; DUBÉ, Pascal; DESJARDINS, Yves; LAJOLO, Franco Maria; GENOVESE, Maria Inés. Comparative study of chemical and phenolic compositions of two species of jaboticaba: *Myrciaria jaboticaba* (Vell.) Berg and *Myrciaria cauliflora* (Mart.) O. Berg. **Food Research International**, [S. l.], v. 54, n. 1, p. 468–477, 2013. DOI: 10.1016/j.foodres.2013.07.018.

ALEZANDRO, Marcela Roquim; GRANATO, Daniel; GENOVESE, Maria Inés. Jaboticaba (*Myrciaria jaboticaba* (Vell.) Berg), a Brazilian grape-like fruit, improves plasma lipid profile in streptozotocin-mediated oxidative stress in diabetic rats. **Food Research International**, [S. l.], v. 54, n. 1, p. 650–659, 2013. DOI: 10.1016/j.foodres.2013.07.041. Disponível em: <http://dx.doi.org/10.1016/j.foodres.2013.07.041>.

ANHÊ, Fernando F. et al. A polyphenol-rich cranberry extract reverses insulin resistance and hepatic steatosis independently of body weight loss. **Molecular Metabolism**, [S. l.], v. 6, n. 12, p. 1563–1573, 2017. DOI: 10.1016/j.molmet.2017.10.003. Disponível em: <https://doi.org/10.1016/j.molmet.2017.10.003>.

AOAC. **AOAC Official Method of Analysis**. 18. ed. Gaithersburg: AOAC International, 2005.

ARHA, Deepti et al. Isoalantolactone derivative promotes glucose utilization in skeletal muscle cells and increases energy expenditure in db/db mice via activating AMPK-dependent signaling. **Molecular and Cellular Endocrinology**, [S. l.], v. 460, p. 134–151, 2018. DOI: 10.1016/j.mce.2017.07.015. Disponível em: <https://doi.org/10.1016/j.mce.2017.07.015>.

BALISTEIRO, Diully Mata; ARAUJO, Renata Luise De; GIACAGLIA, Luciano Ricardo; GENOVESE, Maria Inés. Effect of clarified Brazilian native fruit juices on postprandial glycemia in healthy subjects. **Food Research International**, [S. l.], v. 100, n. August, p. 196–203, 2017. DOI: 10.1016/j.foodres.2017.08.044.

BAO, Yifan; XIAO, Jianbo; WENG, Zebin; LU, Xinyi; SHEN, Xinchun; WANG, Fang. A

phenolic glycoside from *Moringa oleifera* Lam. improves the carbohydrate and lipid metabolisms through AMPK in db/db mice. **Food Chemistry**, [S. l.], v. 311, n. November 2019, p. 125948, 2020. DOI: 10.1016/j.foodchem.2019.125948. Disponível em: <https://doi.org/10.1016/j.foodchem.2019.125948>.

BASELGA-ESCUADERO, Laura; PASCUAL-SERRANO, Aïda; RIBAS-LATRE, Aleix; CASANOVA, Ester; SALVADÓ, M. Josepa; AROLA, Lluís; AROLA-ARNAL, Anna; BLADÉ, Cinta. Long-term supplementation with a low dose of proanthocyanidins normalized liver miR-33a and miR-122 levels in high-fat diet-induced obese rats. **Nutrition Research**, [S. l.], v. 35, n. 4, p. 337–345, 2015. DOI: 10.1016/j.nutres.2015.02.008. Disponível em: <http://dx.doi.org/10.1016/j.nutres.2015.02.008>.

BASTOS, Deborah H. M.; ROGERO, Marcelo M.; ARÊAS, Jose A. G. Mecanismos de ação de compostos bioativos dos alimentos no contexto de processos inflamatórios relacionados à obesidade. **Arq Bras Endocrinol Metab**, [S. l.], v. 53, n. 5, p. 646–56, 2009. DOI: 10.1590/S0004-27302009000500017.

BATISTA, Ângela Giovana et al. Intake of jaboricaba peel attenuates oxidative stress in tissues and reduces circulating saturated lipids of rats with high-fat diet-induced obesity. **Journal of Functional Foods**, [S. l.], v. 6, n. 1, p. 450–461, 2014. DOI: 10.1016/j.jff.2013.11.011.

BELLIK, Yuva; BOUKRAË, Laïd; ALZHRANI, Hasan A.; BAKHOTMAH, Balkees A.; ABDELLAH, Fatiha; HAMMOUDI, S. M.; IGUER-OUADA, Mokrane. Molecular mechanism underlying anti-inflammatory and anti-allergic activities of phytochemicals: an update. **Molecules (Basel, Switzerland)**, [S. l.], v. 18, n. 1, p. 322–353, 2012. DOI: 10.3390/molecules18010322.

BIDEN, Trevor J.; BOSLEM, Ebru; CHU, Kwan Yi; SUE, Nancy. Lipotoxic endoplasmic reticulum stress,  $\beta$  cell failure, and type 2 diabetes mellitus. **Trends in endocrinology and metabolism: TEM**, [S. l.], v. 25, n. 8, p. 389–398, 2014. DOI: 10.1016/j.tem.2014.02.003. Disponível em: <http://www.ncbi.nlm.nih.gov/pubmed/24656915>.

BOUTAGY, Nabil E.; MCMILLAN, Ryan P.; FRISARD, Madlyn I.; HULVER, Matthew W.; TRANSLATIONAL, Fralin; TECH, Virginia; CORE, Metabolic Phenotyping; TECH, Virginia. Metabolic endotoxemia with obesity: Is it real and is it relevant? **Biochimie**, [S. l.], v. 124, n. 2016, p. 11–20, 2016. DOI: 10.1016/j.biochi.2015.06.020.

BRESCIANI, Letizia et al. Absorption profile of (Poly)phenolic compounds after consumption of three food supplements containing 36 different fruits, vegetables, and berries. **Nutrients**, [S. l.], v. 9, n. 3, p. 1–17, 2017. DOI: 10.3390/nu9030194.

BUCHHOLZ, Tina; MELZIG, Matthias F. Medicinal Plants Traditionally Used for Treatment of Obesity and Diabetes Mellitus - Screening for Pancreatic Lipase and  $\alpha$ -Amylase Inhibition. **Phytotherapy Research**, [S. l.], v. 30, n. 2, p. 260–266, 2016. DOI: 10.1002/ptr.5525.

CASTANER, Olga; GODAY, Albert; PARK, Yong-Moon; LEE, Seung-Hwan; MAGKOS, Faidon; SHIOW, Sue-Anne Toh Ee; SCHRÖDER, Helmut. The Gut Microbiome Profile in Obesity: A Systematic Review. **International Journal of Endocrinology**, [S. l.], v. 2018, p. 1–2, 2018. DOI: 10.1155/2018/9109451.

CERULLI, Antonietta; NAPOLITANO, Assunta; MASULLO, Milena; HOŠEK, Jan; PIZZA, Cosimo; PIACENTE, Sonia. Chestnut shells (Italian cultivar “Marrone di Roccadaspide” PGI): Antioxidant activity and chemical investigation with in depth LC-HRMS/MSn rationalization of tannins. **Food Research International**, [S. l.], 2020. DOI: 10.1016/j.foodres.2019.108787.

CITADIN, Idemir; DANNER, Moeses Andriago;; SASSO, Simone Aparecida Zolet. Jabuticabeiras. **Revista Brasileira de Fruticultura**, [S. l.], v. 32, n. 2, p. 343–656, 2010.

CLIFFORD, Michael N.; SCALBERT, Augustin. Review Ellagitannins – nature , occurrence and dietary burden. **Journal of the Science of Food and Agriculture**, [S. l.], v. 80, n. November 1999, p. 1118–1125, 2000. DOI: 10.1002/(SICI)1097-0010(20000515).

CROZIER, Alan; JAGANATH, Indu B.; CLIFFORD, Michael N. Dietary phenolics: chemistry, bioavailability and effects on health. **Natural product reports**, [S. l.], v. 26, n. 8, p. 1001–1043, 2009. DOI: 10.1039/b802662a.

DEL RIO, Daniele; RODRIGUEZ-MATEOS, Ana; SPENCER, Jeremy P. E. E.; TOGNOLINI, Massimiliano; BORGES, Gina; CROZIER, Alan. Dietary (poly)phenolics in human health: Structures, bioavailability, and evidence of protective effects against chronic diseases. **Antioxidants and Redox Signaling**, [S. l.], v. 18, n. 14, p. 1818–1892, 2013. DOI: 10.1089/ars.2012.4581. Disponível em: <http://www.ncbi.nlm.nih.gov/pubmed/22794138%255Cnhttp://www.pubmedcentral.nih.gov/articlerender.fcgi?artid=3619154&tool=pmcentrez&rendertype=abstract>.

DI DONNA, Leonardo; IACOPETTA, Domenico; CAPPELLO, Anna R.; GALLUCCI, Giselda; MARTELLO, Emanuela; FIORILLO, Marco; DOLCE, Vincenza; SINDONA, Giovanni. Hypocholesterolaemic activity of 3-hydroxy-3-methyl-glutaryl flavanones enriched fraction from bergamot fruit (*Citrus bergamia*): “In vivo” studies. **Journal of Functional Foods**, [S. l.], v. 7, n. 1, p. 558–568, 2014. DOI: 10.1016/j.jff.2013.12.029.

DONADO-PESTANA, Carlos M.; BELCHIOR, Thiago; GENOVESE, Maria Inés. Phenolic compounds from cagaita (*Eugenia dysenterica* DC.) fruit prevent body weight and fat mass gain induced by a high-fat, high-sucrose diet. **Food Research International**, [S. l.], v. 77, p. 177–185, 2015. DOI: 10.1016/j.foodres.2015.06.044. Disponível em: <http://dx.doi.org/10.1016/j.foodres.2015.06.044>.

DONADO-PESTANA, Carlos M.; DOS SANTOS-DONADO, Priscila R.; DAZA, Luis Daniel; BELCHIOR, Thiago; FESTUCCIA, William T.; GENOVESE, Maria Inés. Cagaita fruit (*Eugenia dysenterica* DC.) and obesity: Role of polyphenols on already established obesity. **Food Research International**, [S. l.], v. 103, n. September 2017, p. 40–47, 2018. DOI: 10.1016/j.foodres.2017.10.011.

DONADO-PESTANA, Carlos M.; PESSOA, Érika V. M.; RODRIGUES, Larissa; MOURA, Márcio H. C.; SANTOS-DONADO, Priscila R.; CASTRO, Érique; FESTUCCIA, William T.; GENOVESE, Maria Inés. Polyphenols of cambuci (*Campomanesia phaea* (O. Berg.) fruit ameliorate insulin resistance and hepatic steatosis in obese mice. **Food Chemistry**, [S. l.], p. 128169, 2020. DOI: 10.1016/j.foodchem.2020.128169. Disponível em: <https://doi.org/10.1016/j.foodchem.2020.128169>.

EMANUELA, Faloia; GRAZIA, Michetti; MARCO, De Robertis; MARIA PAOLA, Luconi; GIORGIO, Furlani; MARCO, Boscaro. Inflammation as a link between obesity and

metabolic syndrome. **Journal of Nutrition and Metabolism**, [S. l.], v. 2012, 2012. DOI: 10.1155/2012/476380.

EVEN, P. C.; NADKARNI, N. A. Indirect calorimetry in laboratory mice and rats: principles, practical considerations, interpretation and perspectives. **AJP: Regulatory, Integrative and Comparative Physiology**, [S. l.], v. 303, n. 5, p. R459–R476, 2012. DOI: 10.1152/ajpregu.00137.2012. Disponível em: <http://ajpregu.physiology.org/cgi/doi/10.1152/ajpregu.00137.2012>.

GARCÍA-VILLALBA, Rocío et al. Validated Method for the Characterization and Quantification of Extractable and Nonextractable Ellagitannins after Acid Hydrolysis in Pomegranate Fruits, Juices, and Extracts. **Journal of Agricultural and Food Chemistry**, [S. l.], v. 63, n. 29, p. 6555–6566, 2015. DOI: 10.1021/acs.jafc.5b02062.

GARCÍA, Carlos J.; GIL, María I.; TOMAS-BARBERAN, Francisco A. LC–MS untargeted metabolomics reveals early biomarkers to predict browning of fresh-cut lettuce. **Postharvest Biology and Technology**, [S. l.], v. 146, n. August, p. 9–17, 2018. DOI: 10.1016/j.postharvbio.2018.07.011. Disponível em: <https://doi.org/10.1016/j.postharvbio.2018.07.011>.

GENOVESE, M. I.; PINTO, M. D. S.; GONCALVES, A. E. S. S.; LAJOLO, F. M.; DA SILVA PINTO, M.; DE SOUZA SCHMIDT GONCALVES, A. E.; LAJOLO, F. M. Bioactive Compounds and Antioxidant Capacity of Exotic Fruits and Commercial Frozen Pulps from Brazil. **Food Science and Technology International**, [S. l.], v. 14, n. 3, p. 207–214, 2008. DOI: 10.1177/1082013208092151. Disponível em: <http://fst.sagepub.com/cgi/doi/10.1177/1082013208092151>.

GORROCHATEGUI, Eva; JAUMOT, Joaquim; LACORTE, Sílvia; TAULER, Romà. Data analysis strategies for targeted and untargeted LC-MS metabolomic studies: Overview and workflow. **TrAC - Trends in Analytical Chemistry**, [S. l.], v. 82, p. 425–442, 2016. DOI: 10.1016/j.trac.2016.07.004. Disponível em: <http://dx.doi.org/10.1016/j.trac.2016.07.004>.

HANHINEVA, Kati; TÖRRÖNEN, Riitta; BONDIA-PONS, Isabel; PEKKINEN, Jenna; KOLEHMAINEN, Marjukka; MYKKÄNEN, Hannu; POUTANEN, Kaisa. Impact of dietary polyphenols on carbohydrate metabolism. **International Journal of Molecular**

**Sciences**, [S. l.], v. 11, n. 4, p. 1365–1402, 2010. DOI: 10.3390/ijms11041365.

HARA, Atsushi; RADIN, Norman S. Lipid extraction of tissues with a low-toxicity solvent. **Analytical Biochemistry**, [S. l.], v. 90, n. 1, p. 420–426, 1978. DOI: 10.1016/0003-2697(78)90046-5. Disponível em: <http://www.sciencedirect.com/science/article/pii/0003269778900465>.

HARIRI, Niloofar; THIBAUT, Louise. High-fat diet-induced obesity in animal models. **Nutrition research reviews**, [S. l.], v. 23, n. 2, p. 270–99, 2010. DOI: 10.1017/S0954422410000168. Disponível em: [http://journals.cambridge.org/abstract\\_S0954422410000168](http://journals.cambridge.org/abstract_S0954422410000168).

HOTAMISLIGIL, Gokhan S. Inflammation and metabolic disorders. **Nature**, [S. l.], v. 444, n. 7121, p. 860–867, 2006. DOI: 10.1038/nature05485. Disponível em: <http://dx.doi.org/10.1038/nature05485>.

HSU, Jeng Dong; WU, Chia Chun; HUNG, Chi Nan; WANG, Chau Jong; HUANG, Hui Pei. *Myrciaria cauliflora* extract improves diabetic nephropathy via suppression of oxidative stress and inflammation in streptozotocin-nicotinamide mice. **Journal of Food and Drug Analysis**, [S. l.], v. 24, n. 4, p. 730–737, 2016. DOI: 10.1016/j.jfda.2016.03.009.

HUANG, Xingjun; LIU, Guihua; GUO, Jiao; SU, Zhengquan. The PI3K/AKT pathway in obesity and type 2 diabetes. **International Journal of Biological Sciences**, [S. l.], v. 14, n. 11, p. 1483–1496, 2018. DOI: 10.7150/ijbs.27173. Disponível em: <http://www.ijbs.com/v14p1483.htm>.

IBGE. **Pesquisa nacional de saúde 2013: Ciclos de vida**. Rio de Janeiro: Ministério da Saúde, 2015. DOI: ISSN 0101-4234.

INADA, Kim Ohanna Pimenta; SILVA, Tamirys Barcellos Revorêdo; LOBO, Leandro Araújo; DOMINGUES, Regina Maria Cavalcante Pilotto; PERRONE, Daniel; MONTEIRO, Mariana. Bioaccessibility of phenolic compounds of jaboticaba (*Plinia jaboticaba*) peel and seed after simulated gastrointestinal digestion and gut microbiota fermentation. **Journal of Functional Foods**, [S. l.], v. 67, n. November 2019, p. 103851, 2020. DOI: 10.1016/j.jff.2020.103851. Disponível em: <https://doi.org/10.1016/j.jff.2020.103851>.

KAMIO, Naoya; SUZUKI, Takuma; WATANABE, Yuto; SUHARA, Yoshitomo; OSAKABE, Naomi. A single oral dose of flavan-3-ols enhances energy expenditure by sympathetic nerve stimulation in mice. **Free Radical Biology and Medicine**, [S. l.], v. 91, p. 256–263, 2016. DOI: 10.1016/j.freeradbiomed.2015.12.030. Disponível em: <http://dx.doi.org/10.1016/j.freeradbiomed.2015.12.030>.

KAN, Juan; CHEN, Cuicui; HUO, Tongbin; XIE, Wangjin; HUI, Yaoyao; LIU, Jun; JIN, Chang Hai. Polyphenolic-enriched peach peels extract regulates lipid metabolism and improves the gut microbiota composition in high fat diet-fed mice. **Journal of Functional Foods**, [S. l.], v. 72, n. July, p. 104082, 2020. DOI: 10.1016/j.jff.2020.104082. Disponível em: <https://doi.org/10.1016/j.jff.2020.104082>.

KANAMOTO, Yuki; YAMASHITA, Yoko; NANBA, Fumio; YOSHIDA, Tadashi; TSUDA, Takanori; FUKUDA, Itsuko; NAKAMURA-TSURUTA, Sachiko; ASHIDA, Hitoshi. A black soybean seed coat extract prevents obesity and glucose intolerance by up-regulating uncoupling proteins and down-regulating inflammatory cytokines in high-fat diet-fed mice. **Journal of Agricultural and Food Chemistry**, [S. l.], v. 59, n. 16, p. 8985–8993, 2011. DOI: 10.1021/jf201471p.

KANG, Chao et al. Gut microbiota mediates the protective effects of dietary capsaicin against chronic low-grade inflammation and associated obesity induced by high-fat diet. **mBio**, [S. l.], v. 8, n. 3, p. 1–15, 2017. DOI: 10.1128/mBio.00470-17.

KENNEDY, A.; MARTINEZ, K.; CHUANG, C. C.; LAPOINT, K.; MCINTOSH, M. Saturated Fatty Acid-Mediated Inflammation and Insulin Resistance in Adipose Tissue: Mechanisms of Action and Implications. **Journal of Nutrition**, [S. l.], v. 139, n. 1, p. 1–4, 2008. DOI: 10.3945/jn.108.098269. Disponível em: <http://jn.nutrition.org/cgi/doi/10.3945/jn.108.098269>.

KHAMZINA, Leila; VEILLEUX, Alain; BERGERON, Sébastien; MARETTE, André. Increased activation of the mammalian target of rapamycin pathway in liver and skeletal muscle of obese rats: Possible involvement in obesity-linked insulin resistance. **Endocrinology**, [S. l.], v. 146, n. 3, p. 1473–1481, 2005. DOI: 10.1210/en.2004-0921.

KIM, Sang Nam et al. Antiobesity effects of coumestrol through expansion and activation of brown adipose tissue metabolism. **Journal of Nutritional Biochemistry**, [S. l.], v. 76, p. 108300, 2020. DOI: 10.1016/j.jnutbio.2019.108300. Disponível em: <https://doi.org/10.1016/j.jnutbio.2019.108300>.

KITRYTĖ, Vaida; NARKEVIČIŪTĖ, Aistė; TAMKUTĖ, Laura; SYRPAS, Michail; PUKALSKIENĖ, Milda; VENSKUTONIS, Petras Rimantas. Consecutive high-pressure and enzyme assisted fractionation of blackberry (*Rubus fruticosus* L.) pomace into functional ingredients: Process optimization and product characterization. **Food Chemistry**, [S. l.], 2020. DOI: 10.1016/j.foodchem.2019.126072.

KOWALSKA, Katarzyna; OLEJNIK, Anna; ZIELIŃSKA-WASIELICA, Joanna; OLKOWICZ, Mariola. Raspberry (*Rubus idaeus* L.) fruit extract decreases oxidation markers, improves lipid metabolism and reduces adipose tissue inflammation in hypertrophied 3T3-L1 adipocytes. **Journal of Functional Foods**, [S. l.], v. 62, n. May, 2019. DOI: 10.1016/j.jff.2019.103568.

LACROIX, Isabelle M. E.; LI-CHAN, Eunice C. Y. Overview of food products and dietary constituents with antidiabetic properties and their putative mechanisms of action: A natural approach to complement pharmacotherapy in the management of diabetes. **Molecular Nutrition and Food Research**, [S. l.], v. 58, n. 1, p. 61–78, 2014. DOI: 10.1002/mnfr.201300223. Disponível em: <http://doi.wiley.com/10.1002/mnfr.201300223>.

LAMAS, C. A. et al. Jaboticaba extract prevents prediabetes and liver steatosis in high-fat-fed aging mice. **Journal of Functional Foods**, [S. l.], v. 47, n. June, p. 434–446, 2018. DOI: 10.1016/j.jff.2018.06.005. Disponível em: <https://doi.org/10.1016/j.jff.2018.06.005>.

LEE, Dong Young; KIM, Hyun Woo; YANG, Heejung; SUNG, Sang Hyun. Hydrolyzable tannins from the fruits of *Terminalia chebula* Retz and their  $\alpha$ -glucosidase inhibitory activities. **Phytochemistry**, [S. l.], 2017. DOI: 10.1016/j.phytochem.2017.02.006.

LEMIEUX, Christian; PICARD, Frédéric; LABRIE, Fernand; RICHARD, Denis; DESHAIES, Yves. The estrogen antagonist EM-652 and dehydroepiandrosterone prevent diet- and ovariectomy-induced obesity. **Obesity Research**, [S. l.], v. 11, n. 3,

p. 477–490, 2003. DOI: 10.1038/oby.2003.65. Disponível em: <http://www.ncbi.nlm.nih.gov/pubmed/12634448%5Cnhttp://onlinelibrary.wiley.com/doi/10.1038/oby.2003.65/asset/oby.2003.65.pdf?v=1&t=hja2f9ix&s=016584df4b147f8b8d1cc62f094c230862699d03>.

LI, Hua; PARK, Hye Mi Ho Yong Hye Mi; JI, Hyeon Seon; HAN, Jisu; KIM, Sang Kyum; PARK, Hye Mi Ho Yong Hye Mi; JEONG, Tae Sook. Phenolic-enriched blueberry-leaf extract attenuates glucose homeostasis, pancreatic  $\beta$ -cell function, and insulin sensitivity in high-fat diet–induced diabetic mice. **Nutrition Research**, [S. l.], v. 73, p. 83–96, 2020. a. DOI: 10.1016/j.nutres.2019.09.005. Disponível em: <https://doi.org/10.1016/j.nutres.2019.09.005>.

LI, Yulan; CHEN, Dan; ZHANG, Feng; LIN, Yuping; MA, Yage; ZHAO, Shenglan; CHEN, Chaoyin; WANG, Xiaoshuang; LIU, Ji. Preventive effect of pressed degreased walnut meal extracts on T2DM rats by regulating glucolipid metabolism and modulating gut bacteria flora. **Journal of Functional Foods**, [S. l.], 2020. b. DOI: 10.1016/j.jff.2019.103694.

MAGALHÃES, Luís M.; SANTOS, Fernando; SEGUNDO, Marcela A.; REIS, Salette; LIMA, José L. F. C. Rapid microplate high-throughput methodology for assessment of Folin-Ciocalteu reducing capacity. **Talanta**, [S. l.], v. 83, n. 2, p. 441–447, 2010. DOI: 10.1016/j.talanta.2010.09.042.

MANNING, Brendan D.; TOKER, Alex. AKT/PKB Signaling: Navigating the Network. **Cell**, [S. l.], v. 169, n. 3, p. 381–405, 2017. DOI: 10.1016/j.cell.2017.04.001. Disponível em: <http://dx.doi.org/10.1016/j.cell.2017.04.001>.

MARQUES, Tamara R.; CAETANO, Aline A.; SIMÃO, Anderson A.; CASTRO, Flávia Cíntia de O.; RAMOS, Vinicius de Oliveira; CORRÊA, Angelita D. Metanolic extract of *Malpighia emarginata* bagasse: Phenolic compounds and inhibitory potential on digestive enzymes. **Brazilian Journal of Pharmacognosy**, [S. l.], v. 26, n. 2, p. 191–196, 2016. DOI: 10.1016/j.bjp.2015.08.015. Disponível em: <http://dx.doi.org/10.1016/j.bjp.2015.08.015>.

MARRELLI, Mariangela; LOIZZO, Monica Rosa; NICOLETTI, Marcello; MENICHINI, Francesco; CONFORTI, Filomena. Inhibition of key enzymes linked to obesity by

preparations from mediterranean dietary plants: effects on  $\alpha$ -amylase and pancreatic lipase activities. **Plant Foods for Human Nutrition**, [S. l.], v. 68, n. 4, p. 340–346, 2013. DOI: 10.1007/s11130-013-0390-9.

MIRANDA, A. M.; STELUTI, J.; FISBERG, R. M.; MARCHIONI, D. M. Dietary intake and food contributors of polyphenols in adults and elderly adults of Sao Paulo: a population-based study. **British Journal of Nutrition**, [S. l.], v. 115, n. 6, p. 1061–1070, 2016. DOI: 10.1017/S0007114515005061. Disponível em: [http://www.journals.cambridge.org/abstract\\_S0007114515005061](http://www.journals.cambridge.org/abstract_S0007114515005061).

MOLINA-GARCÍA, L.; MARTÍNEZ-EXPÓSITO, R.; FERNÁNDEZ-DE CÓRDOVA, M. L.; LLORENT-MARTÍNEZ, E. J. Determination of the Phenolic Profile and Antioxidant Activity of Leaves and Fruits of Spanish Quercus coccifera. **Journal of Chemistry**, [S. l.], v. 2018, 2018. DOI: 10.1155/2018/2573270.

MOURA, Márcio Hércules Caldas; CUNHA, Maria Gabriela; ALEZANDRO, Marcela Roquim; GENOVESE, Maria Inés. Phenolic-rich jaboticaba (*Plinia jaboticaba* (Vell.) Berg) extracts prevent high-fat-sucrose diet-induced obesity in C57BL/6 mice. **Food Research International**, [S. l.], v. 107, n. January, p. 48–60, 2018. DOI: 10.1016/j.foodres.2018.01.071. Disponível em: <https://doi.org/10.1016/j.foodres.2018.01.071>.

MYERS, Norman; FONSECA, Gustavo a B.; MITTERMEIER, Russell a; FONSECA, G. a B.; KENT, Jennifer. Biodiversity hotspots for conservation priorities. **Nature**, [S. l.], v. 403, n. 6772, p. 853–858, 2000. DOI: 10.1038/35002501. Disponível em: <http://www.ncbi.nlm.nih.gov/pubmed/10706275>.

NELSON, David L.; COX, Michael M. **Princípios de Bioquímica de Lehninger**. 6. ed. Porto Alegre: Artmed, 2014. DOI: 10.2307/j.ctvk8vxxm.7.

OOI, Der Jiun; AZMI, Nur Hanisah; IMAM, Mustapha Umar; ALITHEEN, Noorjahan Banu; ISMAIL, Maznah. Curculigoside and polyphenol-rich ethyl acetate fraction of *Molineria latifolia* rhizome improved glucose uptake via potential mTOR/AKT activated GLUT4 translocation. **Journal of Food and Drug Analysis**, [S. l.], v. 26, n. 4, p. 1253–1264, 2018. DOI: 10.1016/j.jfda.2018.03.003. Disponível em: <https://doi.org/10.1016/j.jfda.2018.03.003>.

PALACIOS-GONZÁLEZ, Berenice et al. Genistein increases the thermogenic program of subcutaneous WAT and increases energy expenditure in mice. **Journal of Nutritional Biochemistry**, [S. l.], v. 68, p. 59–68, 2019. DOI: 10.1016/j.jnutbio.2019.03.012.

PARLEE, Sebastian D.; LENTZ, Stephen I.; MORI, Hiroyuki; MACDOUGALD, Ormond A. Quantifying Size and Number of Adipocytes in Adipose Tissue. **Methods Enzymol**, [S. l.], v. 537, n. 1, p. 93–122, 2014. DOI: 10.1038/jid.2014.371.

PATEL, Payal S.; BURAS, Eric D.; BALASUBRAMANYAM, A. The Role of the Immune System in Obesity and Insulin Resistance. **Journal of Obesity**, [S. l.], v. 2013, p. 1–9, 2013. DOI: <http://dx.doi.org/10.1155/2013/616193>.

PERDICARO, Diahann J.; RODRIGUEZ LANZI, Cecilia; GAMBARTE TUDELA, Julián; MIATELLO, Roberto M.; OTEIZA, Patricia I.; VAZQUEZ PRIETO, Marcela A. Quercetin attenuates adipose hypertrophy, in part through activation of adipogenesis in rats fed a high-fat diet. **Journal of Nutritional Biochemistry**, [S. l.], v. 79, p. 108352, 2020. DOI: 10.1016/j.jnutbio.2020.108352. Disponível em: <https://doi.org/10.1016/j.jnutbio.2020.108352>.

PEREIRA, Luciane Dias; BARBOSA, João Marcos Gonçalves; RIBEIRO DA SILVA, Antonio Jorge; FERRI, Pedro Henrique; SANTOS, Suzana Costa. Polyphenol and Ellagitannin Constituents of Jaboticaba (*Myrciaria cauliflora*) and Chemical Variability at Different Stages of Fruit Development. **Journal of Agricultural and Food Chemistry**, [S. l.], v. 65, n. 6, p. 1209–1219, 2017. DOI: 10.1021/acs.jafc.6b02929.

PERRY, Rachel J.; SAMUEL, Varman T.; PETERSEN, Kitt F.; SHULMAN, Gerald I. The role of hepatic lipids in hepatic insulin resistance and type 2 diabetes. **Nature**, [S. l.], v. 510, n. 7503, p. 84–91, 2014. DOI: 10.1038/nature13478. Disponível em: <http://www.nature.com/doi/10.1038/nature13478> <http://www.ncbi.nlm.nih.gov/pubmed/24899308>.

**PHE. Excess Weight and COVID-19 Insights from new evidence About Public Health England.** London.

PLAZA, Merichel; BATISTA, Ângela Giovana; CAZARIN, Cinthia Baú Betim; SANDAHL, Margareta; TURNER, Charlotta; ÖSTMAN, Elin; MARÓSTICA JÚNIOR,

Mário Roberto. Characterization of antioxidant polyphenols from *Myrciaria jaboticaba* peel and their effects on glucose metabolism and antioxidant status: A pilot clinical study. **Food Chemistry**, [S. l.], v. 211, p. 185–197, 2016. DOI: 10.1016/j.foodchem.2016.04.142. Disponível em: <http://dx.doi.org/10.1016/j.foodchem.2016.04.142>.

PRIOR, Ronald L.; FAN, Ellen; JI, Hongping; HOWELL, Amy; NIO, Christian; PAYNE, Mark J.; REED, Jess; PAYNE, Mark J.; REED, Jess. Multi-laboratory validation of a standard method for quantifying proanthocyanidins in cranberry powders. **Journal of the Science of Food and Agriculture**, [S. l.], v. 90, n. 9, p. 1473–1478, 2010. DOI: 10.1002/jsfa.3966. Disponível em: <http://doi.wiley.com/10.1002/jsfa.3966>.

QIIME2. **Moving Pictures tutorial**. 2020. Disponível em: <https://docs.qiime2.org/2020.2/>. Acesso em: 1 mar. 2020.

QUATRIN, A. et al. Characterization and quantification of tannins, flavonols, anthocyanins and matrix-bound polyphenols from *jaboticaba* fruit peel: A comparison between *Myrciaria trunciflora* and *M. jaboticaba*. **Journal of Food Composition and Analysis**, [S. l.], v. 78, n. June 2018, p. 59–74, 2019. DOI: 10.1016/j.jfca.2019.01.018. Disponível em: <https://doi.org/10.1016/j.jfca.2019.01.018>.

REEVES, Philip G.; NIELSEN, Forrest H.; FAHEY, George C. AIN-93 Purified Diets for Laboratory Rodents: Final Report of the American Institute of Nutrition Ad of the AIN-76A Rodent Diet Hoc Writing Committee on the Reformulation of the AIN-76A Rodent Diet. **The Journal of Nutrition**, [S. l.], v. 123, p. 1939–1951, 1993.

ROBERTS, Christian K.; HEVENER, Andrea L.; BARNARD, R. James. Metabolic Syndrome and Insulin Resistance: Underlying Causes and Modification by Exercise Training. **Comprehensive Physiology**, [S. l.], v. 3, n. 1, p. 1–58, 2014. DOI: 10.1002/cphy.c110062.Metabolic.

SALOMONE, Federico et al. Higher phenolic acid intake independently associates with lower prevalence of insulin resistance and non-alcoholic fatty liver disease. **JHEP Reports**, [S. l.], v. 2, n. 2, p. 100069, 2020. DOI: 10.1016/j.jhepr.2020.100069. Disponível em: <http://dx.doi.org/10.1016/j.jhepr.2020.100069>.

SHEIKHOLESLAMI, Mahsa N.; GÓMEZ-CANELA, Cristian; BARRON, Leon P.;

BARATA, Carlos; VOSOUGH, Maryam; TAULER, Roma. Untargeted metabolomics changes on *Gammarus pulex* induced by propranolol, triclosan, and nimesulide pharmaceutical drugs. **Chemosphere**, [S. l.], v. 260, 2020. DOI: 10.1016/j.chemosphere.2020.127479.

SHIMIZU, Tomohiko; MIURA, Shin-Ichiro; TANIGAWA, Hiroyuki; KUWANO, Takashi; ZHANG, Bo; UEHARA, Yoshinari; SAKU, Keijiro. Rosuvastatin Activates ATP-Binding Cassette Transporter A1-Dependent Efflux Ex Vivo and Promotes Reverse Cholesterol Transport in Macrophage Cells in Mice Fed a High-Fat Diet. **Arteriosclerosis, thrombosis, and vascular biology**, [S. l.], v. 34, n. 10, p. 2246–53, 2014. DOI: 10.1161/ATVBAHA.114.303715. Disponível em: <http://www.ncbi.nlm.nih.gov/pubmed/25104799>.

SILVA, Maria Elizabeth Rossi. Obesidade e metabolismo de carboidratos: a diabetes. In: MANCINI, Marcio C. (org.). **Tratado da Obesidade**. 2. ed. Rio de Janeiro: Guanabara Koogan, 2015. p. 265.

SILVA, Rangel Moreira; PEREIRA, Luciane Dias; VÉRAS, Jefferson Hollanda; VALE, Camila Regina Do; CHEN-CHEN, Lee; SANTOS, Suzana da Costa. Protective effect and induction of DNA repair by *Myrciaria cauliflora* seed extract and pedunculagin on cyclophosphamide-induced genotoxicity. **Mutation Research - Genetic Toxicology and Environmental Mutagenesis**, [S. l.], v. 810, p. 40–47, 2016. DOI: 10.1016/j.mrgentox.2016.10.001.

SUGUINO, Eduardo; MARTINS, A. N.; TURCO, P. H. N.; CIVIDANES, T. M. S.; FARIA, A. M. A cultura da jabuticabeira. **Pesquisa & Tecnologia**, [S. l.], v. 9, n. 1, 2012. Disponível em: <http://www.aptaregional.sp.gov.br>.

TABARELLI, Marcelo. Biodiversidade na Mata Atlântica brasileira Desafios e oportunidades para a conservação da biodiversidade na Mata Atlântica brasileira. **Megadiversidades**, [S. l.], v. 1, n. July 2015, p. 132–138, 2005.

TANAKA, Miori; SUGAMA, Ayako; SUMI, Kanako; SHIMIZU, Kozue; KISHIMOTO, Yoshimi; KONDO, Kazuo; IIDA, Kaoruko. Gallic acid regulates adipocyte hypertrophy and suppresses inflammatory gene expression induced by the paracrine interaction between adipocytes and macrophages in vitro and in vivo. **Nutrition Research**, [S. l.],

v. 73, p. 58–66, 2020. DOI: 10.1016/j.nutres.2019.09.007. Disponível em: <https://doi.org/10.1016/j.nutres.2019.09.007>.

WANG, Shu; MOUSTAID-MOUSSA, Naima; CHEN, Lixia; MO, Huanbiao; SHASTRI, Anuradha; SU, Rui; BAPAT, Priyanka; KWUN, Insook; SHEN, Chwan-Li. Novel insights of dietary polyphenols and obesity. **The Journal of Nutritional Biochemistry**, [S. l.], v. 25, p. 1–18, 2014. DOI: 10.1016/j.jnutbio.2013.09.001. Disponível em: [http://www.jnutbio.com/article/S0955-2863\(13\)00161-7/pdf](http://www.jnutbio.com/article/S0955-2863(13)00161-7/pdf). Acesso em: 13 mar. 2017.

WANG, Yingfeng; SUN, Wenting; ZHENG, Jilin; XU, Can; WANG, Xia; LI, Tianyi; TANG, Yida; LI, Zhongfeng. Urinary metabonomic study of patients with acute coronary syndrome using UPLC-QTOF/MS. **Journal of Chromatography B: Analytical Technologies in the Biomedical and Life Sciences**, [S. l.], v. 1100–1101, n. September, p. 122–130, 2018. DOI: 10.1016/j.jchromb.2018.10.005. Disponível em: <https://doi.org/10.1016/j.jchromb.2018.10.005>.

WHO (World Health Organization). **GLOBAL STATUS REPORT on noncommunicable diseases 2014**. Geneva: WHO Press, 2014. DOI: 10.1016/j.tvjl.2006.05.022. Disponível em: <http://www.ncbi.nlm.nih.gov/pubmed/16904354>.

WHO (World Health Organization). **Global Report on Diabetes**. Geneva: WHO press, 2016. ISBN: 978 92 4 156525 7.

WILLIAMSON, Rachel M. et al. Prevalence of and risk factors for hepatic steatosis and nonalcoholic fatty liver disease in people with type 2 diabetes: The Edinburgh type 2 diabetes study. **Diabetes Care**, [S. l.], v. 34, n. 5, p. 1139–1144, 2011. DOI: 10.2337/dc10-2229.

XIE, Lianghua; SU, Hongming; SUN, Chongde; ZHENG, Xiaodong; CHEN, Wei. Recent advances in understanding the anti-obesity activity of anthocyanins and their biosynthesis in microorganisms. **Trends in Food Science and Technology**, [S. l.], v. 72, n. November 2017, p. 13–24, 2018. DOI: 10.1016/j.tifs.2017.12.002. Disponível em: <https://doi.org/10.1016/j.tifs.2017.12.002>.

YANG, Jieping et al. Cholesterol-lowering effects of dietary pomegranate extract and inulin in mice fed an obesogenic diet. **Journal of Nutritional Biochemistry**, [S. l.], v.

52, p. 62–69, 2018. DOI: 10.1016/j.jnutbio.2017.10.003. Disponível em: <https://doi.org/10.1016/j.jnutbio.2017.10.003>.

YANG, Qiyuan et al. AMPK/ $\alpha$ -Ketoglutarate Axis Dynamically Mediates DNA Demethylation in the Prdm16 Promoter and Brown Adipogenesis. **Cell Metabolism**, [S. l.], v. 24, n. 4, p. 542–554, 2016. DOI: 10.1016/j.cmet.2016.08.010. Disponível em: <http://dx.doi.org/10.1016/j.cmet.2016.08.010>.

YOON, Mee-Sup. The Role of Mammalian Target of Rapamycin (mTOR) in Insulin Signaling. **Nutrients**, [S. l.], v. 9, n. 11, p. 1176, 2017. a. DOI: 10.3390/nu9111176. Disponível em: <http://www.mdpi.com/2072-6643/9/11/1176>.

YOON, Mee Sup. **The role of mammalian target of rapamycin (mTOR) in insulin signaling** **Nutrients**, 2017. b. DOI: 10.3390/nu9111176.

YU, Xuan; WANG, Xin Pei; LEI, Fan; JIANG, Jing Fei; LI, Jun; XING, Dong Ming; DU, Li Jun. Pomegranate leaf attenuates lipid absorption in the small intestine in hyperlipidemic mice by inhibiting lipase activity. **Chinese Journal of Natural Medicines**, [S. l.], v. 15, n. 10, p. 732–739, 2017. DOI: 10.1016/S1875-5364(17)30104-8. Disponível em: [http://dx.doi.org/10.1016/S1875-5364\(17\)30104-8](http://dx.doi.org/10.1016/S1875-5364(17)30104-8).

ZHANG, Qiaozhi; LUNA-VITAL, Diego; MEJIA, Elvira Gonzalez De. Anthocyanins from colored maize ameliorated the inflammatory paracrine interplay between macrophages and adipocytes through regulation of NF- $\kappa$ B and JNK-dependent MAPK pathways. **Journal of Functional Foods**, [S. l.], v. 54, n. January, p. 175–186, 2019. DOI: 10.1016/j.jff.2019.01.016. Disponível em: <https://doi.org/10.1016/j.jff.2019.01.016>.

ZHANG, Ruifen et al. Rice bran phenolic extract supplementation ameliorates impaired lipid metabolism in high-fat-diet fed mice through AMPK activation in liver. **Journal of Functional Foods**, [S. l.], v. 73, n. April, p. 104131, 2020. DOI: 10.1016/j.jff.2020.104131. Disponível em: <https://doi.org/10.1016/j.jff.2020.104131>.

ZIEBA, D. A.; BIERNAT, W.; BARĆ, J. Roles of leptin and resistin in metabolism, reproduction, and leptin resistance. **Domestic Animal Endocrinology**, [S. l.], 2020. DOI: 10.1016/j.domaniend.2020.106472.

ZIMMET, Paul; ALBERTI, K. G. M. M.; SHAW, Jonathan. Global and societal implications of the diabetes epidemic. **Nature**, [S. l.], v. 414, n. 6865, p. 782–787, 2001. DOI: 10.1038/414782a.